T 306

A STUDY
ON SOME MOLECULAR CHANGES IN DYES INDUCED BY PREMICELLAR IONIC SURFACTANTS

A thesis submitted in part fulfillment of the requirements
for the Degree of
Doctor of Philosophy

By

ANISHA DUTTA

Registration No. 032 of 2010

Department of Chemical Sciences
School of Sciences
Tezpur University, Tezpur
Assam, India

July, 2014

Dedicated to Papa and Maa

(Dr. Amarendra Nath Dutta & Mrs. Anuradha Dutta)

&

My Teachers

Study on Some Molecular Changes in Dyes Induced by Premicellar Ionic Surfactants

ABSTRACT

The present thesis describes a study of the molecular changes of three aqueous dyes induced by ionic surfactants by spectroscopic and surface tension measurements. The inferences from the experimental study have been supported by Density Functional Theory (DFT)-Time Dependent Density Functional Theory (TD-DFT) study. The thesis has been organized in four major chapters which deal with different aspects of the study as follows:

I. Introduction: Narrates the salient features of the surfactants, the dyes, background of the dye-surfactant interactions, the motivation behind, the objectives and the strategy of the present research work.

II. Materials and method: Describes the materials used and the methods adopted in the research work.

III. Results and Discussion: Presents the findings, their analysis, their interpretation, explanation and elucidation of the useful information.

IV. Conclusions: Summarizes the important findings.

Chapter I

I. Introduction

Chapter I is a brief introduction of the thesis. It contains a brief narration of the surfactants, the dyes, the earlier work done on dye-surfactant systems, the lacunae that remain in the research area and the motivation that inspires us to carry out the present research work.

Surfactants are amphiphiles characterized by a hydrophilic head group and a hydrophobic hydrocarbon tail. They form monolayers at interfaces in solutions and thus have the ability to reduce the surface/interfacial tension of solutions. They can form organised structures called micelle or reverse micelle in aqueous and nonaqueous solutions, respectively, when the concentration of the surfactants reaches the critical concentration known as the Critical Micelle Concentration (CMC) of the surfactants. Aqueous dye-surfactant systems have been extensively investigated and exploited for understanding the fundamental properties of surfactants as well as for their efficient applications in various fields due to convenience of monitoring the behavior of dyes through spectral changes.

ABSTRACT

Surfactant assemblies can tune the electronic spectra of solution of dyes and thus we can say that they can alter the molecular structure of the dyes in their aqueous solutions. The spectral changes of the ionic dyes in presence of oppositely charged surfactants below their CMC have been attributed to various types of interactions, *viz.*, formation of dye-surfactant salts, dye-surfactant ionpairs (DSIPs), dye-rich induced micelles, self-assembly of the dye-surfactant complexes, change in the chromophore microenvironment, induced dimerization, keto-enol tautomerism and ionpair aggregation.

However, some of these interactions are still not unequivocally ascertained and the study on the interactive forces operative in these systems are not yet sufficient to arrive at definite conclusions. The molecular interactions which facilitate the change in the structure of the dye on binding to surfactants in the submicellar concentration ranges need better understanding. Therefore, an attempt has been made to understand the nature of forces operative in these systems explicitly by using UV-Vis absorption and fluorescence spectroscopy and surface tension measurements. A study of the changes in the molecular structure of two synthetic dyes - Methyl Orange (MO) and Acridine Orange (AO) of different charge types, and also the physicochemical behavior of a natural dye – Curcumin in different surfactants has been presented in the thesis.

The reported *cis-trans* isomerism of MO in the premicellar cationic surfactants has been systematically investigated both experimentally and theoretically. We wanted to examine the possibility of acid-base interaction of AO in addition to the well-known aggregation in premicellar anionic surfactants. In the case of Curcumin, we have made an attempt to clearly understand the stabilization of the β-diketo form of curcumin in presence of submicellar ionic surfactants of both charge types with focus on the effect of higher ionic strength and on the surface tension behavior of the surfactants in presence of curcumin. To understand the microscopic details of the observed interactions in the chosen dye-surfactant systems, we have carried out DFT-TDDFT calculations.

Chapter II

This chapter contains the description of the materials chosen and the methods adopted in the study. The sources of the chemicals, the preparation of experimental solutions and recording of absorption and fluorescence spectra and surface tension have been described in this chapter.

II.1. Materials and Methods

II.1.1. Materials: Three dyes and nine surfactants were chosen for our study. The stock solutions and the experimental solutions were prepared in double distilled water. Low ionic strength (*I= 0.01*) buffer systems were used.

II.2. Experimental

II.2.1. Instrumental analysis: The UV-visible spectra were recorded on a Shimadzu UV-2550 UV-visible double beam spectrophotometer with matched pair of cells of 1 cm path length using thermostated cell holder. Fluorescence spectra were recorded on a Perkin Elmer LS 55 Fluorescence Spectrophotometer. The surface tensions were determined by using a platinum ring with a Do Nouy tensiometer model 276 of JENCON, Kolkata. The *p*Hs were determined by using an Orion Five Star multiparameter kit ion meter (USA), μ-*p*H systems.

II.2.2. Preparations of solutions: The experimental solutions were prepared by mixing definite volume of dye, surfactant and buffer from their stock solutions.

II.2.3. Methodology: Freshly prepared stock surfactant solutions were used to avoid hydrolysis on standing. The experimental solutions were prepared by mixing the components. The dye was added just before recording the data to avoid any error that would arise due to degradation of the dye.

II.2. Computational: The details of the software and the method used are:

II.2.1. Software: Gaussian 09

II.2.2. Method: *ab initio* Density Functional Theory (DFT) combined with time Dependent-Density Functional Theory (TD-DFT).

II.2.3. Functional: B3LYP stands for Becke, 3-parameter, Lee-Yang-Parr.

II.2.4. Basis set: 6-31+g(d,p) basis set for all the atoms.

II.2.5. Solvent effects: The solvent effects were considered employing the self-consistent reaction field (SCRF) method with Polarized Continuum Model (PCM).

II.2.6. Methodology: The free dye molecules as well their complexes with surfactants were optimized. The computational cost was reduced by replacing the long tail non-conjugated alkyl chains of the surfactants with ethyl moiety which would not change the low energy properties significantly at least in the submicellar concentration range. The optimized structures were taken for the TD-DFT calculations.

Chapter III

III. Results and Discussions

This chapter describes the experimental results, their analysis and interpretation. For systematic organization, this chapter has been divided into three major sections. The first section (III.1.) and second section (III.2.) deals with *cis-trans* isomerism and acid-base interactions of the two synthetic dyes, viz., methyl orange and acridine orange, respectively, in the presence of oppositely charged submicellar surfactants. The third section (III.3.) is divided into two sub-sections (III.3.1) and (III.3.2) which deal with the study of the keto-enol tautamerism of the natural dye, viz., curcumin, in presence of cationic and anionic surfactants, respectively.

III.1. *Cis-trans* isomerism of methyl orange in cationic premicelles

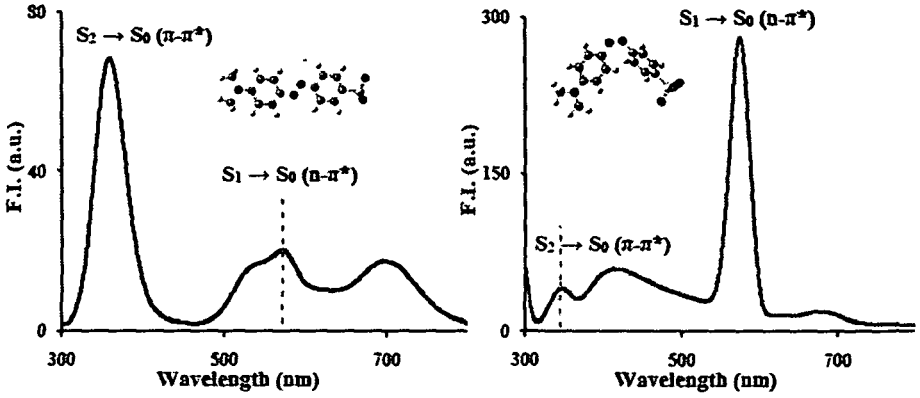

The interaction of aqueous MO with cationic surfactants stabilizing its *cis*-form and exhibiting an UV band around 368 nm has been studied by UV-visible and fluorescence spectroscopy, and surface tensiometry in presence of submicellar concentration of the surfactants. TD-DFT has also been used to predict the molecular structure and excitation energies of the interaction product in the ground state.

MO form ionpairs with cationic surfactants as revealed by surface tension and UV-visible studies. The *cis*-isomer of MO which absorbs at 368 nm, is stabilized in the premicelles formed by the ionpairs and has been found to be fluorescence active when excited at wavelength $\leq$ 270 nm. An intense fluorescence band with maximum at 575 nm along with a broad moderate intensity band in the range of 370-530 nm and a low intensity band at 361 nm have been observed. The hydrophobic interaction between the surfactant tail and the hydrophobic groups of MO facilitate the twisting of MO for which the symmetry forbidden $S_1 \rightarrow S_0$ (n-π^*) transition becomes allowed and MO stabilizes in the *cis* form indicated by the increase in the intensity at 575. The fluorescence and hence the

cis-isomer again disappear when normal micelles are formed above the normal CMC of the surfactant.

Optimizations of both the isomeric forms of MO complexed with CTAB fragment (EA) shows that the MO_{cis}.EA is stable over the MO_{trans}.EA complex by ≈ 2.94 kJ mol^{-1}. Theoretical peaks at 375.18 nm and 375.21 nm were observed in case of free MO_{cis} and MO_{cis} complexed with CTAB, respectively. Thus, the theoretical results also indicate stabilization of the *cis* form of MO by premicellar cationic surfactants.

III.2. Protonation of Acridine Orange in Dye-surfactant Ionpair Micelles

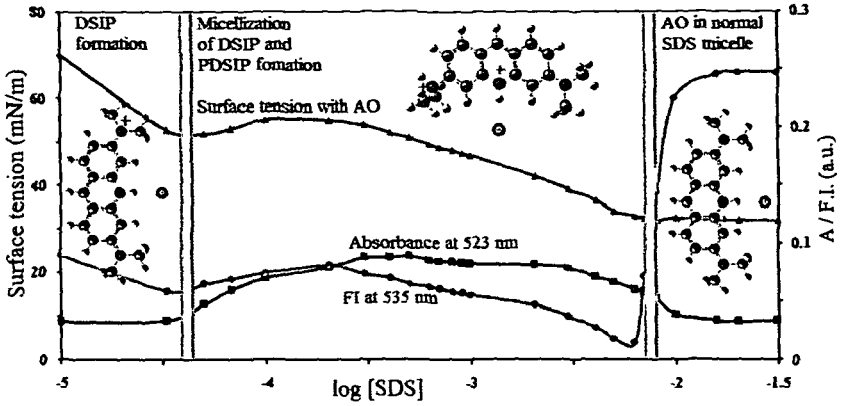

The behavior of aqueous AO in presence of submicellar anionic surfactants has been studied through UV-visible, fluorescence spectroscopy and surface tension measurements. UV-visible spectra of AO in submicellar aqueous solutions of anionic surfactants have been compared to the spectra of AO in varying concentration of concentrated H_2SO_4. TD-DFT has been used to predict the possible site of protonation of AO.

An observed increase in absorption in the 510-580 nm region of the UV-visible spectra of AO in submicellar anionic surfactant solutions has been attributed to protonation of AO in the dye-surfactant ionpair (the PDSIP). This PDSIP formation takes place in addition to the well known induced dimerization (H-aggregation) of AO. The surface tension measurements clearly show two critical micelle concentrations (CMCs) in the dye-surfactant system: the lower one (CMC_{IP}) corresponds to micellization of the DSIP, and the higher one (CMC*) corresponds to the normal micellization of the anionic surfactant. The efficiencies of the DSIP and the anionic surfactant in the systems have been determined.

TD-DFT of the optimized free dye and the ionpair with the surfactant reveals that protonation at the terminal dimethylamino N-atom of AO is a favoured site. The calculated absorption maximum for protonated AO and PDSIP was found to be 475.22 nm

and 478.94 nm, respectively. The computational results agree with the red-shift of the cationic dye when it gets protonated in presence of anionic surfactant.

III.3. Stabilization of the β-diketo tautomer of curcumin in premicellar ionic surfactants

Ke *et al.* have reported that the β-diketo form of curcumin is stabilized by a cationic surfactant, *viz.*, dodecyltyimethylammonium bromide (DTAB) in submicellar concentrations at *p*H 5.00. This was followed by a spectral study by Baruah. It is important to acknowledge the inherent chemical features of the curcumin molecule, specially, because the antioxidant activity of curcumin is attributed to its diketo tautomer. Therefore, we extended the study to surface tension and a detail steady state fluorescence measurements and TD-DFT calculation. To have a complete picture of the interaction, UV-visible study was also done. We also have examined the salt effect on the keto-enol tautomerism of curcumin observed in the premicellar solutions.

III.3.1. Curcumin in Submicellar Cationic Surfactant Solutions

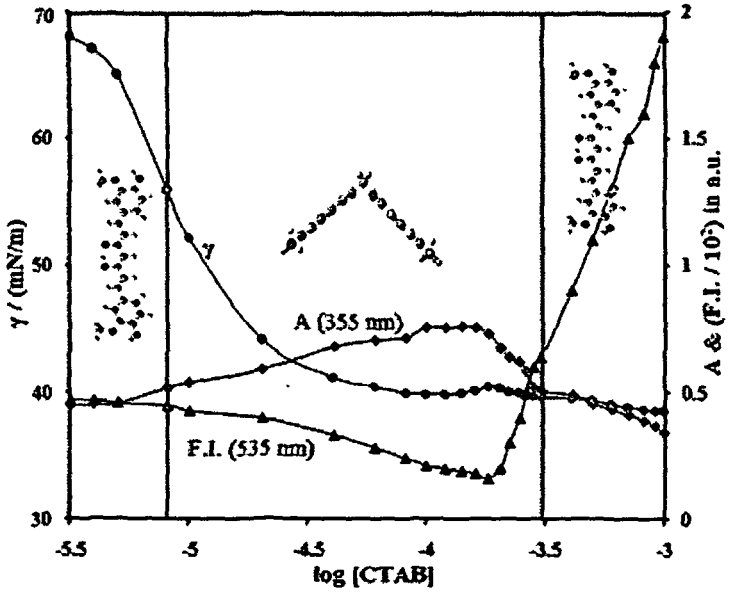

The interaction of aqueous curcumin with cationic surfactants of varying chain lengths and head group, stabilizing its β-diketo tautomer and exhibiting an UV band around 355 nm, has been studied in buffered aqueous solutions in the *p*H range of 2.00-7.50 in presence of submicellar concentration of the surfactants.

The plots of surface tension of the aqueous solutions of the cationic surfactants as a function of surfactant concentrations in the presence of curcumin indicated that curcumin forms electrostatic ionpair complexes due to cooperative attractive forces between the

partial negative charges of the electron rich electronegative O-atoms of curcumin and the positively charged cationic surfactant head groups, thus behaving like nonionic surfactant. The curcumin-surfactant complexes break down as the curcumin-surfactant complex micelles change to normal surfactant micelles as the concentration of the surfactants increase above the normal CMC in the buffered solutions. An observed secondary salt effect on the interaction indicates the involvement of a proton in the interaction.

DFT study showed that in presence of CTAB fragment (EA), the β-diketo curcumin stabilizes with the orientation of the electronegative oxygen atoms towards the positive moiety which otherwise takes an anti-orientation. From natural population analysis (NPA), we find that there is a small amount of fractional charge transfer from diketo curcumin to CTAB. Theoretical peaks were observed at 350.36 nm for diketo curcumin and 369.22 nm, 368.72 nm for diketo curcumin complexed with EA.

III.3.2. Curcumin in Submicellar Anionic Surfactant Solutions

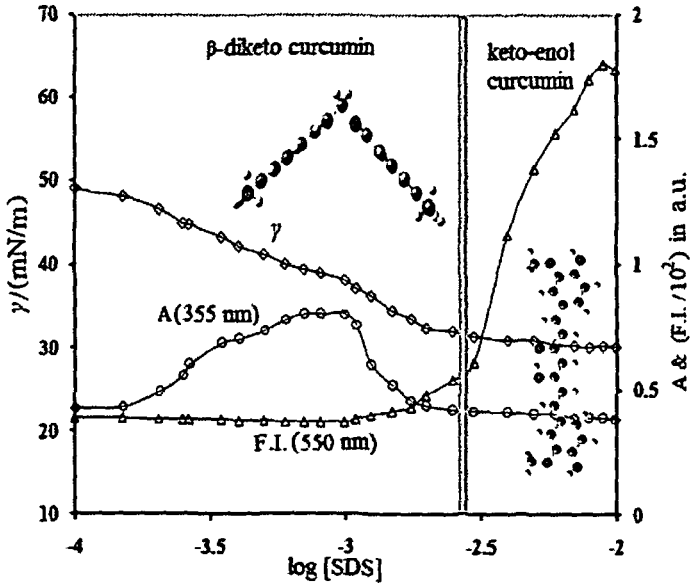

The mechanism of the interaction, for the newly observed UV band of aqueous curcumin, in presence of anionic surfactants, *viz.*, sodium dodecylsulfate (SDS), sodium dodecylbenzenesulfonate (SDBS), sodium dodecylsulfonate (SDSN) in buffered aqueous solutions was studied.

The diketo curcumin interacts with surrounding water through H-bond formation with the oxygen atoms of the carbonyl groups and then the H-atom bound to one of the oxygen atoms binds with the dodecylsulfate group of the surfactant. The H-bond with either of the oxygen atoms, more likely to that of the sulfate group, may be close to a protonation. Thus, the monomeric surfactant stabilizes the twisted diketo curcumin by

means of a dye-surfactant complex involving H-bond formation in the acidic and neutral *p*H ranges.

The, β-diketo curcumin-SDS complex is more stabilized than the keto-enol complex by ≈ 4-5 kcal M^{-1}. Formation of the complex by the diketo form decreases the HOMO-LUMO energy by about 0.45 eV. From NPA calculation, we also find that there is a small amount of fractional charge transfer from diketo curcumin to SDS fragment (ES). Ground state TD-DFT calculations showed absorption peaks at 350.36 nm for diketo curcumin and 366.93 nm, 362.03 nm for diketo curcumin complexed with ES.

Chapter IV

IV. Conclusions

This chapter summarizes the conclusions drawn from the present study on the interactions in the chosen aqueous dyes-surfactant systems. The main conclusions drawn are as follows:

1. The *cis*-isomer of MO, stabilized in the premicelles formed by the MO-cationic surfactant ionpairs has been found to be fluorescent active when excited at wavelength ≤ 270 nm. The major fluorescence band at 575 nm has been attributed to $S_1 \rightarrow S_0$ (n-π^*) fluorescence unlike the other azobenzenes where the $S_2 \rightarrow S_0$ (π-π^*) fluorescence which is usually reported.
2. AO in aqueous submicellar anionic surfactants solutions forms PDSIP in the premicelles of DSIPs in addition to the well known dimerization of the dye. The PDSIP formation by AO is entropy driven and stronger with SDS than with SDBS.
3. The β-diketo curcumin-SDS complex is more stabilized than the keto-enol complex by ≈ 4-5 kcal M^{-1}. In presence of CTAB, the β-diketo curcumin is stabilized with the orientation of the electronegative oxygen atoms towards the positive moiety which would otherwise take an anti-orientation. There is charge transfer from diketo curcumin to CTAB and SDS. An observed secondary salt-effect indicates the involvement of a proton in the mechanism of the interaction with surfactants of both the charge types.

List of Publications

A major portion of the work described here in the theses has been already published as mentioned below.

1. "Fluorescence behavior of *cis*-methyl orange stabilized in cationic premicelles", A. Dutta and R.K Dutta, ***Spectrochim. Acta A*** 126 (2014) 270-279.

2. Protonation of acridine orange in dye-surfactant ion pair micelles", A. Dutta and R.K. Dutta, ***J. Mol. Liq.*** 178 (2013) 25-30.
3. "Stabilization of diketo tautomer of curcumin by premicellar cationic surfactants: UV-Vis, fluorescence, tensiometric and TD-DFT evidences", A. Dutta, B. Boruah, P.M. Saikia, R.K. Dutta, ***J. Mol. Liq.*** 187 (2013) 350-358.
4. "Stabilization of diketo tautomer of curcumin by premicellar anionic surfactants: UV-Vis, fluorescence, tensiometric and TD-DFT evidences", A. Dutta, B. Boruah, A.K. Manna, B. Gohain, P.M. Saikia, R.K. Dutta, ***Spectrochim. Acta A*** 104 (2013) 150-157.
5. "Time-dependent density functional theory (TDDFT) modeling of protonated dye-surfactant ion pair", A. Dutta and R.K. Dutta (to be communicated).

DECLARATION BY THE CANDIDATE

I hereby declare that the thesis entitled "***A Study on Some Molecular Changes in Dyes Induced by Premicellar Ionic Surfactants***" being submitted to the Department of Chemical Sciences, Tezpur University, is a record of original research work carried out by me under the supervision of **Dr. Robin K. Dutta.**

Any text, figure, result or design that is not of my own devising is appropriately referenced in order to give credit to the original author (s). All sources of assistance have been assigned due acknowledgement.

I also declare that neither this work as a whole nor a part of it has been submitted to any other university or institute for any other Degree, Diploma or Award.

Anisha Dutta

Place: Tezpur University (Anisha Dutta)

Date: 25/07/2014

TEZPUR UNIVERSITY

(A Central University Established by an Act of Parliament)

NAPAAM, TEZPUR-784028

DISTRICT: SONITPUR :: ASSAM :: INDIA

Ph: 03712-267008 (O) 9435006674 (M) Fax: 03712-267006 Email: robind@tezu.ernet.in

This is to certify that the thesis entitled "***A Study on Some Molecular Changes in Dyes Induced by Premicellar Ionic Surfactants***" submitted to the Tezpur University in the Department of *Chemical Sciences* under the School of Sciences, in partial fulfillment for the award of the Degree of Doctor of Philosophy in Science, is a record of research work carried out by Ms. Anisha Dutta under my supervision and guidance.

All helps received by her from various sources have been duly acknowledged.

No part of this thesis has been submitted elsewhere for award of any other Degree.

Place: Tezpur University
Date: 25/7/2014

(Dr. Robin Kumar Dutta)
Professor
Department of Chemical
Sciences School of Sciences

Acknowledgement

This Ph. D dissertation is the culmination of five wonderful years of my research experience and ardent learning. The words in these pages are not mere words but are what I actually feel for. I would like to acknowledge each person who has in any way helped and supported me and have been instrumental during the course of my research. Without them it would not have been possible to put each step forward and reach at the stage of completion.

At the very outset, I would like to express my sincere gratitude to my research supervisor, Dr, Robin Kumar Dutta, Prof., Chemical Sciences, Tezpur University. I would remain ever debtful towards him for his untiring guidance, intellectuality and encouragement during the entire research work, without which it would have not been possible for me to reach at this stage of writing my Ph. D Dissertation. He has always given me the benefit of his honesty and forthright opinion whenever I would seek for it and has always proven to be beneficial. His urge to do something for the society and his love for the Assamese culture always inspires me. I am grateful to Dr. (Mrs.) Meera Dutta baideu for her encouragement and I would like to share my love with Narji and Tora.

I thank to Almighty, who I believe to be with me every moment and showering His blessings upon me. I am always grateful to Papa who provides a constant source of encouragement to succeed without ever putting me under pressure. He has always been an example who strives for perfection with utmost patience though I am not an owner of either of the two. The energy and stamina with which he approaches his work even at this age has always been a great example and there has never been any doubt what drives him. I am eternally grateful to Maa who has always given me the moral support whenever I am down. Her prayer for me was what sustained me thus far.

With the deepest sense of gratitude, I would like to thank my doctoral committee members, Prof. S. K. Dolui and Prof. R. C. Deka, Department of Chemical Sciences, for their constant inspiration and valuable suggestions during my research work. I would like to thank every faculty member of the Department of Chemical Sciences for their encouraging words and helpful advice.

I would like to express my appreciation to Dr. B. Gohain, Technical Officer, Department of Chemical Sciences, Tezpur University whom I never hesitated to approach for anything regarding my research work.

I would like to offer my deepest gratitude to Dr. Swapan K. Pati, JNCASR, Bangalore with whom I learnt some computational work for a period of four months. I thank him for allowing me to use the Gaussian 09 software under his license. I can never forget the guidance of

the research scholars in his group, Dr Prakash Parida, and Dr Arun K, Manna in this regard who helped me even through phone.

I am very much thankful to Mr Arup Chakrabarty, Mr Biraj Borah, Mr Sankur Phukan, Mr Raju Borah, Mr Nipu Dutta, Mr Manoranjan Sarma, our technical staff members and Mr Hemanta Gogoi, Mr Babul Kalita and Ms Bobita Das, our office staff for their help in many aspects. I am grateful to all the staff of the administrative community of Tezpur University.

I thank Tezpur University for the Institutional Fellowship for the period 2009-2012. The UGC for the BSR Fellowship and the Council of Scientific and Industrial Research (CSIR) for the SRF as financial assistance to complete the research work staying away from home.

I want to share my love and gratitude with my friends specially Amrita, Bondita, Kosturika, Sikha, Samadrita, Madhulekha, Prarthana, Nibedita, Najima, Rasna, Zenith, Chandan, Surajit, Murshid, Deepak, Dipannita and pranamita, You always stand by me in my happy and sad times.

I would like to thank my brother in law Mr Rajaa Bharali and my sister Mrs Mrigakshi Dutta Bharali for their loving support, patience and understanding throughout the course of my studies, so that I might pursue this endeavour. I would like thank all my family members.

I would like to thank Mr Shyamal Gogoi, my husband for always standing by me and supporting me in my adverse situations.

I would also like to thank my colleagues in the laboratory Suresh da, Bornali ba, Shreemoyee ba, Sweety, Barsha, and Anup, for discussions that have spawned many of the ideas used in doing this research work. Thanks to all for providing useful suggestions on the manuscript for their help and cooperation.

I am also thankful to all my friends and well wishers in the Dept. of Chemical Sciences, Tezpur University for their valuable support.

I would like to thank Google for being a constant source of information that helped me throughout the research work. I am grateful to all the authors cited in this thesis without whom I would have been unable to step forward.

Finally, I would like to thank the authority of Tezpur University for granting me the permission to do this work.

I would probably forget what I have been through; however, I will keep all the courage and confidence throughout my entire life.

Anisha Dutta

CONTENTS Pages

CONTENTS

List of Tables

List of Abbreviations

AR	Analytical reagent
AO	Acridine Orange
CMC	Critical Micelle Concentration
CMC^*	CMC of pure surfactant in water
$CMC^/$	CMC of aqueous surfactant solution in presence of dye
CMC_{IP}	CMC of dye-surfactant ionpair
CMC_c	CMC of curcumin-surfactant complex
CTAB	Cetyltrimethylammonium bromide
CPB	Cetyltrimethylammonium bromide
CPC	Cetyltrimethylammonium chloride
DSIP	Dye-surfactant ionpair
DTAB	Dodecyltrimethylammonium bromide
PDSIP	Protonated dye-surfactant ionpair
MO	Methyl Orange
pC_{20}	Efficiency of surfactant
pK_a	Negative logarithm of equilibrium constant
pH	Potential of hydrogen ion concentration
SDS	Sodium dodecylsulfate / sodium laurylsulfate
SDBS	Sodium dodecylbenzene sulfate
SDSN	Sodium dodecyl sulfonate / sodium sulfonate
TTAB	Tetradecyltrimethylammonium bromide
TX-100	Triton X-100 (Iso-octlylphenoxy-polyethoxy-ethanol)
Γ_s	Surface Excess Concentration
HF	Hartree Fock
LSDA	Local Spin Density Approximation

VWN	Vosko, Wilk, and Nusair 1980 correlation functional

List of Symbols used in the thesis

K	Kelvin
R	Gas constant
T	Temperature
χ	mole fraction
K_a	acid dissociation constant
μ	micro
μ	Chemical potential
a	activity
m	milli
mN/m	milliNewton/metre
g	gram
I	ionic strength
γ	surface tension
J	Joule
M	molar

INTRODUCTION

I. Introduction

This chapter briefly narrates the salient features of the surfactants, the dyes, the background, the motivation, the objectives and the strategy of the present research work.

I.1. Surfactants and micelles

I.1.1. Surfactants

The word '**surfactant**' is a blend of **surface active agents**, which literally means active at surfaces and interfaces[1,2] (boundary between any two phases which are immiscible). The term surfactant was coined by Antara products in 1950[3]. Surfactants are amphiphilic materials possessing both a polar long hydrocarbon "tail" of carbon atoms (7-20 carbon atoms)[1] and polar, usually ionic, "head" groups. An amphiphile exhibits a dual affinity, which can be defined as polar-apolar duality from the physicochemical point of view. The unusual and versatile properties of surfactants in their aqueous solutions can be ascribed to its amphiphilicity. The polar or ionic head group interacts strongly with a polar/aqueous environment, in which it is solvated via dipole-dipole or ion-dipole interactions. In fact, it is the nature of the polar head group which is used to divide surfactants into different categories.

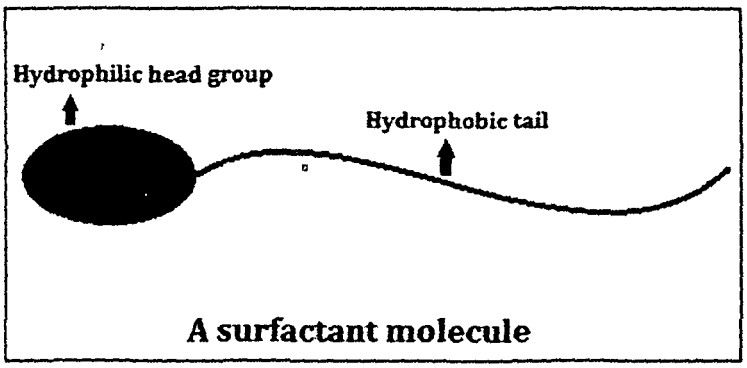

Fig.I.1. A surfactant molecule

Based on the origin, surfactants have been broadly classified into two groups, *viz.*, naturally occurring surfactants and synthetic surfactants. The typical examples of naturally occurring surfactants are lipids and the bile salts. All others are synthetic surfactants. Depending upon the nature of the ionic hydrophilic head group, the synthetic surfactants are primarily classified into four sub classes: (i) anionic, (ii) cationic, (iii) nonionic, and

(iv) zwitterionic. Some common examples of synthetic surfactants of various types are illustrated in the **Table I.1.**

However, a new group of surfactants known as 'gemini surfactant' has also been identified. Gemini surfactants are a different type of surfactants which have been of more scientific interest due to their greater effectiveness in modifying interfacial properties. These surfactant molecules are chemically bonded together by a spacer[4]. The spacer group can be hydrophilic or hydrophobic, flexible or rigid and connects two surfactant moieties at, or near the head group. The name Gemini was coined by Menger[5].

Table I.1. Example of some common surfactants

Class	Examples	Structures
Anionic	Sodium dodecylsulphate	$CH_3(CH_2)_{11}SO_4^-Na^+$
Cationic	Cetyl trimethylammonium bromide	$CH_3(CH_2)_{15}N^+(CH_3)_3Br^-$
Nonionic	Polyoxyethylene octyl phenyl ether	$C_{14}H_{22}O(C_2H_4O)_n$ (n=9-10)
Zwitterionic	Dodecyl betaine	$C_{16}H_{33}NO_2$

I.1.2. Adsorption of Surfactants on Surfaces and Interfaces

Surfactants tend to form monolayers at the surfaces of solutions as well as in the interfaces. Surfactant monolayers are formed in a way such that the hydrophilic headgroups orient towards the polar environment while hydrophobic tails remain in the hydrophobic environment. Adsorption of surfactants at the liquid-vapour (l/v), liquid-liquid (l/l) and solid-liquid (s/l) interfaces are of immense academic and commercial importance utilizing the phenomenon of foaming and emulsification[6]. The nature of layer adsorbed and the manner in which it alters or modifies the surface properties depends on the nature of the surfactant and its interaction with the surface. Depending on the amount of surfactant adsorbed on the interface/surface and the structure of the interfacial/ adsorbed layer (the manner in which the surfactant in oriented at the surface/interface), the surface can become more hydrophilic or more hydrophobic.

I.1.2.1. The Gibbs Adsorption Isotherm

The amount of surfactant adsorbed per unit area of liquid-gas and liquid-liquid cannot be determined directly because of the difficulty in isolating exactly the interfacial region. Therefore, the amount of surfactant adsorbed per unit area of a surface or an interface can be calculated from the surface or interfacial tension values of the surfactants indirectly.

From a plot of surface (interface) tension as a function of surfactant concentration in one of the liquid phases, rather than the adsorption isotherm, is used to describe adsorption at these surfaces. Thus, from such a plot, the amount of surfactant adsorbed per unit area of interface can readily be determined by the use of the Gibbs adsorption equation[1]. The Gibbs adsorption equation at liquid-gas and liquid-liquid interface, in its general form is given as:

$$d\gamma = -\Sigma_i \Gamma_i \, d\mu_i \qquad \text{I.1.}$$

$$d\mu_i = RT d \ln a_i \qquad \text{I.2.}$$

where, $d\gamma$ = the change in surface or interfacial tension of the solvent,

Γ_i = the surface excess concentration of any component of the system

$d\mu$ = the change in chemical potential of any component of the system

a_i = activity of 'i' in bulk phase

I.1.2.2. Surface Excess Concentration of Surfactant

For an interface, the adsorption or surface excess of a given component is defined as the difference between the amount of that component actually present in the system, to that present in a reference system if the bulk concentration in the adjoining phases is maintained up to a chosen geometrical dividing surface (the Gibbs dividing surface)[1]. For measurements on a nonionic surfactant of dilute concentrations (10^{-2} mol dm^{-3} or less), the Gibbs equation is given by the following equation where the activity is replaced by concentration.

$$d\gamma = -2RT \, \Gamma_i \, d \ln C_i \qquad \text{I.3.}$$

$$= -4.606 \, RT \, \Gamma_i \, d \log C_i \qquad \text{I.4.}$$

Where, C_i is the molar concentration of surfactant. When γ is in the mN/m (= mJ/m^2) and $R = 8.31 \times 10^7$ J mol^{-1} K^{-1} then Γ_i is in mol/1000 m^2. Surface excess concentration of a surfactant is a measure of the effectiveness of the surfactant[1] in a medium.

I.1.2.3. Efficiency of a surfactant: pC_{20}

The efficiency is expressed by a quantity termed pC_{20}. It is a useful parameter to compare the performance of a surfactant at the liquid-gas or liquid-liquid interfaces and determines

the 'efficiency' of a surfactant in a medium. pC_{20} is the negative logarithm of the concentration of surfactant in the bulk phase required to produce a 20 mN/m reduction in the surface or interfacial tension of the solvent[1] and is given by:

$$pC_{20} = -\log C_{(-\Delta\gamma = 20)} \qquad \text{I.5.}$$

The efficiency is determined by plotting γ versus log C_1 of the surfactant solution. It has been reported earlier that when the surface (interfacial) tension is reduced by 20 mN/m, *i.e.* at pC_{20}, the surface concentration is 84-99.9 % saturated[1]. The negative logarithm of the bulk phase concentration of surfactant, pC_{20}, in mol dm^{-3}, rather than the concentration C_{20} itself because the negative logarithm can be related to the standard free energy change ΔG° involved in the transfer of the surfactant molecule from the interior of the bulk liquid phase to the surface or an interface. The larger the value of pC_{20}, the more is the surfactant adsorbed at the surface/interface and the more is the surfactant efficient in reducing the surface or interfacial tension. Since, this is a logarithmic relation, a value of pC_{20} one unit greater means ten times the efficiency, that is 1/10 the bulk phase concentration required to produce surface saturation. There is a linear relationship between the efficiency of adsorption at the interfaces and the increase in the number of carbon atoms in a straight-chain hydrophobic group, which reflects the negative free energy of adsorption of a methylene group at these interfaces.

I.1.3. Micellization and CMC

Due to the amphiphilicity, surfactants in aqueous solutions have an inherent tendency to form self aggregates of nearly spherical shape called micelles as the concentration exceeds a certain value (**Fig.I.2**). In aqueous solution, at low concentration, the surfactants remain as single molecules or form monolayers at the surfaces. These amphiphilic molecules distort the water structure and increase the free energy of the system. They concentrate at the surface of the aqueous solution forming a monolayer with the hydrophobic tails oriented away from the solvent thus minimizing the free energy of the solution. Now, when the concentration of the surfactant is increased and reaches the critical value, the surface or interface becomes saturated and starts self-aggregating to form clusters known as the micelles as shown in **Fig.I.2.**

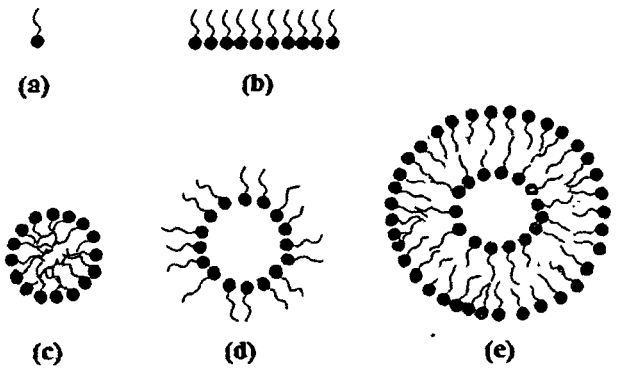

Fig.I.2. Schematic representation of (a) a surfactant monomer, (b) monolayer, (c) a normal micelle, (d) a reverse micelle and (e) a vesicle.

This critical concentration, at which micelle formation starts, characteristic of a surfactant, is called its critical micelle concentration (CMC) as already mentioned. In aqueous or polar solutions, the surfactant molecules orient their hydrophobic tails towards the core of the micelles and the hydrophilic head groups toward the solvent. In nonpolar medium, the aggregates are oriented in such a manner that the polar head groups of the surfactants are shielded from the nonpolar solvent by the hydrocarbon tails. These aggregates have been termed as "reverse micelles". Thus, CMC of a surfactant is a narrow range of concentration rather than a particular concentration[8]. The IUPAC defines CMC as "***There is a relatively small range of concentrations separating the limit below which virtually no micelles are detected and the limit above which virtually all additional surfactant molecules form micelles***". Many of the properties of the surfactant solution appear to change at a differently above and below this range[9] when we plot them against concentration

Since the first inception made by J. McBain[10] and Hartley[11], micelles have been very useful in various fields of science and technology due to their excellent solubilization power and other properties exhibited and have been the subject of excellent reviews, reports and books[10,12-32]. The CMC can be determined by plotting the changes in the various physical properties viz. surface tension, electrical conductance, light scattering, refractive index, viscosity, turbidity, osmotic pressure, spectral changes and solubilization against the concentrations of surfactants which is illustrated by Preston's classic graph[19,33-37], (**Fig.I.3**).

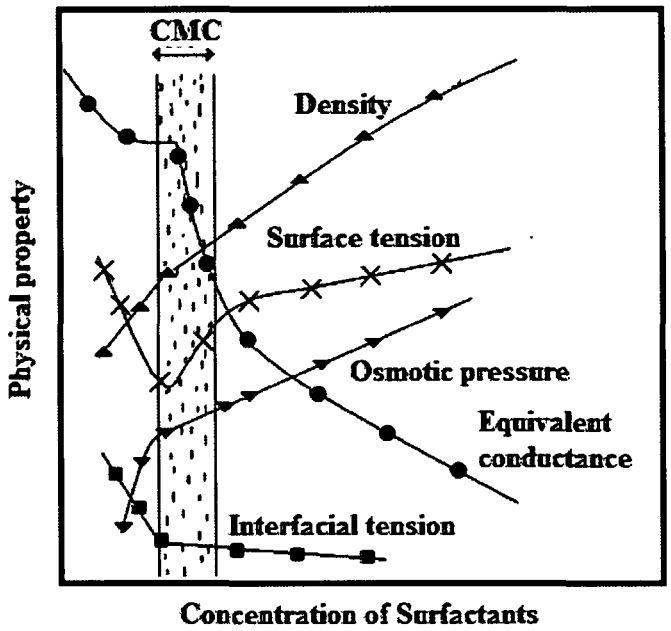

Fig.I.3. Changes of some physical properties of aqueous surfactant solution (in arbitrary scale) with concentration of the surfactant[1].

The CMCs of some common surfactants at 298 K in aqueous medium are shown in **Table I.2**[1,12-14]. The CMC of surfactants depend on a number of factors: (a) the length and structure of hydrophobic carbon chain, (b) the nature of the head group, (c) the presence of additives, (d) the temperature, etc[19,33-37].

Table I.2. The literature values[1] of the CMCs of some common surfactants at 298K in water.

Surfactant	CMC / (mol dm^{-3})
Sodium Dodecyl Sulphate (SDS)	8.20×10^{-3}
Sodium Dodecyl Benzene Sulphonate (SDBS)	1.20×10^{-3}
Sodium Dodecyl Sulphonate (SDSN)	1.22×10^{-2}
Cetyl trimethylammonium bromide (CTAB)	9.20×10^{-4}
Tetradecyl trimethylammonium bromide (TTAB)	3.60×10^{-3}
Dodecyl trimethylammonium bromide (DTAB)	1.60×10^{-2}
Cetyltrimethyl pyridinium chloride (CPC)	9.00×10^{-4}
Cetyltrimethyl pyridinium bromide (CPB)	9.20×10^{-4}
Iso-octylphenoxy-polyethoxy-ethanol (Triton X – 100)	3.00×10^{-5}

1.1.4. Thermodynamics of micellization

Micellization takes place spontaneously due to the decrease of free energy. The primary driving force is the hydrophobic force, though both hydrophobic and electrostatic interactions are responsible for micellization. The large negative value of ΔG^{o} is mainly due to the large positive values of ΔS. The entropies of micellization even when negative are much smaller than $T\Delta S$[1] giving negative free energies. The positive entropy change during micellization has been attributed to firstly, due the destruction of the ordered structure of the water molecules surrounding the hydrophobic tails of the monomeric surfactant in aqueous medium when the hydrocarbon tails are moved away from the aqueous medium to the interior of the micelle, upon micellization. Secondly, due to an increase in the freedom of the hydrocarbon tails in the nonpolar core of the micelles. The micelle formation thermodynamically has been treated using a mass action model and phase separation model[38], where the standard free energy of micellization ΔG^{o}_{mic} is described by **Eq. I.6**,

$$\Delta G^{o}_{mic} = -RT\ln\chi_{cmc} \qquad \text{I.6.}$$

where, χ_{cmc} is the mole fraction of the surfactant at CMC

I.1.5. Micellar features

Surfactant monomers aggregate to form micelles and each micelle consists of a definite number of surfactant molecules known as **aggregation number**. Thus, an **aggregation number** (N) is a description of the number of surfactant monomers present in a micelle once the CMC has been reached. Each micelle consists of aggregation number usually ranging from 10 to 150, which determines its general size and shape[21,39,40]. The size and shape of the micelle formed in aqueous medium is important in determining various properties such as viscosity, cloud point determination and also the capacity to solubilize the water insoluble substance etc. The sizes of the micelles normally cover the range of 1-10 nm[21,40].

Ionic micelle forms an electrical double layer. The Stern layer encompasses the interfacial region containing the head groups in the electrical double layer formed by the ionic micelles and it extends to about one half of the counterions associated with the micelle and water[19,41,42].

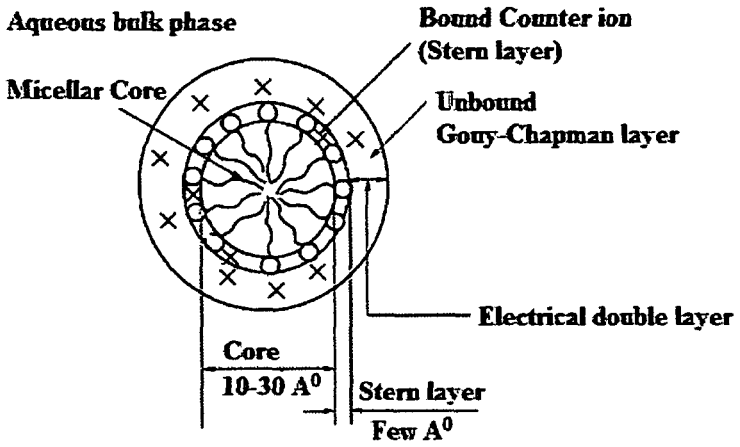

Fig.I.4. A two dimensional representation of the regions of a spherical micelle: ∿∿ hydrocarbon chain, O-head group, X-counterion[41].

However, in case of nonionic micelles, the hydrated polyoxyethylene chains comprise the outer region[36]. A pictorial representation of a spherical micelle with illustration of its different regions is shown in **Fig.I.4**. The micelle can assume different shapes depending on the nature of the surfactant and its concentration[15,43-49]. Some of the principal morphological structures are shown in **Fig.I.5**.

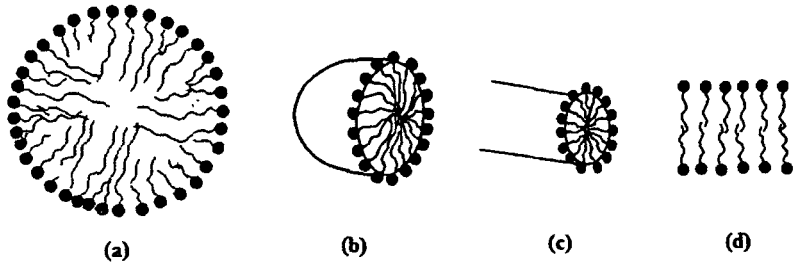

Fig.I.5. The schematic picture of some surfactant micelles: (a) spherical, (b) oblate, (c) cylindrical and (d) lamellar.

The size as well as the shape of micelles is of great theoretical interest, but of very less significant in terms of surfactant applications. However, the more important is the concentration at which the formation of micelle takes place, the critical micelle concentration, since at this concentration, many of the most useful surfactant properties come to play.

Micellization is governed by the hydrophobic interaction between the hydrophobic alkyl chains and the polar repulsion between the head groups[40,50]. Also, in addition to electrostatic repulsions of the surfactant head groups, the repulsions due to the hydration of the head groups also govern the process of micellization. The interfacial tension exerts an opposing force that tends to decrease the effective area of the head group. In the year 1976, Israelachvilli[37] introduced a relationship between the shape of a surfactant monomer and the morphology of a micelle on the basis of the packing parameter approach. Based on the range of the value of the packing parameter, morphology of the aggregates was suggested. The approach was criticized by several authors[51,52]. Later, Dobos[52] introduced a new parameter, *viz.*, micellar proportion, as a parameter to express the time spent by an analyte in the micellar phase in comparison to the whole migration time of the analyte. The determined micellar proportion for various analytes differing in structure and the experimentally determined values were utilized to compare the hydrophobicity and retention ability of the pseudostationary phase.

I.1.6. Assemblies of surfactants other than micelles

Surfactant may self assemble to form a variety of aggregates including the microemulsions and biological membranes apart from the micelles and reverse micelles. If a small amount of oil is added to an aqueous solution of surfactant, the surfactants aggregate around the oil drops. This type of surfactant aggregates is called microemulsion (oil in water, O/W). The term microemulsion was introduced by the English chemist J.H. Schulman in 1959[53] Microemulsions are thermodynamically stable, macroscopically homogeneous dispersions of water-in-oil (W/O)[54-56] or oil in water (O/W) also[57,58]. O/W microemulsions can be formed by dispersing oil in an aqueous surfactant solution and adding a short chain alcohol or amine as a co-surfactant. Sometimes a cosurfactant, usually an alcohol of micelle chain length, is required for microemulsion formation[59,60]. The solubilizing ability of microemulsions is much higher than that of the micellar solutions[61]. Biological membranes are made up of phospholipid bilayers. There are two layers of phosphate "heads" with fatty acid "tails" in the biological membranes[62,63].

I.1.7. Solubilization by micelles

Solubilization into aqueous media is of practical importance in many industrial processes such as detergency[18,64-66], emulsion polymerization[67], micellar catalysis[11,42,68], oil recovery[69-71], drug delivery[58,72], etc. The extent of solubilization of the solubilizate

depends on factors *viz.*, the structure of the surfactant molecule, concentration of the surfactant, molecular properties of the solubilised species, temperature and added electrolytes[73-75]. The locus of solubilization varies with the nature of the solubilizate and is of great importance as it in a way reflects the type of interaction between the micelle and the solubilizate. X-ray diffraction[76,77], UV-visible spectroscopy[78] and NMR spectroscopy[79,80] are the various methods that have been used to determine the sites on solubilization in the micelles. Based on these reports, the solubilizate is believed to be solubilized at different locations in the micelle[1], *viz.*, on the micellar surface, between the hydrophilic head groups, in the layer between the hydrophilic head groups and the first few carbon atoms of the hydrophobic tail and in the nonpolar core of the micelle. Generally, polar solubilizates are solubilized near the micelle surface, whereas non polar solubilizates are solubilized in the non polar micellar core. There is a linear relationship between the free energy of solubilization and the number of carbon atoms of the solubilizate as well as with the number of carbon atoms in the hydrocarbon chain of the surfactants[1,15,81].

A number of experimental techniques have been used to study the solubilization equilibrium, ion-ion, ion-dipole, dipole-dipole as well as hydrophobic interactions of solubilizate with surfactant micelles, such as vapour pressure measurements[82-84], maximum solubility[85], calorimetry[31,86], semi-equilibrium dialysis[87-89], etc. Additives also considerably affect the solubilization process[1,90-94].

I.1.8. Applications of surfactants

The extensive importance of surfactants in practical applications as well as of scientific interest has sparked a plently of published literature on the particular subject. Good beginning points for basics on surfactants are the classic books of Rosen[1], Myers[95] and Mittal[96]. The applications of surfactants in scientific interest and in industries industry are legion, which ranges from primary production processes of the recovery and purification of raw materials used in the mining and petroleum industries, to enhance the quality of products such as paints, cosmetics, pharmaceuticals, and foods. Amphiphiles exhibit properties other than tension lowering and this is the reason they are labeled according to their main use such as: soap, detergent, wetting agent, dispersant, emulsifier, foaming agent, bactericide, corrosion inhibitor, antistatic agent, etc. They are even sometimes known from the name of the structure they are build such as membrane, liquid crystal, microemulsion, liposome, gel or vesicle etc.

Surfactants play an important role in many aspects of our day to day life ranging from the formulation of industrial products to biological applications[97-112]. Starting from the household detergency[1,97], surfactants are used in the production and processing of foods[98-100], in the agrochemicals[101-103], pharmaceuticals[143-107], petroleum product industries[2,108,109], mineral ores[2,108], fuel additives and lubricants[110-111], paints[112,113], coatings and adhesives[114-117], and also in removing hazardous materials from the waste water discharged from industries[118-120]. Moreover due to greater advantages in performance by Gemini surfactants, we can anticipate their use in a multitude of applications[121] ranging from soil remediation and oil recovery to commercial detergents, when a favorable cost/performance ratio is needed to be taken into account.

I.2. The dyes

Dyes have been used since the ancient times. They were extracted from natural sources like plants, flowers and also from animal substances. As early as 1500 B.C., the mummies of Egypt were wrapped in linen strips dyed with indigo or woad. These wrappings although 3500 years old still retain their blue colour. In Greco-Roman period, the indigo was used for the blue colour while red cloth was achieved with the use of kermes insect. One precious animal dye with a glorious history which became available for home consumption in Crete in 1600 B.C. was Tyrian purple. It was derived from crushed sea snails. Almost four million molluscs were required to make one pound of dyestuff. Therefore only rich people could afford to wear colored clothes. In 1856 William Henry Perkin discovered the first synthetic dyestuff 'Mauve' while searching for a cure for malaria. It is an oxidation product of aniline.

Dyes are soluble compounds and possess a specific affinity for the substances for which they are used. A dye must have suitable color, capable to fix on the substrate, light fastness and resistance to water, dilute acids and alkalis. On the other hand, pigments are compounds insoluble in the media in which they are applied and can only be attached with the help of a second compound, for example, by using polymers in paints. Dyes are widely used for coloring textiles, leathers, in printing, photography, thermal writing displays, in lasers etc. Dyes also find important in latest technologies like lasers and displays.

In the year 1876, Witt for the first time showed that color is usually exhibited by a compound containing a group with multiple bonds. These are known as chromophores. The chromophore is a region in the molecule where the energy difference between two different molecular orbitals falls within the range of the visible spectrum. Generally,

chromophores are unsaturated groups like aromatic rings, N=N, C=N, NO, NO_2, quinoid structure etc. On the other hand, there are some groups of atoms attached to a chromophore which modifies the ability of that chromophore to absorb light. These are known as auxochromes. Modifiers like alkyl group that affect the absorption spectra of the dyes can also alter the colour of the dyes. Dyes interact with certain histologic or cytologic structures yielding a color change, known as metachromacy.[122] The metachromic behavior of dyes is used in biological staining.

Three methods for naming the dyes exist. The first method each dye has been issued a C.I. (Colour Index) by the Society of dyes and Colorists, U.K. and has been listed in a series of books known collectively as the Colour Index of "The Society of Dyers and Colorists", Bradfort, U.K., 1971-1982. The rules of the second method of naming are found in the Nonemclature of Organic Chemistry (International Union of Pure and Applied Chemistry, IUPAC, 1957). This second method of classification was implemented by the Chemical Abstracts Service (CAS) in 1965 by issuing a number called "CAS Registry Number" which was unique for each chemical substance. The third system of naming the dyes constitutes the commercial and trivial names for the dyes.

I.3. Dye-surfactant systems

I.3.1. Interactions in the Dye-surfactant systems

The interactions between the dyes and the surfactants both in the premicellar and micellar concentrations of the surfactants have been utilised for a myriad of applications. The combined electrostatic and hydrophobic interactions[21] relate to many biologically important processes. Interactions between oppositely charged dyes and surfactants help us to understand the combined electrostatic and hydrophobic interactions that govern such biological processes. However, the interaction between the oppositely charged dyes and surfactants is not a new aspect of study. In fact this has been the subject of several reports.

Several reports on the spectral changes of the dyes in presence of surfactant medium came into being. In the year 1934, it was Hartley, who for the first time reported that the presence of long chain salts had a very large effect on the color of acidimetric indicator dyes[122]. He correlated the color change of the dyes with the charge of micelles and stated the "Hartley's Sign Rule." According to the Hartley's Sign Rule, the indicator equilibrium of the indicator dye is hardly disturbed if the charge of the indicator (in acid as well its conjugate base form) is of the same sign as that of the micelle. Secondly, if the indicator is neutral in one of its form, the equilibrium is shifted to the acid side by anionic and to the alkaline side by the cationic micelle. Finally, if both forms of the indicator are

of opposite sign to that of the micelle, the direction of displacement depends on some particular factors.

There have been excellent reviews of the scattered literature on dye-surfactant interactions[12,123-126]. Surfactant assemblies, both in micellized and premicellized form are well known for tuning the electronic spectra and sometimes appearance of new bands are accompanied by the disapperance of the original bands of dyes and various chromophores[122-136]. The positions of the absorption bands of the dyes are sensitive to medium; therefore they can be used as reporter molecules for solvatochromatic micropolarity. Solvatochromism is observed in all types of dyes, viz., all classes of synthetic dyes as well as natural dyes. E.g., azo[126,134-160], acridinium[161-179], azine[180-187], cyanine[188-192], triphenylmethane[192-205], anthraquinone[206,207], phenazinium[187,208-214] sulphonapthalein[215-219] and curcumin[220-224].

I.3.2. Dye-surfactant interactions in submicellar surfactant solutions

If a surfactant is added to a solution of a dye at submicellar concentrations, specific molecular interactions takes place between the dye and the surfactant, which primarily occurs with surfactants that are oppositely charged to the dye[123]. Premicellar dye-surfactant aggregate formation and also formation of molecular complexes of having characteristic physicochemical features at concentrations far below CMC of some surfactants is a very well known phenomenon which are exhibited by ionic surfactants in presence of an submicellar ionic dye of opposite charge[211]. The specific changes in the absorption spectral bands of the dyes, characteristic of the dyes, associated with such interactions were attributed to self-assembly of dye-surfactant complex[185,226-228], formation of dye-surfactant salt[226-228], ion-pairs[214,217,218,229-231], dye-rich induced micelles[232-234], induced self-assembly of dyes[234-241], change in the microenvironment of the dye[242] and formation of charge transfer complexes[211,243]. The type of interactions depends mostly on the chemical structure and nature of both of the interacting compounds[123]. The scattered literature on dye-submicellar surfactant systems have been summarized below.

The absorption spectrum of pinacyanol chloride in presence of anionic surfactants was studied and the changes were attributed to the formation of micelle. Based on the spectral changes produced by solubilization of the dyes by the oppositely charged surfactants, Corrin and Harkins[244] developed a method for determination of the CMC of the surfactants. Dutta *et al.*[214] studied the interaction of phenazinium dyes with anionic surfactants in the submicellar concentration ranges and attributed the observed spectral

changes to an induced protonation of Safranin O dye in the dye-surfactant ionpairs. Hiskey and Downey[245] investigated the interaction between octadecyltrimethyl ammonium ions and methyl orange over a *p*H range form 0 to 12. They attributed the spectral changes to an association between the quaternary salt and the basic form methyl orange and reported that the association increased the ionization constant of methyl orange by 6.2 pK_a units. Hiskey and Downey suggested the formation of insoluble dye-surfactant salt at the concentrations of the surfactant far below CMC.

Mukherjee and Mysels[246] used spectrophotometric as well as electrical conductivity measurements of the pynacyanol-sodium dodecylsulphate system identified the presence of two types of dye-surfactant aggregates: (i) below the CMC, a dye-surfactant salt is formed a coarse stable slurry in the presence of more than a stoichiometric amount of surfactant, and (ii) dye-rich micelles, at below and around the CMC, where the water-insoluble dye-detergent salt was solubilized. Guha *et al.*[247] attributed the changes in the UV-visible spectra and the decrease in fluorescence intensity of thionine to be due the formation of a dye-surfactant complex at sodium dodecylsulphate concentrations below the CMC.

Reeves and Harkaway[140] also suggested a model for the metachromism of methyl orange (MO) in the presence of the cationic surfactants. They attributed the spectral change of MO with the submicellar cationic surfactants to formation of surfactant homomicelles. The band is shown to result from a dye-dye stacking interaction rather than from a change in dye geometry. They also added that the variation of the surfactant: dye (S:D) ratio gives distinct absorption bands characteristic of three disperse states: (1) a band similar to that of free dye at S:D ratios near the equivalence point is due to a microcrystalline suspension of the insoluble salt; (2) the dye aggregate band at larger S:D ratios characteristic of mixed micelles having a significant population of dye molecules occurring side-by-side with their molecular axes nearly parallel; and (3) a band similar to that of the dye dissolved in an organic medium at concentrations of the surfactant near the CMC.

Dye-surfactant mixtures are more surface active than CTAB alone at surfactant concentrations near the CMC. Changes in the spectra of Metal-Chrome Azurol S (CAS) in presence of surfactants have been carried out. The reports concluded the formation of submicellar ternary complexes of Be-Chrome Azurol S with cetylpyridinium chloride (CPC)[248] and CTAB[249]. Similar, conclusion was drawn by Callahan *et al.*[205] also. Goturk *et al.*[250] studied the interaction between cationic dye Safranin O with the anionic

surfactants and by the method of continuous variations, also called Job's Method determined the equilibrium molecular complex formation ratio as determined as 1:1. Rodriguez *et al.*[251] reported the formation of premicellar aggregates of the surfactants in presence of pyranene by photophysical methods. In 2013, Rahman *et al.*[252] attributed the spectral changes of malachite green to the binding of monomeric SDS with the carbocationic dye.

From surface tension study, Gohain *et al.*[212,217,218,253] reported the presence of two CMCs - the first CMC corresponding to the micellization of the dye-surfactant ionpairs and the second CMC corresponds to the normal CMC of the surfactant. They reported the deprotonation of some sulphonapthalein and triphenylmethane dyes in the dye-submicellar surfactant ionpair micelles. On the other hand they also reported that some cationic dyes can be further protonated in the presence of submicellar anionic surfactants in the ionpair premicelles formed by the dye-surfactant ionpairs. These ionpair form monolayers on the surface and have high surface tension reducing efficiency. Also, Shahir *et al.*[254] reported the formation of ionpairs of tartrazine with some cationic and Gemini surfactants which migrate to the surface to form ionpair rich monolayer thus exhibiting higher efficiency of the surfactants.

I.3.3. Interaction of dyes with micellized surfactants

Submicellar interactions between oppositely charged dyes and surfactants are electrostatic and hydrophobic induced[253]. However, at CMC or concentrations above CMC of the surfactants, the dyes are found encapsulated[222,255,256], solubilized[257-262], stabilized or partitioned via incorporation into surfactant micelles.[263-269] Generally, hypsochromic and bathochromic shift of the original dye bands are observed upon interaction of a dye with oppositely charged micelles[232,245,246,270-273]. Micelles can affect the pK_a of indicators[161,187,274-276].

The interaction of the various dyes with micelles of different charges has been attributed to various types of interaction mechanisms. Association with micelles[187,268,277], CT complex formation[243], localization at the hydrophobic interior and hydrophilic interface of the micelle[162] were supposed to be the nature of interaction. Moulik *et al.*[243] reported the primary requirement for acridine orange-surfactant (anionic) system was electrostatic interaction; the hydrophobic effect to be secondary and may be also co-operative. Molecular[245] and CT interactions[243], and shift in the pK_a of the dyes[236] were observed in azo dyes in presence of anionic micelles whereas solvatochromism[247],

electrostatic interactions[274] and association with micelles[275] were observed in presence of cationic micelles.

I.4. Changes of the dyes induced by premicellar solutions

I.4.1. Molecular changes in the dyes

Premicellar solutions of ionic surfactants induce specific interactions between the dye and the surfactant, which primarily occurs with surfactants that are oppositely charged to the dye. Complex formation[226-228], salt formation[226], dimerization, aggregation[234-241], etc do not lead to a change in the structure of the dye molecule. Though dimerization or aggregation in dyes is induced by premicellar surfactants, yet, there are other dyes which exist in various isomeric or tautomeric forms. In 1971, Quadrifoglio[135] reported *trans* to *cis* isomerism of azo dyes in presence of cationic polyelectrolyte and with colloidal electrolytes. Moreover, there are other dyes which exist in various tautomeric forms and exhibit specific spectral characteristics in presence of premicellar surfactants. There may be a possibility of tautomerism of these dyes to another form in presence of oppositely charges submicellar surfactants as reported by Ke *et al.*[276] followed by a spectral study by Boruah[277]. Gohain *et al.*[296] focussed on the protonation/deprotonation of the dyes after ionpair formation and reported changes in the spectra of some triphenylmethane, sulphonapthalein and phenazinium dyes. These indicate some acid-base equilibria in these systems. All these interactions occurred in presence of oppositely charged premicellar surfactants. Since, mere ionpair formation does not lead to spectral change, thus, there may be specific interactions in the ionpairs leading to a change in the molecular structure also of some of the dyes.

On the other hand, Time Dependent Density Functional Theory (TDDFT) calculations can be used in reproducing or predicting absorption wavelength of dyes/chromophores[278-293]. The electronic spectra of Pechmann dye family was modelled by TD-DFT and Time Dependent Hartree Fock (TD-HF) *ab-initio* calculations by Kantchev *et al.*[280] They concluded that TD-HF underestimated the UV-Visible absorption maximum, while, pure TD-DFT had led to an overestimation when compared with the experimentally found absorption maximum. Jacquimin *et al.*[281] studied the π-π^* transition of more than 100 organic dyes from the major classes of chromophores by TD-DFT method relying on a large number of basis sets and also solvent models. Bourass *et al.*[282] showed that TD-DFT with a hybrid exchange correlation functional in conjunction with polarized continuum model for solvation with 6-31+g(d,p) basis was reasonably capable

of predicting the excitation energy, the absorption and the emission spectra of five novel organic donor-π acceptor molecules used for dye sensitized solar cells and for organic solar cells. Also, some of the essential parameters related to the photoelectric chemical properties of some Ti (IV)-dye complexes were studied by DFT-TDDFT at the B3LYP/6-31+g (d,p) level of theory[283,284]. It is also noteworthy to mention that TD-DFT calculations can incorporate environmental effects also[289]. Homen-de-Mello *et al.*[290] studied the structure and electronic spectra of some cationic dye dimers. They reported the conformations for the dye dimers and also analysed the variation of interaction energy as a function of the monomer (dye) distance. They also reported the effects of solvation on the theoretical spectra of the cationic dye monomers[291] computed by ZINDO, TD-HF and TD-DFT calculations.

I.4.2. Acid-base equilibrium of the dyes in aqueous medium

The acid-base reactions are proton transfer reactions and the study occupies an indispensable area in chemistry[294,295]. When an acid-base indicator is dissolved in water, it undergoes the following equilibrium

$$A^z \overset{K_{a,w}}{\rightleftharpoons} B^{z-1} + H^+ \qquad \text{I.7.}$$

$$K_a = [B^{z-1}]\,[H^+] / [A^z] \qquad \text{I.8.}$$

where, A^z and B^{z-1} are the acid and the conjugate base, respectively and K_a is the acid dissociation constant. Due to the high values of K_a values, a logarithmic measure of the acid dissociation constant is used. The logarithmic constant, pK_a, which is equal to $-\log_{10} K_a$, is referred to as an acid dissociation constant:

$$pK_a = -\log K_a \qquad \text{I.9.}$$

The acid-base forms absorb light and the absorption by the protonated, A^z and that of the deprotonated, B^{z-1} species are different[296]. Depending on the *p*H of the medium, the above equilibrium (**Eq. I.8**) shifts to the left or right accompanied by the change of color. A characteristic property of an indicator dye is the pK_a, which is the *p*H of the aqueous

indicator solution at which the activity of the acid form of the indicator dye is equal to that of the conjugate base form.

I.5. Lacuna and rational

Dye-submicellar surfactant interactions occupies an important place in the domain of combined electrostatic and hydrophobic study, yet some of these systems have not been settled and demand further study to arrive at definite conclusions. There is an enormous literature on the anionic methyl orange in presence of oppositely charged cationic surfactant. The appearance of the UV-band of the dye in presence of submicellar cationic has been the subject of several reports. Despite several interpretations have been put forward for the appearance of the UV band of MO in submicellar solutions, the matter is not yet unequivocally settled and demand further study using various other tools.

There are reports on the H-aggregation of an acridinium dye, viz., acridine orange but the absorptions in the longer wavelength side of the visible spectrum of the dye has remained unnoticed or has been paid less attention. We anticipate the possibility of occurrence of a protonation of the dye, like that of phenazinium dyes, in the presence of the submicellar anionic surfactants in addition to the well known surfactant induced aggregation of the dye. The system of acridine orange-anionic surfactant system may be studied further to examine the possibility of the sub-micellar surfactant induced protonation.

Curcumin is a natural dye of versatile medicinal activity. Most of the previous studies on curcumin-surfactant systems have been carried out with concentrations of the surfactant above CMC, where the nature of the interactions is somewhat simple and better-known. Curcumin exists in various isomeric forms depending on the polarity of the solvent. Surfactants solutions provide a wide range of polarity. Ke *et al.*[276] reported the stabilization of its β-diketo tautomer by a submicellar cationic surfactant DTAB. The important antioxidant property of curcumin is attributed to its β-diketo tautomeric form. A spectral study of curcumin in presence of submicellar and micellar ionic surfactants in presence as well as in absence of polymers was also carried out by Boruah[277]. However, the detail nature of the interactions leading to the tautomerism including the effect of ionic strength on the mechanism of stabilization of the β-diketo tautomer of curcumin is of immense importance, due to the diverse medicinal importance of the dye, which needs systematic investigation.

Thus, an attempt will be made to understand the nature of forces operative in such systems explicitly by using UV-Vis absorption and fluorescence spectroscopy and surface tension measurements. Our experimental inferences will be supported by Density Functional Theory (DFT) combined with Time Dependent calculations. The computational calculations can give us the microscopic details of the structural stability and the excitation energies of the interaction products between the dye and a premicellar surfactant.

I.6. Aim and objectives

The aim of the present work was to understand the nature of forces operative in aqueous dye-surfactant systems explicitly by using both experimental and computational techniques. The experimental techniques include UV-Vis absorption and fluorescence spectroscopy and surface tension measurements and computational method, viz., Density Functional Theory (DFT) combined with Time Dependent calculations. The computational calculations can give us the microscopic details of the structural stability and the excitation energies of the ground state interaction products between the dye and a premicellar surfactant. A study of the changes in the molecular structure of two synthetic dyes - Methyl Orange (MO) and Acridine Orange (AO) of different charge types, and also the physicochemical behavior of a natural dye – Curcumin in different surfactants was proposed. We aim to have a detail study of curcumin in presence of surfactants of both the charge types in the submicellar medium in buffered with more focus on the mechanism of interaction. The different surfactants were chosen without a tremendous change in structures.

The work was planned as described below:

- Preparation of the aqueous solutions of dyes and surfactants and their mixtures.
- Recording of UV-Vis and fluorescence spectra of the aqueous dye solutions as a function of concentration of surfactants ranging from very low below the CMC of the surfactant to above the CMC.
- Recording of the surface tension values of the aqueous surfactant solutions in the full range in absence and in the presence of the dyes to evaluate the effectiveness and efficiencies of the surfactants in the dye-surfactants systems.
- Comparative study of the surface tension behavior of the dye-surfactant systems with the spectral behavior.

- Performance of DFT-TDDFT calculations on the structures of dyes and surfactants, and their combinations.

Thus, an attempt to understand the nature of forces operative in the above-mentioned systems explicitly by using the experimental methods, viz., UV-Vis absorption and fluorescence spectroscopy and surface tension

At the end of the chapter the author would like to acknowledge all the authors cited in this thesis. The author also apologizes for any lapse which might have occurred due to oversight or not cited or error in judgement.

MATERIALS AND METHODS

II.1. Materials and Methods

Three dyes which include two synthetic and one natural, nine surfactants of different charge types have been used in the present study. The detail description of the dyes and the surfactants used has been given below.

II.1.1. Dyes

Methyl Orange (MO): MO (Product No. M0200), IUPAC name: 4-((4-dimethyl amino) phenyl)-azo) benzenesulfonic acid, FW 327.24g/mol, (mp 300°C), of AR grade was obtained from Rankem, New Delhi, India. The dye was recrystallized from water and dried before use. Transition interval: *p*H 3.1 (red) to 4.4 (yellow). Detailed description of the dye is given in **Table II.1.** Structural formula is shown in **Fig.II.1**.

Acridine Orange (AO): AO (Product No. 61841500251730), IUPAC name: *N,N,N',N'*-Tetramethylacridine-3,6-diamine, FW 301.81 g/mol, (mp 300°C), of AR grade was obtained from Merck, Mumbai, India. The dye was recrystallised from water and dried before use. Transition interval: *p*H 6.80 (yellow) to 8.20 (red). Detailed description of the dye is given in **Table II.1.** Structural formula is shown in **Fig.II.1**.

Curcumin: (Product No. SL09143, CAS No. 458-37-7), IUPAC name: (1E,6E)-1,7-bis(4-hydroxy-3-methoxyphenyl)-1,6-heptadiene-3,5-dione, FW 368.39 g/mol, (mp 175°C), of LR grade was obtained from Sigma Aldrich, USA. The dye was used as such. Detailed description of the dye is given in **Table II.1.** Structural formula is shown in **Fig.II.1.**

Spectrophotometry and melting point determination methods were used to check the purity of all the dyes after recrystallization.

Table II.1. Detail description of the dyes used in the study.

Sl. No.	Name	Charge type	Class/ Compound	CI. No.	Abbreviation
1	Methyl Orange	Anionic	Azo	13025	MO
2	Acridine Orange	Cationic	Acridinium	46005	AO
3	Curcumin	Anionic	Polyphenol	75300	Curcumin

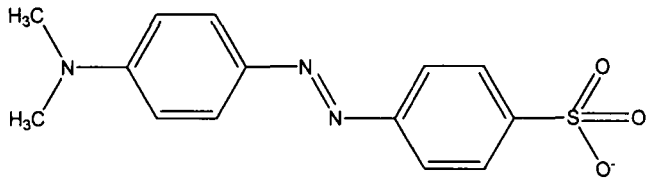

MO (MO^- form)

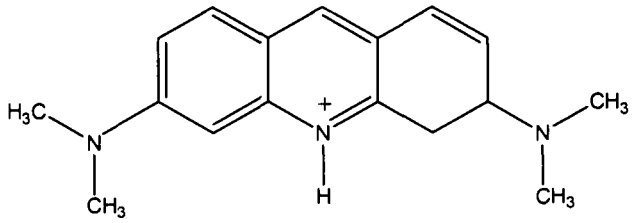

AO (AO^+ form)

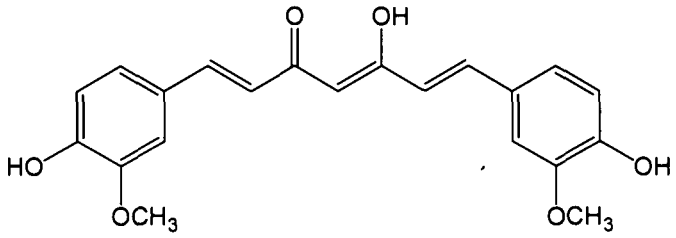

Curcumin (ketoenol form)

Fig.II.1. Structural formulae of the dyes studied.

II.1.2. Surfactants and salts used

SDS: SDS (Batch No. T8261190) FW 288.38 g/mol of electrophoresis grade was obtained from Sisco Research Laboratory, Mumbai, India. To remove the dodecanol impurities, usually present in SDS as a result of hydrolysis, the surfactant was stirred overnight in ether. The samples were then recrystallised twice from ethanol-water mixture and dried thoroughly. The CMC of the surfactant was determined by using a platinum ring with a Do Nouy tensiometer model 276 of JENCON, Kolkata. The CMC was found to be 8.1×10^{-3} mol dm^{-3} in good agreement with the literature value[1]. Structural formula is shown in **Fig. II.2**. Detail description of the surfactant is given in **Table II.2**.

SDSN: SDSN (Batch No. 10,643-7), FW 272.38 g/mol, was obtained from Aldrich Chemical Company, USA. The CMC of the aqueous surfactant solution was determined at 298 K and was found to be 1.25×10^{-2} mol dm^{-3} in good agreement with the literature

value[1] and was used as such. Structural formula is shown in **Fig.II.2**. Detail description of the surfactant is given in **Table II.2**.

SDBS: SDBS (Lot No. 02728JI, Product No. 28,995-7) FW 348.48 g/mol, was obtained from Aldrich Chemical Company, USA. The CMC of the aqueous surfactant solution was measured at 298 K and was found to be 1.25×10^{-2} mol dm^{-3} in good agreement with the literature value[1] and was used as such. Structural formula is shown in **Fig.II.2**. Detail description of the surfactant is given in **Table II.2**.

CTAB: CTAB (Batch No. C01Y-0301-2202-13, Product No.37665), FW 364.45 g/mol, of LR grade was obtained from S.D. Fine Chemicals Limited, Mumbai, India. The CTAB was recrystallized from acetone and dried before use. The measured CMC value 8.90×10^{-4} mol dm^{-3} in pure water at 298 K was in good agreement with the literature value[1]. Structural formula is shown in **Fig.II.2**. Detail description of the surfactant is given in **Table II.2**.

TTAB: TTAB (Lot No. FA005752, Product No. 86,042-5, CAS 1119-97-7), FW 336.41 g/mol, was obtained from Sigma, USA. The measured CMC value (4.0×10^{-3} mol dm^{-3}) of the aqueous surfactant solution was at 298 K and found to be in good agreement with the literature value[1]. Structural formula is shown in **Fig.II.2**. Detail description of the surfactant is given in **Table II.2**.

DTAB: DTAB (Lot No. 19805, Product No. 26876-3, CAS 1119-94-4), FW 308.35 g/mol, was obtained from Sigma, USA. The measured CMC value (1.80×10^{-2} mol dm^{-3}) of the surfactant in pure water at 298 K was found in good agreement with the literature value[1]. Structural formula is shown in **Fig. II.2**. Detail description of the surfactant is given in **Table II.2**.

CPC: CPC (Batch No. 02050, Product No. 027921), MW 358.01 g/mol, was obtained from Central Drug House (CDH) LTD, New Delhi, India. The CPC was recrystallized from acetone and dried before use. The measured CMC value (9.2×10^{-4} mol dm^{-3}) of the surfactant in pure water at 298 K was found in good agreement with the literature value. Structural formula is shown in **Fig.II.2**. Detail description of the surfactant is given in **Table II.2**.

CPB: CPB (Art. 818188), MW 402.46 g/mol, was obtained from Merck, Mumbai, India. The CPC was recrystallized from acetone and dried before use. The measured CMC value ($9.0x10^{-4}$ mol dm^{-3}) of the surfactant in pure water at 298 K was found in good agreement with the literature value. Structural formula is shown in **Fig.II.2**. Detail description of the surfactant is given in **Table II.2**.

Triton X-100: Triton X-100 (Lot No. 10142986, Product No. 9002-93-1, CAS), was obtained from Alfa Aesar, Lancester). The CMC was not determined and was used as such. Structural formula is shown in **Fig.II.2.** Detail description of the surfactant is given in **Table II.2**.

TBAB: Tetrabutylammonium bromide, TBAB (Lot No. 4110132, Product No. 072009), was obtained from Spectrochem, Pvt. Ltd., India. Structural formula is shown in **Fig.II.2.**

KBr: Potassium bromide, KBr (Product No. 051623), was obtained from Spectrochem, Pvt. Ltd., Bombay, India.

Na_2SO_4: Sodium sulphate anhydrous, (CAS No. 7757-82-6), was obtained from Merck, *Mumbai, India*

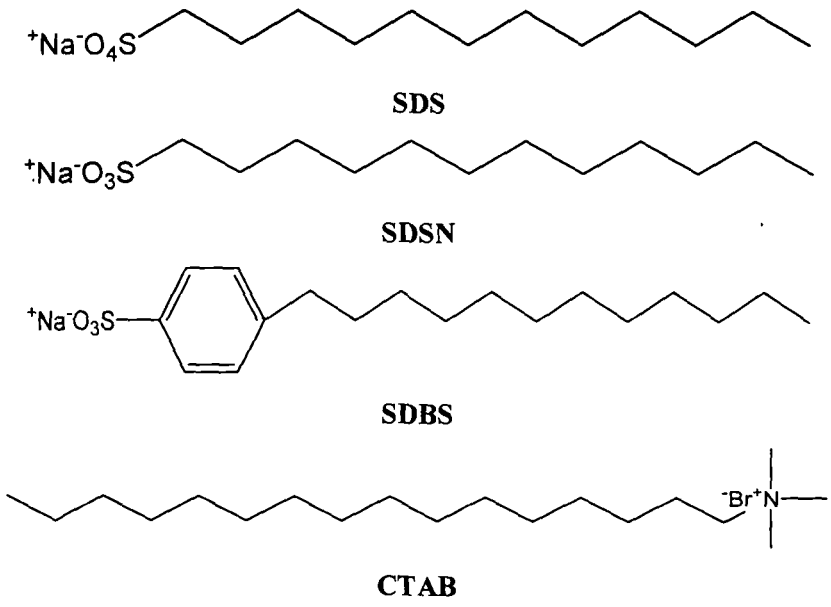

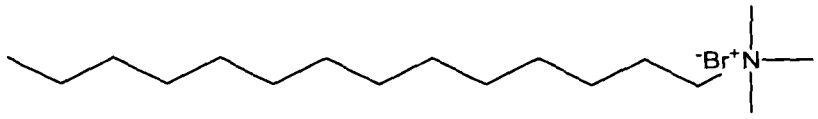

TTAB

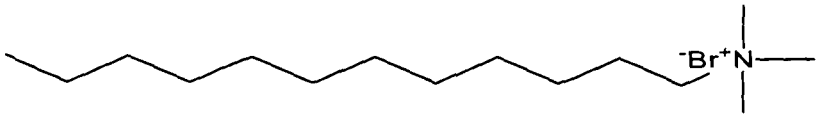

DTAB

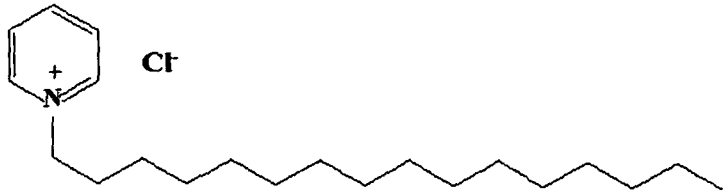

CPC

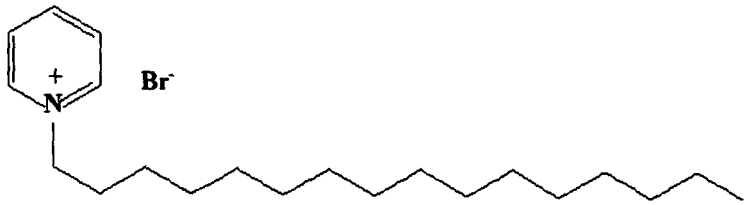

CPB

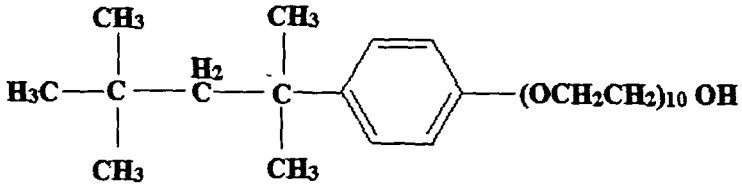

Triton X-100

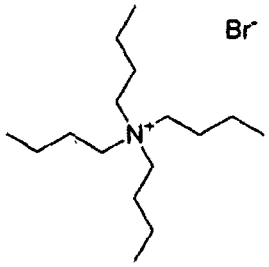

TBAB (salt)

Fig.II.2. Structural formulae of the surfactants studied.

Table II.2. Detail description of the surfactant used in the study.

S.No.	Name	Charge type	Abbreviation
1	Sodium dodecylsulphate	Anionic	SDS
2	Sodium dodecylbenzenesulphonate	Anionic	SDBS
3	Sodium dodecylsulphonate	Anionic	SDSN
4	Hexadecyltrimethylammonium bromide	Cationic	CTAB
5	Tetradecyltrimethylammonium bromide	Cationic	TTAB
6	Dodecyltrimethylammonium bromide	Cationic	DTAB
7	Hexadecyltrimethylpyridinium chloride	Cationic	CPC
8	Hexadecyltrimethylpyridinium bromide	Cationic	CPB
9	Triton X-100	Nonionic	TX-100

II.1.3. Water

Double distilled water of conductivity ~0.1μS, prepared by adding $KMnO_4$ in the first distillation was used in the experiments and for preparing the stock solutions.

II.1.4. Buffer Components

Perrin's low ionic strength (*I= 0.01*) buffer systems were used throughout the study[297]. The buffer components, *viz.*, disodium hydrogen phosphate (Na_2HPO_4), glycine ($H_2NCH_2CO_2H$), potassium dihydrogen phosphate (KH_2PO_4), acetic acid, (CH_3COOH), sodium acetate (CH_3COONa), potassium hydroxide (KOH), sodium metaborate ($Na_2B_4O_7.10\ H_2O$), boric acid (H_3BO_3), sodium chloride (NaCl), hydrochloride acid (HCl), perchloric acid ($HClO_4$), sodium hydroxide (NaOH) etc., were all of AR grade obtained from Merck, Mumbai, India and used as such.

II.2. Experimental

II.2.1. Instrumental analysis

The UV-visible absorption spectra were recorded on Shimadzu U-2550 UV-visible spectrophotometer with a matched pair of cells of 1 cm path length fitted in a thermostated cell holder. Temperature was maintained within ±1K using a circulating cryostat bath connected to the spectrophotometer during the measurements. The sample cell was pre-rinsed with the respective solutions to avoid any loss of dye by adsorption in the cuvette.

Fluorescence spectra were recorded on a Perkin Elmer LS 55 Fluorescence Spectrophotometer with the excitation and emission slit widths set at 8 nm. The temperatures were maintained within ±1 K using a circulating cryostat bath attached to the spectrometer during the measurements.

The surface tensions of the experimental solutions were determined by using a platinum ring with a Do Nouy tensiometer model 276 of JENCON, Kolkata.

The *p*Hs were determined by using an Orion Five Star multiparameter kit ion meter (USA), μ-*p*H systems. The *p*H-meter was calibrated properly with care before the measurements.

All experiments were repeated at least thrice to check reproducibility.

II.2.2. Preparations of solutions

II.2.2.1. Preparation buffer solutions

Double distilled water was used for preparing the buffer solutions. Doubly concentrated stock solutions of buffer components were prepared so that after mixing with the dye and surfactant solutions the resulting experimental solution contains the desired concentrations of the components required for the desired *p*H and the desired ionic strength. The buffer solutions were prepared by following the Perrin's table of buffer systems[297]. The *p*H of the aqueous buffer solutions was found to be unchanged on the addition of the surfactants below their CMC.

II.2.2.2. Preparation of stock solutions of the dyes

As curcumin is poorly soluble in water, for the preparation of 3.8×10^{-4} mol dm^{-3} curcumin solution, 2:3 ration of methanol : water was used. In the final experimental solution the concentration of methanol is 3.0% and that of curcumin is 2.5×10^{-5} mol dm^{-3}.

Similarly, 1.5×10^{-4} mol dm^{-3} stock solutions of Acridine Orange (AO) and Methyl Orange (MO) were prepared by dissolving the required quantity of the dyes in water. In the final experimental solution, the concentration of AO and MO was 1.0×10^{-5} mol dm^{-3}.

II.2.2.3. Preparation of stock solutions of the surfactants

To cover a wide range of surfactant concentrations in the experimental solutions, stock solutions of different surfactant concentrations were prepared in double distilled water.

II.2.2.4. Preparation of experimental solutions

Double distilled was used as solvent for preparing all solutions. Experimental solutions with fixed dye concentration in a wide range of surfactant concentrations have been prepared by volume as shown in a representative table, **Table II.3**. Fixed concentrations of the dyes were chosen in the order to have absorbance in a suitable range.

Table II.3. Preparation of experimental solutions for the determination of binding constant for an aqueous dye-surfactant system at a fixed *p*H.

Sl. No.	Buffer solution (ml) (doubly concentrated)	Aqueous surfactant* (ml)	Water (ml)	Aqueous dye (ml)	Total solution volume (ml)	[Surfactant] in final solution (mol dm^{-3})
1	7.5	0.00	6.5	1	15	0.00
2	7.5	0.15 (0.0001)	6.35	1	15	$1.0x10^{-6}$
3	7.5	0.75 (0.0001)	5.75	1	15	$5.0x10^{-6}$
4	7.5	1.5 (0.0001)	5.0	1	15	$1.0x10^{-5}$
2	7.5	3.0 (0.0001)	3.5	1	15	$2.0x10^{-5}$
3	7.5	6.0 (0.0001)	0.5	1	15	$4.0x10^{-5}$
4	7.5	0.9 (0.001)	5.6	1	15	$6.0x10^{-5}$
5	7.5	1.2 (0.001)	5.3	1	15	$8.0x10^{-5}$
6	7.5	1.5 (0.001)	5.0	1	15	$1.0x10^{-4}$
7	7.5	3.0 (0.001)	3.5	1	15	$2.0x10^{-4}$
8	7.5	6.0 (0.01)	0.5	1	15	$4.0x10^{-4}$
9	7.5	0.9 (0.01)	5.6	1	15	$6.0x10^{-4}$
10	7.5	1.2 (0.01)	5.3	1	15	$8.0x10^{-4}$
11	7.5	1.5 (0.01)	5.0	1	15	$1.0x10^{-3}$
12	7.5	3.0 (0.01)	3.5	1	15	$2.0x10^{-3}$
13	7.5	6.0 (0.10)	0.5	1	15	$4.0x10^{-3}$
14	7.5	0.9 (0.10)	5.6	1	15	$6.0x10^{-3}$
15	7.5	1.2 (0.10)	5.3	1	15	$8.0x10^{-3}$
16	7.5	1.5 (0.10)	5.0	1	15	$1.0x10^{-2}$
17	7.5	3.0 (0.10)	3.5	1	15	$1.2x10^{-2}$
18	7.5	2.1 (0.10)	0.5	1	15	$1.4x10^{-2}$

*Values within parenthesis indicate stock surfactant concentration.

II.2.3. Methodology

Freshly prepared stock surfactant solutions were used to avoid hydrolysis on standing. The experimental solutions were prepared by mixing the components (surfactant, water, dye, buffer) as shown in the **Table II.3**. However, the dye was added just before recording the data in the spectrophotometric study as well in case of the surface tension study to avoid any error that would arise due to degradation of the dye. In case of solutions without any buffer, the volume was made up with water.

II.3. Computational

In order to understand the details of the structural stability and the changes in spectral characteristics, theoretical calculations were also done. The details of the software and the method used are briefed below.

II.3.1. Software: Gaussian 09[298]

II.3.2. Method: *ab initio* Density Functional Theory (DFT) combined with Time Dependent-Density Functional Theory (TD-DFT)[278,279].

II.3.3. Functional: B3LYP[299] (Becke exchange with Lee, Yang and Parr correlation) stands for Becke, 3-parameter, Lee-Yang-Parr. B3LYP combines Becke's 1988 exchange functional with the correlation functional by Lee, Yang, and Parr. Along with the component exchange and correlation functionals, three parameters define the hybrid functional, specifying how much of the exact exchange is mixed in. Becke-3-LYP uses the following mixing scheme involving three mixing parameters:

$E_{xc} = 0.2*E_x(HF) + 0.8*E_x(LSDA) + 0.72*DE_x(B88) + 0.81*E_c(LYP) + 0.19*E_c(VWN)$

II.3.4. Basis set: 6-31+g(d,p) basis set for all the atoms.

Significance of 6-31: The inner shells of the atoms are described using a linear combination of 6 Gaussians, while the valence shell are described using two sets of basis functions, one expanded in a set of 3 Gaussians, and the other in a set of 1 Gaussian.

Significance of + (d,p): An atom in a molecule experiences a nonuniform electric field arising from its nonspherical environment. By adding polarization functions to a basis set for the atom we directly accommodate this effect. In case of first row atoms, d-type functions, which are not occupied in first row atoms, play the role of polarization functions for the atoms Li to F. One denotes this improvement with a star (*) or a (d) when only the heavy atoms are corrected with *d-type* functions, or with two stars (**) (or with a (d,p)) when the hydrogen (or helium) atom is corrected as well with *p-type* functions. The '+' a diffuse function, is a multiple polarization functions.

In our case, we have atoms *viz.*, hydrogen, oxygen, sulphur, nitrogen etc.

II.2.5. Solvent effects: The solvent effects were considered by employing the self-consistent reaction field (SCRF) method with Polarized Continuum Model[300] (PCM). The PCM is a popular method to take into account the solvent effects. The method considers the solvent as a polarisable continuum and does not consider each solvent molecule as a separate molecule which makes the method computationally less costly. This implicit model has the great advantage that the dielectric continuum response can be formulated to represent the response of a statistically averaged solvent, so that meaningful results can be obtained from a single calculation.

II.2.6. Methodology: The free dye molecules as well their complexes with the surfactants were optimized. In order to reduce the computational cost, the surfactants have been modelled by replacing the long tail non-conjugated alkyl chains with ethyl moiety which would not change the low energy properties significantly at least in the submicellar concentration range. The vibrational harmonic frequency calculations were also performed to confirm the local energy minimum structures for all the molecules. The optimized structures were taken for the Time dependent Density Functional Theory calculations (TD-DFT).

RESULTS AND DISCUSSION

III. Results and Discussion

In this chapter the experimental results, their analysis and the interpretation have been discussed. For systematic organization, this chapter has been divided into three major sections, each dealing with a particular molecular interaction involving one of the three dyes, which are described below.

III.1. *Cis-trans* Isomerism of Methyl Orange in Cationic Premicelles*

Aqueous Methyl Orange (MO) shows a band in the visible region with λ_{max} at 464 nm. In presence of submicellar cationic surfactants, the intensity of the 464 nm band decreases and the dye shows a new band with λ_{max} in the UV region of 368 nm to 378 nm, depending on the surfactant, which has been the subject of several reports[135,137,141-145,149-151].

Quadrifoglio *et al.*[135] attributed the appearance of the UV band of MO in presence of polyelectrolytes and colloidal electrolyte to a conformational change of the dye from the *trans* to the *cis* form. Reeves and Harkaway attributed the UV band of MO observed in aqueous solutions of cationic polymers to the formation of higher aggregates of MO[137]. Vijlder suggested that a change in the chromophore environment of MO caused by replacement of hydrating water dipoles by metal cation was responsible for the *cis-trans* isomerism of the dye[141]. On the basis of circular dichroism experiments, Dawber *et al.* ruled out the formation of MO dimers as a reason for the appearance of the UV-band[142]. Karukstis *et al.*[300] assumed that an increased hydrophobic interaction of the azo group of MO with the alkyl chains of the alkyltrimethylammonium bromide surfactants led to the appearance of the UV band. Alehyen *et al.*[143] proposed that mono and bis-quaternary ammonium surfactants bind with MO in aqueous submicellar solutions to cause the UV band. Dutta *et al.*[151] proposed the formation of 'water structure enforced ionpairs' to explain the appearance of the UV band. Buwalda *et al.* assumed the spectral changes to be due to aggregation of the surfactant-dye ionpair[149,150]. Rafati *et al.*[144] and Simon *et al.*[145] have reported the ionpair formation of MO with cationic surfactant. However, mere ionpair formation does not lead to such spectral changes[146]. Thus, despite several interpretations have been put forward for the appearance of the UV- band of MO in submicellar solutions, the matter is not yet unequivocally settled and demand further study using various other tools.

This work has been published in **Spectrochim. Acta A 126 (2014) 270-279.*

III.1.1. Electronic absorption of MO in submicellar cationic surfactant solutions

Although the changes in absorption behavior of aqueous MO caused by cationic surfactants are well-studied, the absorption spectra of MO in the presence of CTAB of varying concentrations are presented in **Fig.III.1** for clarity and completeness. The absorption band at 464 nm of MO initially decreases gradually on addition of CTAB in the submicellar concentrations of the surfactant up to 8.0×10^{-4} mol dm^{-3} with a simultaneous appearance of a band in the UV region with absorption maximum at 368 nm[135,137,141-145,149-151]. On further addition of the surfactant, the UV band gradually disappears with simultaneous appearance of a visible band at 430 nm which remains unaffected at above the CMC of the surfactant. The band at 430 nm is due to the stabilization of MO in the non polar core of CTAB micelles[151,301].

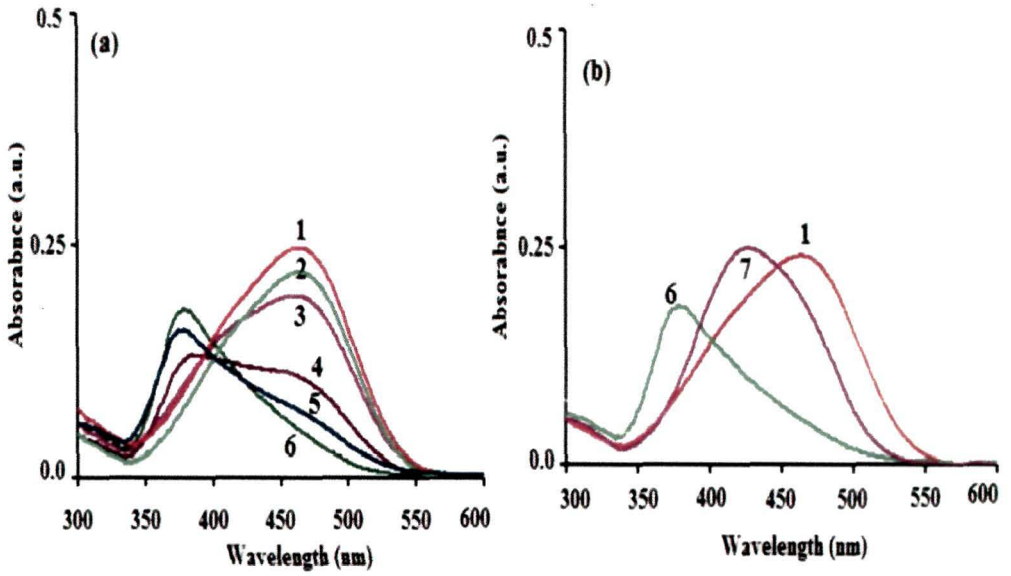

Fig.III.1. The UV-Vis spectra of 1.0×10^{-5} mol dm^{-3} aqueous MO in presence of varying CTAB concentrations. [CTAB] / (mmol dm^{-3}) = (1) 0.00 (2) 0.005 (3) 0.01 (4) 0.05 (5) 0.10 (6) 0.50 (7) 0.80.

II.1.2. Fluorescence spectra of MO

There is no report on fluorescence of MO in water or in other systems such as submicellar cationic surfactants except that of MO bound to nanoparticles[147,148]. We have observed that MO shows fluorescence bands at 361 and 575 nm in aqueous solutions. The fluorescence intensity (FI) of the 575 nm band significantly increases in the presence of submicellar cationic surfactants. The coincidence of the observed increase in the FI and

the appearance of the UV band in the presence of submicellar cationic surfactants is interesting since fluorescence behavior depends on the polarity of the microenvironment of a chromophore[302]. A systematic study of the fluorescence behavior may throw light on the interactions involving the ionpairs leading to UV band and hence on the factors stabilizing the *cis* isomer of MO. Therefore, it was thought worthwhile to investigate the detail steady state fluorescence behavior of aqueous MO in absence and in the presence of cationic surfactants of varying chain length as well as head group.

III.1.3. Corrections for shading and inner filtering of fluorescence intensity

'Shading' and 'inner filter effects' [303,304] may arise due to addition of a foreign substance (in our case, the surfactants) to the probe (in our case, aqueous MO solutions) and lead to an additional absorbance of the excitation light or to an absorbance of the emitted fluorescence, of the probe, by the foreign substance. However, the alkyltrimethylammonium bromide surfactants (CTAB, TTAB and DTAB) do not absorb at all in the entire wavelength range of 200 nm to 800 nm (**Fig.III.2**). We have excited MO at 270 nm for our studies and therefore the excitation light, in the presence of the alkyltrimethylammonium bromide surfactants, has been used for the excitation of MO alone and is observed that the emitted light of MO is intact. On the other hand, the alkylpyridinium bromide surfactants (CPC and CPB) absorb in the range 231 nm to 272 nm with a maximum absorbance at 257 nm. They have very weak absorptions at the excitation wavelength, 270 nm and hence there may be a small shading effect by these surfactants. However, since the surfactants do not absorb in the wavelength range of the emission (300 nm to 800 nm), there is no inner filter affect due to the surfactants. So, the FIs in case of CPC and CPB have been corrected by considering the absorbance of CPC and CPB at the excitation wavelength by using the following equation suggested by Weert[304] at each surfactant concentration:

$$F_{corr} = F_{obs} * 10^{\frac{A_{exc} + A_{em}}{2}} \qquad \text{III.1.}$$

where, F_{corr} is the corrected fluorescence value, F_{obs} the measured fluorescence value, A_{exc} the absorption value at the excitation wavelength, and A_{em} the absorption value at the emission wavelength.

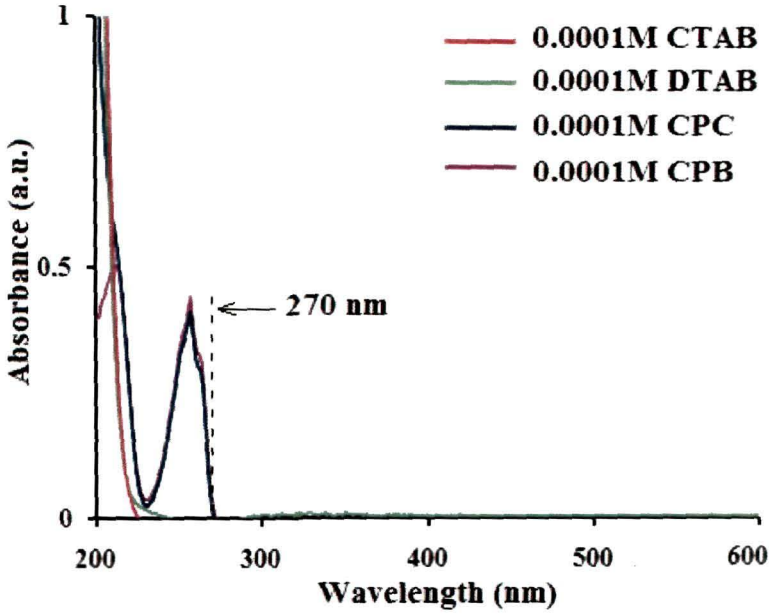

Fig.III.2. Absorbance of the alkyltrimethylammonium bromide (CTAB and DTAB) and alkylpyridinium surfactants (CPC and CPB) in the wavelength region 200 nm to 600 nm.

III.1.4. Steady state fluorescence spectra of Aqueous MO

To see the emission properties of aqueous MO, we excited the molecule at five wavelengths *viz.*, 250 nm, 270 nm, 290 nm, 368 nm and 464 nm. The steady state fluorescence spectra of aqueous MO at the different excitation wavelengths are shown in **Fig.III.3.** Two peaks were observed at 361 nm and 575 nm in the emission spectra of MO when excited at wavelengths $\leq$ 290 nm whereas only one peak at 575 nm was observed on excitation at wavelengths $\geq$ 368 nm. With the change in the excitation wavelength from 250 nm to 464 nm, the positions of both the 361 nm band and the 575 nm band in the emission spectra remained unchanged, which suggests that these bands are true emission bands and not due to any second order diffraction of the excitation light[305,306]. It is reported that usually, azobenzenes show an intense emission band around 428 nm corresponding to a π-π^* transition and a weak emission band in the higher wavelength side corresponding to a symmetry forbidden n-π^* transition[307-309]. A rotation around the NN double bond is also induced by the π-π^* excitation[309]. However, it has been observed with MO that the excitation of MO with higher wavelengths lowered the intensity of the 575 nm band but there was no definite trend in intensity change in the 361 nm band on changing the excitation wavelength.

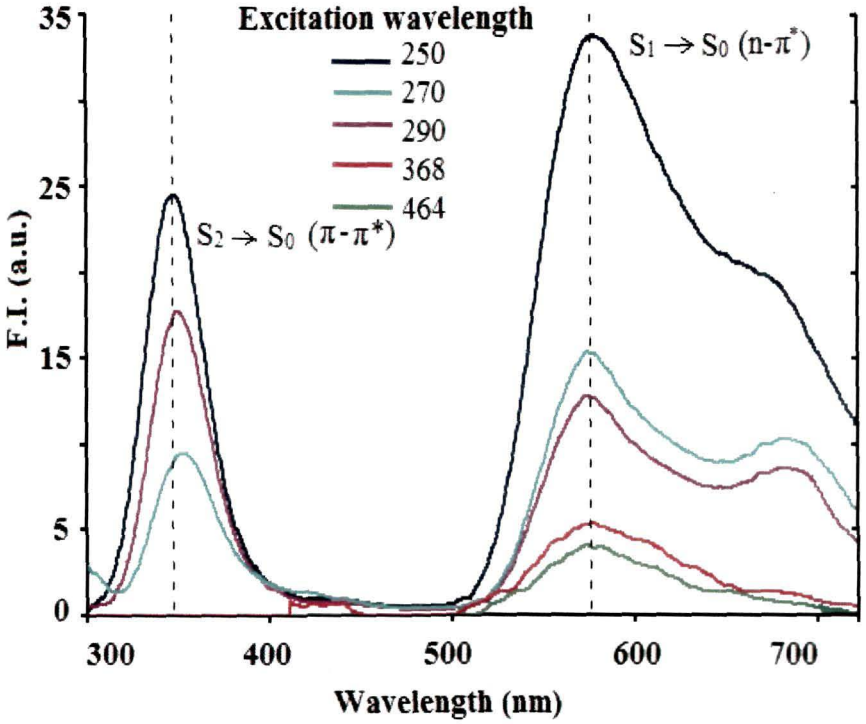

Fig.III.3. Fluorescence spectra of aqueous MO (1.0×10^{-5} mol dm^{-3}) at different excitation wavelengths.

A fluorescence excitation in the azo π-π^* transition leads to an overall *trans* to *cis* conversion, while excitation in the n-π^* transition leads to an overall *cis* to *trans* conversion[307].

III.1.5. Fluorescence of MO in presence of premicellar cationic surfactants

Excitation of aqueous MO in presence of submicellar CTAB (3.0×10^{-5} mol dm^{-3}) resulted in the emission of a greenish yellow light in the UV-chamber but no such emission was observed in the absence of CTAB (**Fig.III.4**). Green-yellow light falls in the wavelength region ≈ 550-570 nm. This observation indicates that the 575 nm band observed in presence of submicellar CTAB is an emission band of MO.

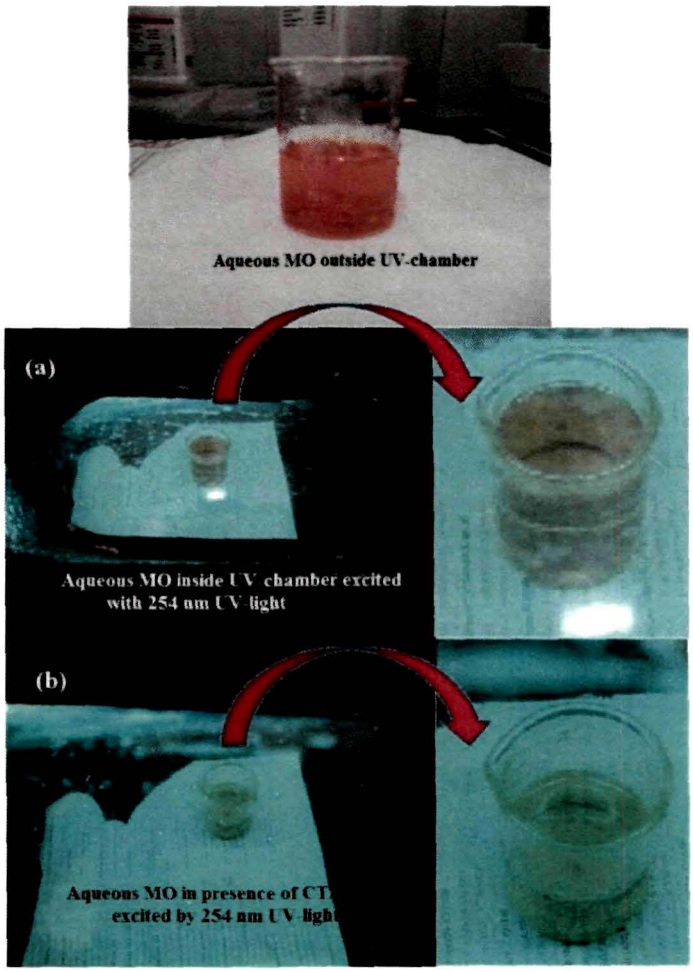

Fig.III.4. The emission of green-yellow light from aqueous solutions of MO in (a) absence of CTAB, and (b) presence of 3.0×10^{-5} mol dm^{-3} CTAB, as observed in a UV-chamber.

In order to examine the behavior of both of the fluorescence bands of MO in the presence of CTAB, we excited aqueous MO at 270 nm in the presence of varying CTAB concentrations (**Fig.III.5**). In absence of CTAB (**spectra 1 of Fig.III.5.(a)**), an intense emission band of MO is peaked at 361 nm whereas a weak band is peaked at 575 nm which may be assigned to the $S_2 \rightarrow S_0$ (π-π^*) and the $S_1 \rightarrow S_0$ (n-π^*) transitions, respectively like the usual azobenzenes[307,308].

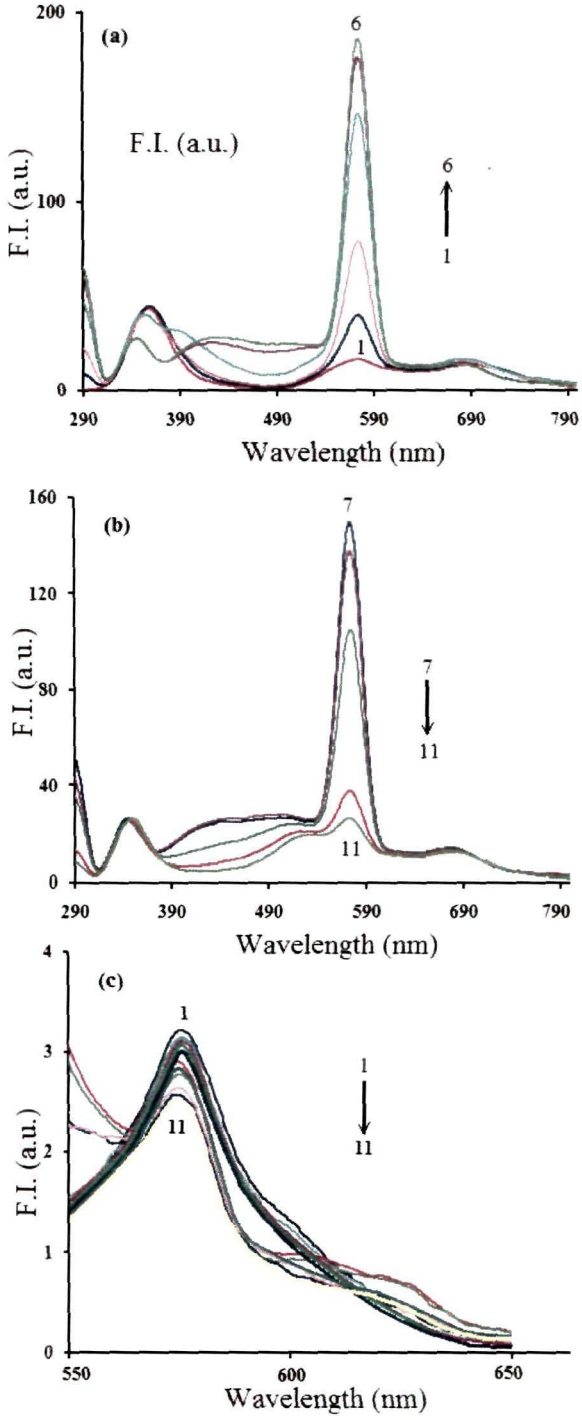

Fig.III.5. Fluorescence spectra of $1.0x10^{-5}$ mol dm^{-3} MO in presence of varying CTAB concentrations. [CTAB] / (mmol dm^{-3}) = **(a):** (1) 0.00, (2) 0.03, (3) 0.06, (4) 0.09, (5) 0.30 and (6) 0.60; **(b):** (7) 0.80, (8) 0.90, (9) 1.00 and (10) 1.50; with 270 nm as the excitation wavelength. **(c)** Fluorescence spectra of $1.0x10^{-5}$ mol dm^{-3} MO when excited at 464 nm of [CTAB] = 0.00 to 1.50 mmol dm^{-3}.

On increasing the concentration of CTAB above $3.0x10^{-5}$ mol dm^{-3}, within the submicellar concentration range, we have observed that the intensity of the band at 361 nm does not show any significant change whereas there is about 20 times increase in the intensity of the band at 575 nm. In presence of submicellar CTAB, the major steady-state fluorescence $S_1 \rightarrow S_0$ (n-π^*) transition is at 575 nm which is energetically lower than that of the $S_2 \rightarrow S_0$ (π-π^*) transition. The increase in the intensity values of the $S_1 \rightarrow S_0$ (n-π^*) transition in presence of submicellar CTAB compared to that of $S_2 \rightarrow S_0$ (π-π^*) transition indicate that the major component of the steady-state fluorescence for MO is the S_1 fluorescence and not the S_2 fluorescence unlike that of the usual azobenzenes[309]. The symmetry forbidden $S_1 \rightarrow S_0$ (n-π^*) transition of azobenzenes is allowed in the case of MO due to a distortion of the molecule along the coordinates, *viz.*, a properly symmetrized twistings around the CN bonds[310]. In the present case, the hydrophobic interaction between the surfactant tail of CTAB and the hydrophobic phenyl groups of MO may facilitate the twisting of MO and stabilizes it in the *cis* form, as indicated by the increase in the intensity of the $S_1 \rightarrow S_0$ (n-π^*) transition at 575 nm in presence of submicellar CTAB (**Fig.III.5**). Thus, the decrease in the π-π^* band and increase in the n-π^* band of MO in the presence of submicellar CTAB indicates that the dominant form here is the *cis*-isomer[307].

At [CTAB] concentration of $8.1x10^{-4}$ mol dm^{-3}, MO reverts back to its *trans* form in the CTAB micelles. The CMC of CTAB is $9.10x10^{-4}$ mol dm^{-3} which may be lowered by the presence of dyes to $\approx 6.0x10^{-5}$ mol dm^{-3} (ref.218) due to formation of CTAB-dye premicellar aggregates. So, the reversal of MO to the *trans* form at $8.1x10^{-4}$ mol dm^{-3} CTAB may correspond to the disappearance of the premicellar CTAB-MO aggregates, where the *cis* form is stabilized, into the pure micelles of CTAB, where the *trans* form of MO is stabilized.

The fluorescence response of MO in presence of the cationic surfactants also show a low intensity peak at $\approx$ 690 nm and hump at around 420 nm. This hump around 420 nm shifts to a position at 510 nm on changing the concentration of the surfactant. We may assign the peak at 690 nm, which neither shifts its position nor changes its intensity significantly on addition of CTAB, to be due to other transitions such as the $S_2 \rightarrow S_1$. It can be noted that when MO was excited at 464 nm, an increase in the concentration of CTAB decreases the intensity of the main emission band of MO at 575 nm (**Fig.III.5(c) and Fig.III.6**) with a slight increase in the intensity around 625 nm (**Fig.III.5(c)**).

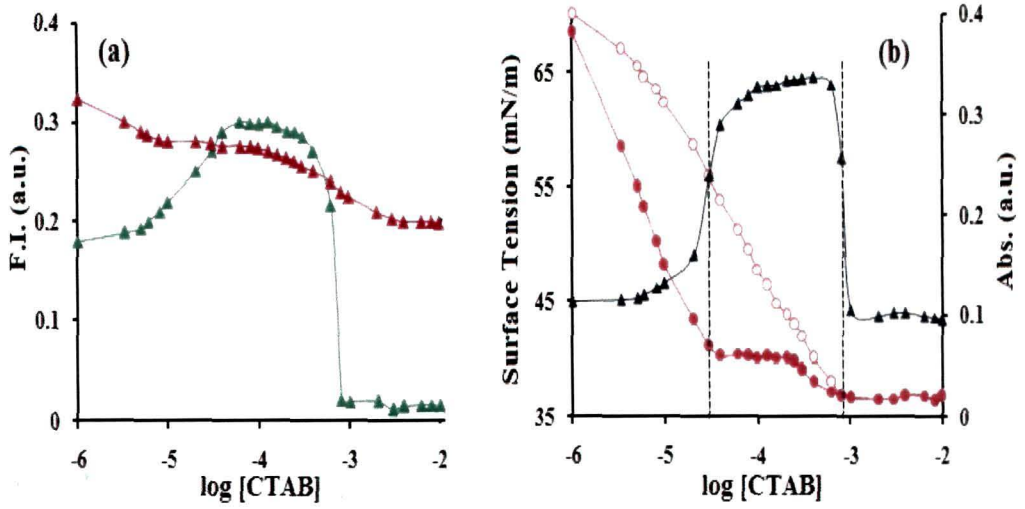

Fig.III.6. Plot of FI, absorbance and γ of MO ($1.0x10^{-5}$ mol dm^{-3}), as a function of concentration of CTAB at 298 (±1) K. **(a)** FI at 575 nm ($S_1 \rightarrow S_0$ (n-π*)) excited at 270 nm (▲), FI at 575 nm ($S_1 \rightarrow S_0$ (n-π*)) excited at 464 nm (▲), and **(b)** absorbances at 368 nm (▲), γ in the presence (●), and in absence ( ) of MO.

III.1.6. Surface tension behavior

The variations in the surface tension, γ, of the aqueous alkyltrimethylammonium bromide surfactant as well of the alkylpyridinium surfactants in absence and in presence of $1.0x10^{-5}$ mol dm^{-3} MO are shown in **Fig.III.7.** The plots of the absorbances at the λ_{max} of the UV band of MO are also included in this figure. In the absence of MO, the surface tension of the surfactants reduces gradually and at some concentration attains a minimum and becomes constant, the concentration being the CMC of the surfactant in absence of any other substance, CMC^* (ref. 212,218,254). The plots of surface tension (γ) *vs.* log [CTAB] in the presence of $1.0x10^{-5}$ mol dm^{-3} MO shows that firstly, on addition of CTAB (**Fig.III.6**) in the submicellar concentration range, the surface tension decreases much more rapidly in the presence of MO than that in its absence. It is known that nonionic surfactants have greater surface tension reducing efficiency than that of the ionic surfactants[1]. The observed better surface tension reduction by the interaction product than the surfactant alone can be attributed to the formation of close-packed dye-surfactant ionpair (DSIP) which behave like a nonionic surfactant. Similar observations were reported earlier in the cases of other oppositely charged dye-surfactant systems[212,217,218,254].

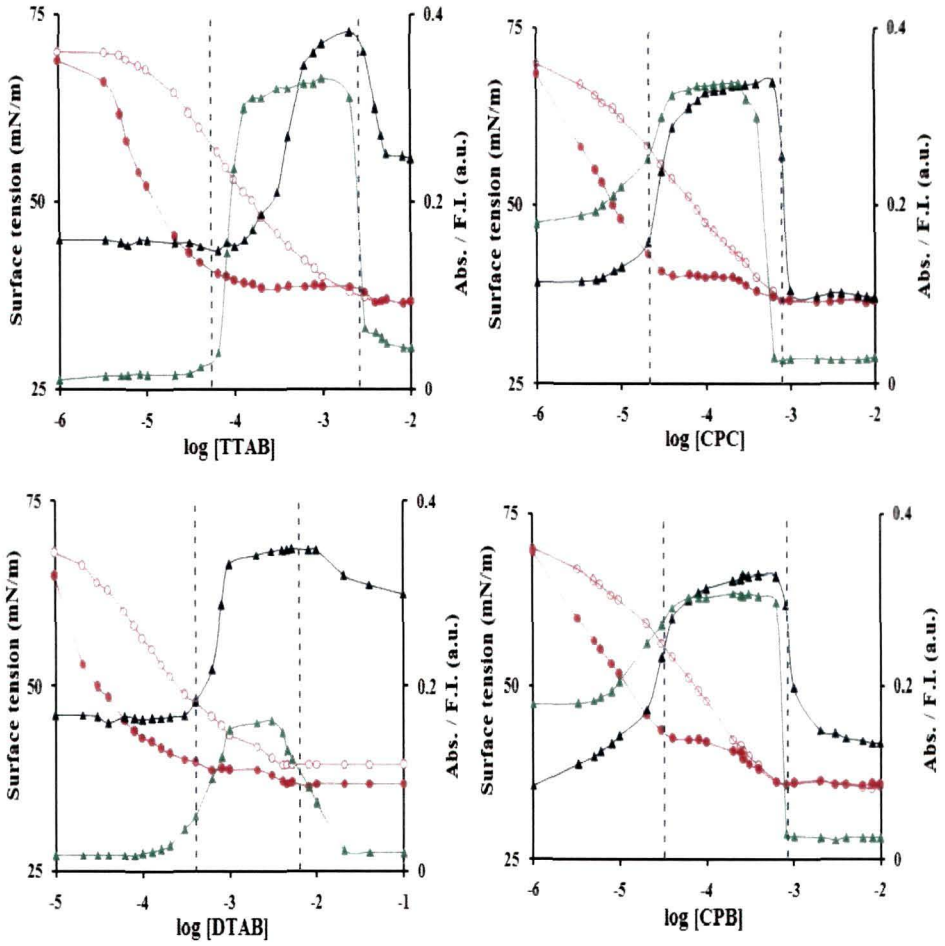

Fig.III.7. Plots of FI, absorbance and γ of MO ($1.0x10^{-5}$ mol dm^{-3}), as a function of concentration of TTAB, DTAB, CPC and CPB at 298 (±1) K. Symbols: FI at 575 nm (▲) (the $S_1 \rightarrow S_0$ (n-π*)) excited at 270 nm; γ in the presence (•), absence ( ) of MO; absorbances at 368 nm (for CPC and CPC) and 377 nm (TTAB and DTAB) (▲). Vertical dotted lines indicate CMCs.

Secondly, we can note the existence of two well-separated and distinct CMCs in the premicellar surface tension curve at CTAB concentrations of ≈ $3.01x10^{-5}$ mol dm^{-3} and ≈ $8.10x10^{-4}$ mol dm^{-3} in the presence of the dye as shown in **Fig.III.6.** The second CMC is the CMC* as indicated by the plots of γ for the aqueous surfactant alone. Above $8.10x10^{-4}$ mol dm^{-3} of CTAB, the γ values in absence and in the presence of MO are exactly equal indicating the formation of normal CTAB micelles above this concentration even in the presence of the dye. Thus, the first CMC, (CMC_{IP}) can be attributed to micellization of the DSIP, whereas, the second one, (CMC*) can be attributed to the formation of normal micelles of CTAB. The surface tension of solution is affected by any change in the

Table III.1. pC_{20}, surface excess concentration (Γs), CMC_{IP} and CMC* of the cationic surfactants in the presence of MO at 298 (±1) K.

Surfactant	CMC* /mM	pC_{20}		Γ_s (mmol/1000m^2)		CMC_{IP}/mM
		a	b	a	b	
CPC	0.81 (0.91)	4.39	5.00	1.44	1.01	0.030
CPB	6.31 (0.92)	4.21	4.79	1.47	0.95	0.040
CTAB	0.91 (0.91)	4.22	4.79	1.33	0.83	0.051
TTAB	4.01 (3.70)	3.79	4.63	1.04	0.82	0.204
DTAB	12.1 (16.0)	3.52	4.39	0.94	0.89	0.316

Experimental error limit = ±5%, values in parentheses indicates the CMC values form literature.

a In absence of MO

b In presence of MO

structure of the monolayer at the air/water interface. The DSIP has a larger head group and surface area per DSIP molecule compared to that of CTAB alone which results in the lower CMC of DSIP than that of CTAB alone[311]. The ionpair formation is a pronounced interaction and it exists in the monolayer. The formation of the air-water (a/w) interfacial monolayer by the DSIP in the present case can be compared with the reported a/w monolayer of CTAB in presence of *p*-tosylate counterion[311]. The area per surfactant molecule in the monolayer of CTAB was reported to increase by one-quarter to generate space for the p-tosylate ions within the monolayer. The CTAB-MO ionpair bears a larger head group thus it forms aggregation with a lesser number of molecules leading to a lower CMC. The pC_{20}, the negative logarithm of the concentration of the surfactant required to reduce the surface tension by 20 mN/m, is a measure of the efficiency of the surfactant[1]. The pC_{20} of the surfactants in presence of MO has been found much greater than that in the absence of the MO (**Table III.1**). The efficiency increased with increase in the chain length of the surfactants in absence as well as in presence of the dye. The surface tension

behavior of MO showed similar trends in the presence of all cationic surfactants but the effects decreased with decrease in the surfactant chain length.

The excess surface concentration at the surface saturation of the surfactants, *viz*, Γ_s has been calculated using the Gibbs adsorption equation commonly used for nonionic surfactants[1]:

$$d\gamma = -4.606\ RT\ \Gamma_s\ d\log C_1 \qquad \text{III.2.}$$

where, $d\gamma$ is the surface tension at the surface saturation and C_1 is the surfactant concentration.

The Γ_s of the cationic surfactants in presence of MO have been found to be smaller than that in absence of MO. This is consistent with the fact that a larger surface area is required for the formation of the ionpair. From the plots (**Fig.III.7**), it is seen that the γ values at CMC_{IP} are greater than that at CMC^*. This indicates that the effectiveness of the surfactant in presence of MO is less than that in its absence. CPC and CPB surfactants are found to be more effective and exhibit a higher surface excess value compared to that of the alkyltrimethylammonium surfactants. The observed greater effectiveness as well as higher Γ_s values of these surfactants carrying pyridinium head groups indicate that the pyridinium head groups may contribute towards better packing of the ionpairs compared to the trialkylammonium head group of CTAB. Moreover, Cl^- is reported to have larger contribution than Br^- counterion towards micellization[146] and other submicellar dye-surfactant interactions[146,312].

III.1.7. Correlation between the spectral and the surface tension behavior

It has been reported that cationic surfactants have the ability to deprotonate an anionic dye in certain premicellar aggregates of closed-packed DSIPs[218]. However, there is no replaceable proton in the base form of MO, in which MO exists in pure water. So, we can rule out the possibility of deprotonation of MO. We have observed that aqueous MO obeys the Beer-Lambert's law up to a concentration of 1.0×10^{-3} mol dm^{-3} indicating absence of dimerization of MO under such conditions. We also did not observe poor solubility of MO-CTAB complex showing the UV band[234]. Therefore, the UV band is unlikely to be due to dimerization of MO-CTAB ionpairs.

We can also rule out the possibility of appearance of the UV band merely due to MO-cationic surfactant aggregation because had there been only ionpair aggregation, we

would not get two CMCs and the surface tension would keep on decreasing continuously without any break in the plot of surface tension *vs.* log [surfactant] (**Fig.III.7**). It is seen from the figure that the UV-band which is attributed to the *cis* form of MO appears at CMC_{IP} Now what is the driving force that converts *trans* MO to *cis* MO?

The DSIPs starts forming micelles of their own as the surfactant concentration exceeds the CMC_{IP}. These DSIP micelles are small and compact aggregates where the dye molecule in the *trans* form experiences a steric strain. Under this situation, the MO molecule will prefer a conformation with the minimum strain. Thus, the hydrophobic tails of CTAB molecules in the DSIP micelles interact with the phenyl groups of *trans* MO, distort the dye molecules and reduce the molecular volume[313] of MO in the DSIP micelles, converting MO to its *cis* isomer. The twisted V-shape allows more hydrophobic interaction between the surfactant tail and the two hydrophobic phenyl groups. When there is DSIP micelle formation at [CTAB] concentration of 3.05×10^{-5} mol dm^{-3}, the dye remains at the highly polar surface region of the CTAB dominated small DSIP-CTAB mixed micelles, where the polar *cis* form is favored. Hypsochromic shifting of the band of a conjugated system by about 96 nm can be attributed as to have attained a structure with restriction in the conjugation like in case of the polyphenolic curcumin[276].

The surface tension behavior suggests that the air/water interfacial monolayer breaks down as the CTAB concentration approaches the CMC*. This coincides with gradual but complete replacement of the DSIP in the air/water interfacial monolayer by the surfactant (CTAB) at CMC*. The shift of the λ_{max} of MO from 377 nm to 430 nm above the second CMC suggests that the DSIP's too break down and form normal micelles of CTAB above CMC* and the dye exists only in the *trans* form solubilized in the nonpolar CTAB micelles.

We get three distinct regions in the plot of the FI of MO at 575 nm *versus* the concentration of CTAB (**Fig.III.6**). There is an initial slow and gradual increase in the intensity up to [CTAB] = 3.05×10^{-5} mol dm^{-3}, then there is a steep increase above [CTAB] = 3.05×10^{-5} mol dm^{-3}. The FI remains almost steady in the concentration range 8.10×10^{-5} – 4.07×10^{-4} mol dm^{-3}. Then there is a steep decrease in the intensity of the band at [CTAB] above 6.00×10^{-4} mol dm^{-3} and then above 1.00×10^{-3} mol dm^{-3}, the FI levels off. It is interesting to note the coincidence of the appearance of the UV band and the increase in the FI of MO in the submicellar concentrations where MO exists in the micelles of the DSIP. The increase in the FI in the CTAB concentration range is unusual because the FI is expected to decrease due to a likely positioning of MO in a highly polar surface region of the DSIP micelles. Also, above the normal CMC of the surfactant, the FI of MO is again

decreased whereas it is expected to increase due to possible transfer of MO to the nonpolar core of the micelles. This unusual fluorescence behavior of MO in the presence of the submicellar and micellar surfactants may be due to the greater fluorescence of the *cis* form compared to that of the *trans* form, a factor that dominates over the polarity factor. The difference in the spectral properties of the two forms may be reflected in the TD-DFT results of the two forms complexed with the cationic surfactant.

The appearance and gradual shifting of the hump from 420 nm to 510 nm in the fluorescence spectra (**Fig.III.5(a,b)**) can be attributed to the change in the microenvironment of MO on increasing the concentration of the cationic surfactant – MO being in the DSIPs, then in the DSIP micelles above CMC_{IP} and finally in the micellar core above CMC*. At these situations MO may be stabilized in intermediate conformations other than exactly the *trans* and the *cis* isomers. These changes in the microenvironment of MO in the premicellar aggregates can be compared to the defect states as in solids which play a significant role in the fluorescence process in this region (370 nm – 520 nm)[314].

III.1.8. DFT optimized structures of *cis* form, *trans* form and DSIP

The DFT optimized structures of the individual molecules and the DSIP are shown in **Fig.III.8**. The *trans* to *cis* isomerization of an azobenzene moiety changes its dipole moment, structural geometry, and optical spectrum. The estimated water phase DFT dipole moments for the ground state of the basic *trans*, basic *cis*, MO_{trans}.EA and the MO_{cis}.EA are 28.60, 39.92, 8.54 and 25.77, respectively. The calculated dipole moments are found to be smaller for the *trans* form than for the *cis* form. From the fully optimized geometries, we find that free *trans* MO stabilizes in planar geometry while the *cis* form stabilizes in a twisted geometry with an angle of 124.43 between the two phenyl rings around the azo group (N1-N2-C33 in **Table III.2**) which is increased by ~ 0.2 A° on complexation with EA. The conversion from *trans* to *cis* MO decreased the distance between the C-atom and the O-atom of the terminal methyl and sulphonate groups respectively, from 14.59 to 5.5 Å.

Optimization of both the isomeric forms of MO complexed with EA shows that the MO_{cis}.EA is stable over the MO_{trans}.EA complex by ≈ 2.94 kJ $mole^{-1}$. We find that the shortest distance of separation (as measured from the nearest O-atom of the terminal sulfonate group of MO_{cis} and the nearest H-atom of the terminal methyl group of EA) in *cis*-MO.EA is 2.35 A° while 2.31 A° in case of MO_{trans}.EA in water phase.

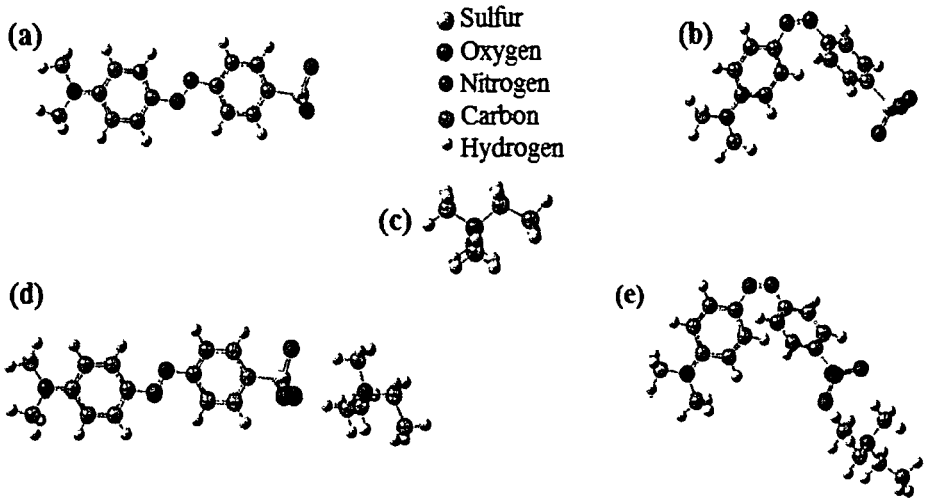

Fig.III.8. DFT optimized structures of individual molecules and the ionpair complexes. (a) MO_{trans}, (b) MO_{cis}, (c) EA^+, (d) $MO_{trans}^- EA^+$, (e) $MO_{cis}^- EA^+$.

Table III.2. Some structural parameters (bond length, bond angle and torsion angle) for each system. The values in bracket correspond to gaseous phase.

System	N1-N2 (A°)	N1-C3 N2-C22	C5-C3-N1-N2 (ring with methyl groups) N1-N2-C22-C24 (ring with sulfonate group) (°)	Shortest distance of approach of EA^+ (A°)
			***Trans* MO**	
MO anion trans	1.269 (1.263)	1.396 1.416	179.976 179.843	
$MO^-•EA^+$	1.269 (1.262)	1.395 1.416	179.150 177.852	2.312
			***Cis* MO**	
MO anion cis	1.262 (1.256)	1.411 1.431	160.024 129.848	
$MO^-•EA^+$	1.262 (1.254)	1.411 1.431	161.004 129.420	2.353

To be noted that the inclusion of the solvent effects reduces the stabilization energy significantly while increases the shortest distance between MO and cationic EA because of the presence of significant solvent screening effect. This geometrical change associated with *trans* to *cis* isomerization of azobenzenes is significant, and can be used to destroy or rearrange the order of an organized media.

The UV-Vis study has already demonstrated that MO absorbs at lower energy region (464 nm) which shifts to a high energy wavelength in presence of a cationic surfactant. We supposed that this is the consequence of dye-surfactant ionpair induced *trans* to *cis* isomerism of MO. Consequently, a possibility of preferred complexation of the EA^+ with *cis* MO compared with its planar *trans* MO isomeric form exists and could rationalize the current experimental band shifts. Presumably, we have considered the complexes of *cis* MO and EA^+ for further investigation of optical properties.

III.1.9. Prediction of the spectral properties of *cis* and *trans* forms of MO

To understand the observed shifts in the peak position in the UV-Vis absorption spectra of MO in presence of the cationic surfactants we have carried out TD-DFT of excitation energies on the ground state optimized geometries of the free dye as well as for their complexes with CTAB in both water and gas phase. **Fig.III.9** shows the plots of the absorption spectra and **Table III.3** includes the corresponding stabilization energies, absorption wavelengths (λ_{max}), oscillator strengths, transition dipole moments, and the molecular orbitals involved in the main excited states together with the error (%) in λ_{max} with respect to the experimentally observed values in the aqueous solution. The calculated results for MO_{trans}, λ_{max} = 446.11 nm is in quantitative agreement with the current experimental findings (λ_{max} = 464 nm) within a percentage error of 3.85% in water phase. We also obtained theoretical peaks at 375.18 and 375.21 nm in case of free MO_{cis} and MO_{cis} complexed with EA, respectively, with strong absorptions resulting mainly from the HOMO to LUMO and HOMO-1 to LUMO electronic excitations of appreciable oscillator strength (0.34) (**Table III.3**) as obtained at 368 nm in our experiments at cationic surfactant concentrations $\approx 2\times10^{-5}$ mol dm^{-3}. Thus the calculated absorption spectra of the *trans* and the *cis* forms of MO quantitatively match with their experimentally obtained absorption wavelengths.

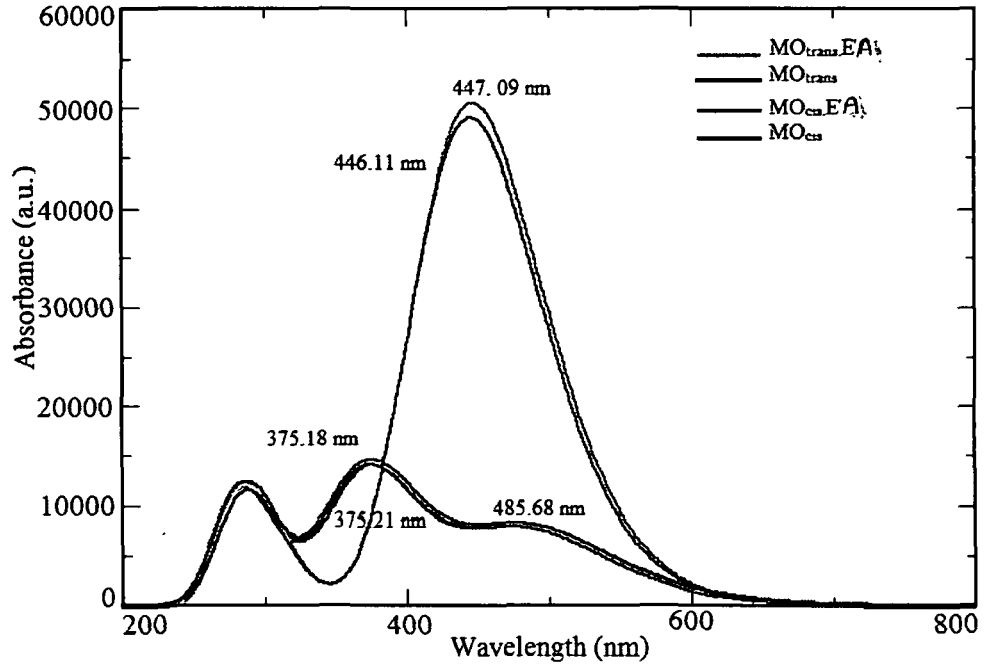

Fig.III.9. Computed spectra of the individual molecules and the DSIPs.

The enhancement of FI of the 575 nm fluorescence band of MO in the DSIP micelles may be attributed to the *cis* form where the electronic excitation is possible through absorption around 375 nm band (though the excitation wavelength was 270 nm) which then fluoresce at 575 nm (**Fig.III.5(a,b)**). This is supported by the fact that there was no fluorescence enhancement when excited at 464 nm because the electronic excitation around 375 nm is not possible with excitation at 464 nm (**Fig.III.5(c)**).

The experimental UV-Vis spectra showed the appearance of a new band at the higher energy side of MO in aqueous solution of submicellar range of CTAB, which we attribute to the formation of the *cis* form of the dye. To rationalize these observations, we focus on the occupation of relevant frontier molecular orbitals (FMOs) (**Fig.III.10**) responsible for these higher energy electronic transitions.

Table III.3. Stabilization energy for the ionpair complex (kJ mol^{-1}), oscillator strength (f), transition dipole moment (μ_x, μ_y, μ_y), molecular orbital contribution (H=HOMO and L=LUMO), and corresponding absorption wavelength (λ_{max}) for each system.

System	Stabilization energy (kJ $mole^{-1}$)	f	μ_x	μ_y	μ_z	Transition	λ_{max}	Error in λ_{max} (%)[a]
				***Trans* MO**				
MO anion trans		1.2096	28.57	1.26	0.004	H→L=0.706	446.11	3.85
						H-2→L=0.685	315.88	
		0.0481				H-3→L=0.15		
$MO^{-}•EA^{+}$	-10.23	1.2246	7.18	-2.32	2.37	H→L=0.698	447.09	3.64
						H-1→L=0.103		
		0.0019				H-3→L=0.544	311.26	
						H-2→L=0.44		
				***Cis* MO**				
MO anion cis		0.1956	39.90	0.58	-1.10	H→L=0.58	487.20	
						H-1→L=0.101		
		0.3404				H→L=0.38		
						H-1→L=0.55	375.18	0.48
$MO^{-}•EA^{+}$	-13.12`	0.1914	7.87	24.02	-5.97	H→L=0.57	485.68	
						H-1→L=0.38		
		0.3468				H-1→L=0.54	375.21	0.47
						H→L+2=0.11		

[a]Error (%) corresponds to the difference between the calculated λ_{max} (nm) and the experimental values in aqueous solutions.

From the FMOs, it is seen that in the *trans* form, the L and L+1 are delocalized over the entire molecule while the H is localized in the central part of the molecule. In case of the *cis* form, the H, L, L+1 are delocalized over both the arms of the molecule with a kink in the central azo group. On complexation of the *cis* MO with EA, there is no significant change in the FMOs, however, complexation brings about changes in the symmetry of the lobes of the relevant FMOs. These changes may significantly render the electronic transition energy towards higher energy values. Thus, experimental and computational results are in good agreement on the appearance of the UV band in that MO

isomerizes to the *cis* form in the DSIP micelles in the presence of submicellar cationic surfactants.

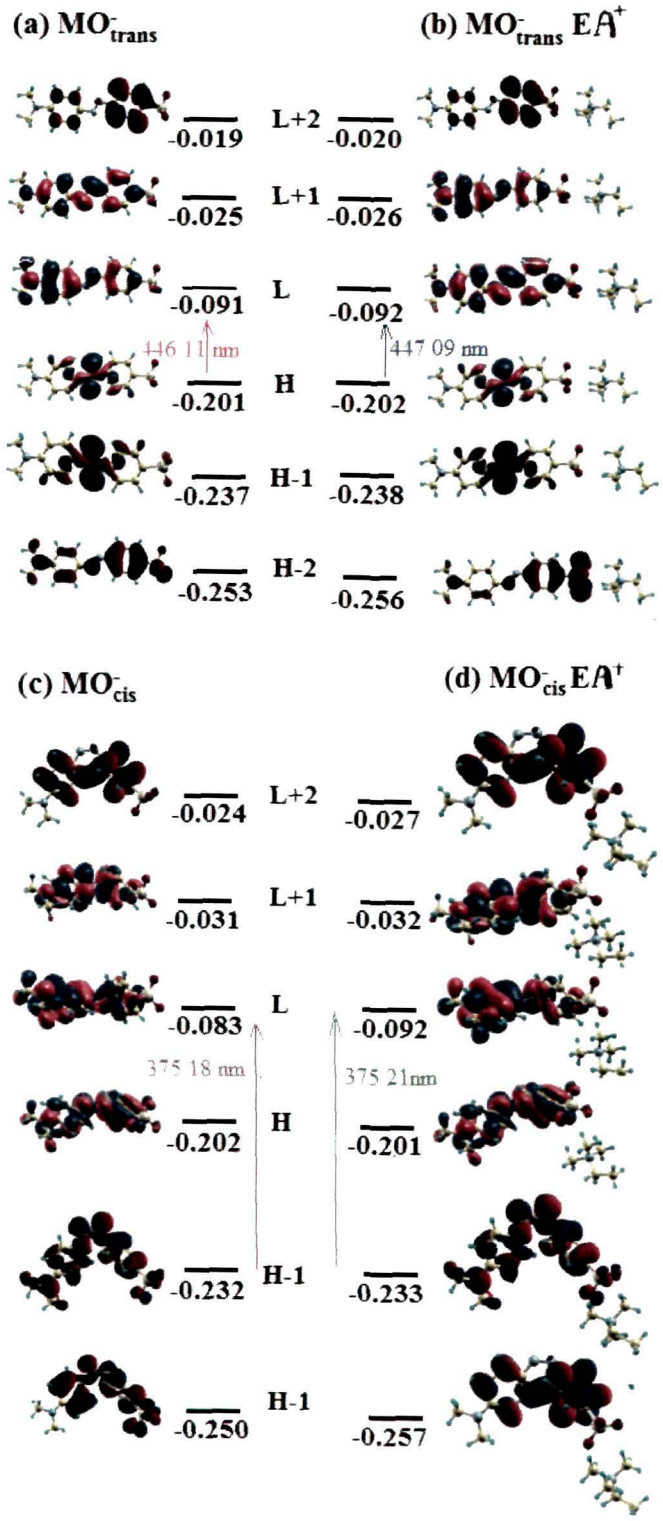

Fig.III.10. Orbital energies of FMOs and their wave function plots together with the corresponding transitions.

III.2. Protonation of Acridine Orange in Dye-surfactant Ionpair Micelles*

Phenazinium dyes are known to be protonated in the dye-surfactant ionpairs (DSIP) formed in aqueous submicellar anionic surfactants solutions[214]. Recently, spectroscopic and tensiometric studies revealed that other cationic dyes, *viz.*, neutral red[212] and triphenylmethane dyes[217] form protonated dye-surfactant ionpairs (PDSIP) on micellization of their DSIP in aqueous submicellar anionic surfactant solutions. Neutralization of electric charge due to close packed ionpair formation was assumed to generate strong hydrophobicity in the ionpair and redistribute electron densities in the dye ion, which lead to further protonation of the cationic dyes. On the other hand, some sulphonapthalein dyes were reported to undergo further deprotonation in their DSIPs formed in presence of submicellar cationic surfactants[218]. It has also been shown that submicellar cationic surfactants can further deprotonate the sulphonapthalein dyes[218] from their monoanionic forms to their dianionic forms in their DSIP micelles even below the pK_a in water.

It is well-known that AO undergoes aggregation in submicellar anionic surfactant solutions[243]. However, the detail of the micelle formation process in aqueous AO-anionic surfactant system is not known. In a preliminary investigation, we had observed some changes in the low energy side of the spectra of aqueous AO in premicellar solutions of anionic surfactants, *viz.*, sodium dodecylsulfate (SDS) and sodium dodecylbenzenesulfonic acid (SDBS) which were not paid enough attention earlier. While spectrophotometric study is a suitable tool to monitor the protonation-deprotonation equilibrium or the existence of the different forms of the dye, surface tension measurements give the surface tension as well micelle forming behavior of the surfactants in presence of the dye. In addition to that, fluorescence measurements provide insight to the microenvironmental variations of the dye in the premicellar and micellar concentration ranges of the surfactant in the presence of the dye. We thought it worthwhile to systematically study the low energy side of the spectra of aqueous AO in premicellar solutions of anionic surfactants in order to study the premicellar behavior of the AO-anionic surfactant system, in general, and to see if any protonation of the dye also takes place in addition to the reported dimerization, in particular.

Part of this work has been published in* ***J. Mol. Liq.* *178 (2013) 25-30.*

We also carried out theoretical calculations using time dependent density functional theory (TD-DFT) on the AO dye and the model dye-surfactant systems in order to verify the experimental results.

III.2.1. Electronic absorption spectra of AO in the low-energy region

The spectra of $1.0x10^{-5}$ mol dm^{-3} aqueous AO show a maximum absorbance at 491 nm and a shoulder at 469 nm which have been attributed to the monomeric AOH^+ and the dimeric $(AOH)_2^{2+}$ forms of AO, respectively[171]. The variation in the band and the shoulder of the spectra observed in presence of submicellar sodium dodecylsulfate were studied by Moulik *et al.* and attributed to dye-surfactant complex formation and induced dimerization dye-surfactant mixed micelle formation[243]. In the presence of submicellar SDS, in addition to the increase in the dimer band (469 nm) at the cost of the monomer band (491 nm), there is an increase in the absorbances in the higher wavelength range (508-580 nm) of the AO spectra as can be seen in **Fig.III.11(a),** which has not been paid enough attention so far[315-317]. As no maximum was observed in the 508-580 nm region, we have estimated the absorption λ_{max} to be 523 from the difference of spectra 1 and 5 of **Fig.III.11(a).** We have observed an isosbestic point (Q) at 508 nm in the presence of SDS from $0.5x10^{-4}$ to $4.0x10^{-4}$ mol dm^3 indicating the presence of an equilibrium condition between two forms of AO. The absorptions in the 508-580 nm range starts decreasing as [SDS] exceeds $4.0x10^{-4}$ mol dm^{-3} and totally disappears above $8.0x10^{-3}$ mol dm^{-3} with the reappearance of the monomeric AO band (**Fig.III.11(b)).**

The spectra of $1.0x10^{-5}$ mol dm^{-3} aqueous AO show a maximum absorbance at 491 nm and a shoulder at 469 nm which have been attributed to the monomeric AOH^+ and the dimeric $(AOH)_2^{2+}$ forms of AO, respectively[171]. Increasing the concentration of SDS in aqueous AO gives a series of spectra that pass through an isosbestic point (Q) at 508 nm (**Fig.III.11**). It is to be noted that the absorbances between 508-580 nm gradually increased on increasing the SDS concentration above $3.2x10^{-5}$ mol dm^{-3} up to $4.0x10^{-4}$ mol dm^{-3}. This occurred simultaneously with a gradual appearance of the band due to the dimer and a rapid decrease in the absorbances of the band of the monomeric dye. Thereafter, the absorbances in the 508-580 nm range remained almost unchanged up to $3.0x10^{-3}$ mol dm^{-3} of SDS but gradually disappeared with a corresponding sharp increase in the intensity of the monomer band as the concentration of SDS was increased to $8.2x10^{-3}$ mol dm^{-3} (**Fig.III.11.(b)**). The λ_{max} of the monomer band also shifted while increasing in the intensity and finally settled at 496 nm.

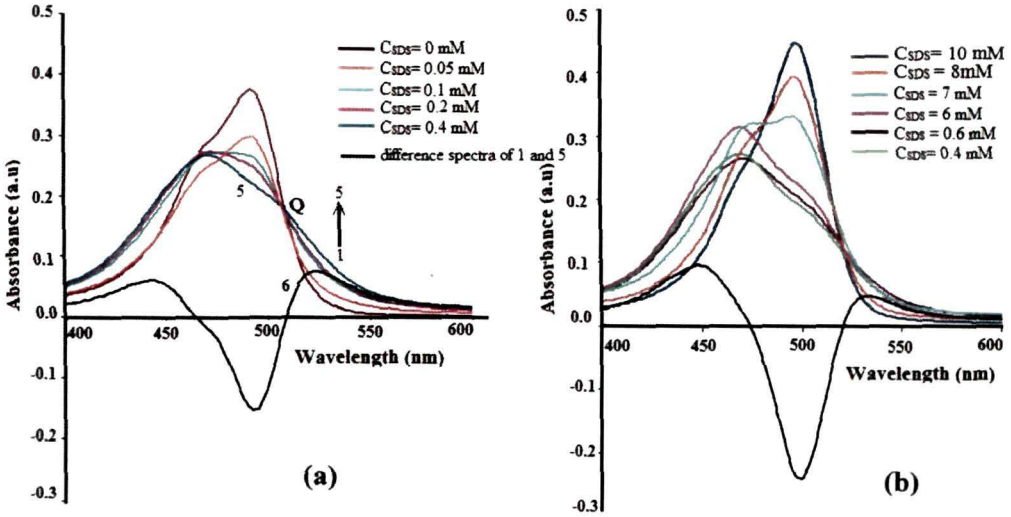

Fig.III.11. The effect of variation in the spectra of AO ($1x10^{-5}$ mol dm^{-3}) in presence of SDS 298K ($\pm$1).

A bathochromic shift observed in another acridine dye, *viz.*, proflavine in presence of submicellar SDS was attributed to J-aggregate of the dye[179], whereas, the aggregation reported in the case of AO is H-aggregation (hypsochromic)[243,315]. On the other hand, it is interesting to note that AO shows increase in the absorbances in the same range (508-580 nm) in presence of concentrated H_2SO_4 analogous to that as reported in case of Safranin O[214]. The difference spectra (**Spectra 4 in Fig.III.12**) obtained by subtracting the spectra 3 from spectra 1 gives the λ_{max} of the new higher wavelength absorption band as 530 nm which is close to that observed in presence of the submicellar surfactants. The AO spectra observed in presence of H_2SO_4 also passed through an isosbestic point (Q') at 514 nm (**Fig.III.12**). The pK_a of AO is reported to be 10.2, which corresponds to the protonation of the nonionic form of AO to the monocationic form[171,316]. Thus, the observed absorbance in the higher wavelength range in the presence of concentrated H_2SO_4 is due to protonation of the monocationic form of AO (AOH^+) to the dicationic (AOH_2^{2+}) form. Therefore, the absorptions in the 508-580 nm region in the presence of submicellar SDS also may be due to formation of the doubly protonated dye. Though ionic micelles can shift pK_a of dyes only up to about 2 units[122,180], the ionic submicellar surfactants are

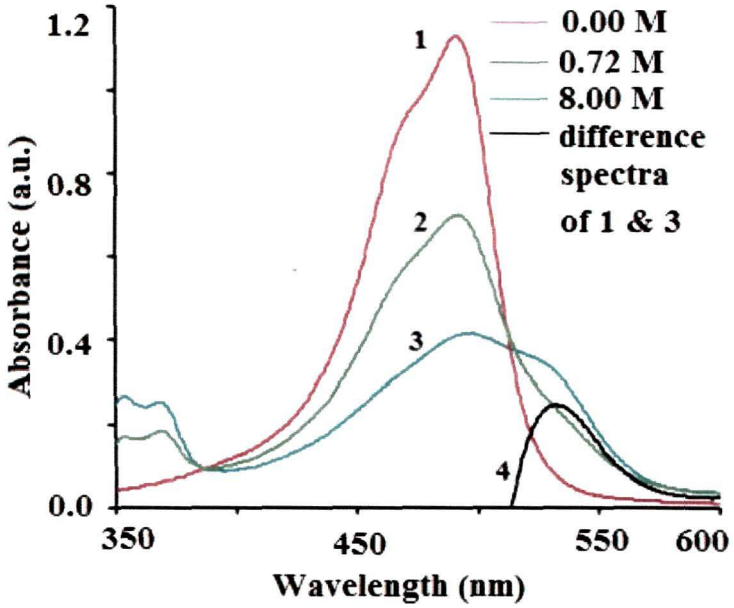

Fig.III.12. Effect of H_2SO_4 on the spectra of AO ($2.5x10^{-5}$ mol dm^{-3}) at 298K (±1).

reported to shift the pK_a of some oppositely charged dyes up to 5-6 units[212,217,218,253]. Though SDS may not make the solution acidic as H_2SO_4, it may provide a local environment to the dye in the SDIP through a strong electron withdrawing effect arising from combined hydrophobic-electrostatic interactions. Thus, it is possible to attribute the observed increase in the absorbances in the 508-580 nm regions to protonation of AO.

Analogous absorption behavior of $1.0x10^{-5}$ mol dm^{-3} AO has been observed with another anionic surfactant, *viz.*, SDBS. But we have not observed the increased absorption of AO in the higher wavelength range around 523 nm with Triton X 100, $(CH_3)_2C_6H_4(OCH_2CH_2)_{10}OH$ (a nonionic surfactant) and also with CTAB, hexadecyltrimethylammonium bromide (a cationic surfactant) in the submicellar concentration range which indicates that, as is in the case of induced dimerization[243], the opposite charge on the dye and the surfactant, *i.e.*, ionpair formation, is a primary requirement for the interaction leading to the absorptions of AO around 523 nm. However, mere ionpair formation cannot lead to such spectral changes[146].

The *p*H of the above aqueous dye-surfactant solutions was ≈ 6.60 where the dye is in the singly protonated form, AOH^+. It is possible that the absorbances of AO around 523 nm in the submicellar SDS may be due to the doubly protonated dye, AOH_2^{2+} formed by protonation of the AOH^+ form, caused by a local acidic effect of the DS^- ion in the DSIP, as is reported in other similar systems[212,214]. Thus, the isosbestic point at 508 nm in the

spectra can be attributed to an equilibrium condition between the DSIP and protonated DSIP (PDSIP), $AOH_2^{2+}SDS^-$. The PDSIP probably breaks down as normal micelles are formed on approaching the CMC of SDS in pure water, CMC* = $8.2x10^{-3}$ mol dm^{-3} (ref.218).

III.2.2. Surface tension study

The plots of surface tension vs. log [SDS] in the presence of $1.0x10^{-5}$ mol dm^{-3} AO (**Fig.III.13**) revealed some interesting facts. Firstly, on addition of SDS in the submicellar concentration range, the surface tension decreases much more rapidly in the presence of AO than that in its absence. This means the interaction product between an SDS monomer and AO has a higher efficiency than SDS as was reported in similar systems[212,217,218,253,254]. The value of pC_{20}, has been estimated to be 3.39 and 3.09 in presence and in the absence of the dye, respectively (**Table III.4**). Nonionic surfactants have greater efficiency than the ionic surfactants. The present increase in the efficiency of
the surfactant in presence of the dye can be attributed to the formation of the DSIP. Since the electrical charges in the close packed DSIP are practically neutralized, the DSIP behaves like a nonionic surfactant having higher efficiency than the surfactant alone. The higher efficiency of the DSIP surfactant also suggests that the DSIP retains its electrically neutral character upon micellization[1].

Secondly, there exists two well-separated and distinct CMC's at SDS concentrations of $\approx 5.01x10^{-5}$ mol dm^{-3} and $\approx 8.2x10^{-3}$ mol dm^{-3} in the presence of the dye as shown in **Fig.III.13(a)** as reported in similar systems. Interestingly, the second CMC is the CMC of SDS in pure water (CMC*) as has been indicated by the surface tension vs. log [SDS] plot in the absence of the dye. Above $8.2x10^{-3}$ mol dm^{-3} of SDS the surface tensions in absence and in the presence of AO are exactly equal indicating formation of normal SDS micelles above this concentration even in the presence of the dye. Thus, the first CMC, (CMC_{IP}) can be rightly attributed to micellization of the DSIP whereas the second one, (CMC*) can be attributed to the formation of normal micelles of SDS.

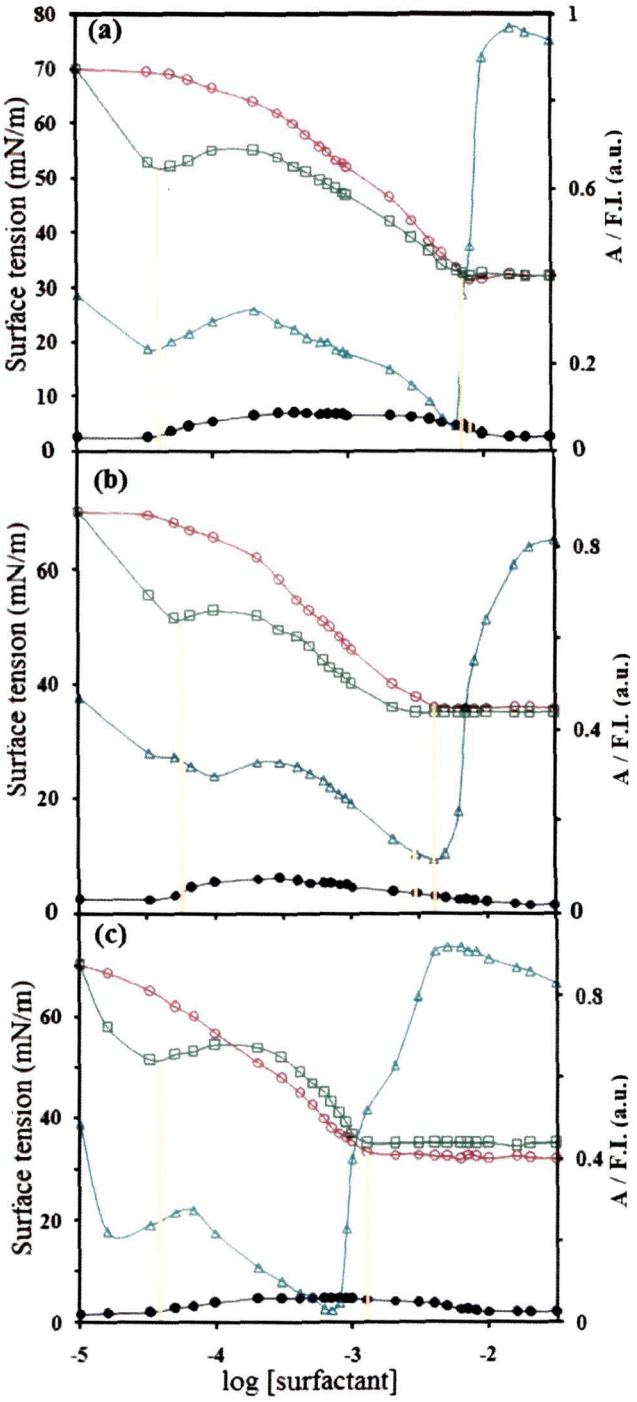

Fig.III.13. Plots of surface tension (mN/m), absorbance and fluorescence intensity of aqueous AO (1×10^{-5} mol dm^{-3}) solutions as a function of logarithm of the concentration of SDS (a) and SDBS (b) at 298K (±1). Symbols: surface tension in the presence (□) and absence ( ) of AO, absorbances at 523nm (●), fluorescence intensity ($/10^3$) at 535 nm ( ).

Table III.4: Critical micelle concentration of the surfactants in water (CMC^*), as DSIP (CMC_{IP}) and the surfactant in the presence of the buffer (CMC*), and pC_{20} in absence and in presence of buffer and AO ($1x10^{-5}$ mol dm^{-3}) at 298K.

Surfactant	(CMC*±0.05) /(10^{-3} M)		pC_{20}				(CMC_{IP} ± 0.1) /(10^{-5} mol dm^{-3})
	without buffer	with buffer	without buffer		with buffer		
			without dye	with dye	without dye	with Dye	With dye
SDS	8.1 8.2 [a]	4.27	3.09	3.39 4.17[b]	3.15	3.52 4.30[b]	5.1 5.1[b]
SDBS	1.25 1.20 [a]	0.91	3.69	4.31 4.61[b]	3.52	4.17 4.48[b]	3.3 3.3[b]

[a] Literature values from Ref. [1,318]

[b]Corresponds to [AO] = $2.5x10^{-5}$ mol dm^{-3}

The DSIP formation between AO and SDS in the present case can be considered equivalent to formation of a nonionic surfactant with a larger head group. The nonionic DSIP is expected to have a high affinity towards the a/w interface and occupies larger surface area per surfactant resulting in greater efficiency and lower CMC than SDS alone[212].

Thirdly, the absorbances above 508 nm started to increase as the surfactant concentration approached the CMC_{IP}. The increase in the absorbance in the 508–580 range can be due to second protonation of the dye caused by high electric potential at the DSIP micelle (or mixed micelle[243]) surface as reported in the cases of cationic triphenylmethane dyes and other phenazinium dyes under similar conditions[253] The presence of a minimum in the surface tension of SDS was attributed to the presence of impurities like dodecanol or Ca^{2+} or Mg^{2+} ions and a slight increase after the minimum was attributed to their solubilization[319]. However, as ionic surfactants are in general less efficient than nonionic surfactants, the observed increase in the surface tension above CMC_{IP} in the present case can be attributed to the presence of some ionic character of the DSIP surfactant in the DSIP micelles, which is possible through the formation of the PDSIPs. Finally, the PDSIP

band disappears with corresponding increase in the absorbance of the micelle solubilized monomeric AO on approaching the second CMC (CMC*) at $8.2x10^{-3}$ mol dm^{-3}. The observed surface tension behavior and the spectral changes suggest that the PDSIP in the ionpair micelles and in the air/water interfacial monolayer breaks down as the SDS concentration approaches the CMC*. SDBS showed analogous surface tension behavior in presence of $1.0x10^{-5}$ mol dm^{-3} AO (**Fig.III.13(c)**). SDBS also shows two well separated CMC's in the presence of AO (**Table III.4**). CMC* = $1.0x1^{-3}$ mol dm^{-3} and CMC_{IP} = $3.3x10^{-5}$ mol dm^{-3}. The pC_{20} values have increased in the presence of higher concentration of the dye ($2.5x10^{-5}$ mol dm^{-3}) in cases of both SDS and SDBS indicating formation of more DSIPs at the higher concentration of the dye.

III.2.3. Fluorescence intensity increases due to PDSIP

The changes in the steady state fluorescence intensities (FI) of $1.0x10^{-5}$ mol dm^{-3} AO in presence of varying concentrations of SDS are also shown in **Fig.III.13(a)** The fluorescence spectra of AO in presence of varying concentration of SDS is shown in **Fig.III.14.** We as well as Luo and Shen[320] did not observe any fluorescence band at 620 nm as was reported by Ban *et al.*[321] at [AO] = 0.20 mmol dm^{-3}. This may be due to the reason that the concentration of the induced dimer is very low at the experimental concentrations of AO in our case and in the case of Luo and Shen. The FI initially decreased with increase in SDS concentration, showed a minimum near the CMC_{IP} at $3.2x10^{-5}$ mol dm^{-3} of SDS, then increased to a maximum at $2.0x10^{-4}$ mol dm^{-3}, then started to decrease rapidly showing another minimum near the CMC* at $6.3x10^{-3}$ mol dm^{-3} and then finally increased rapidly (**Fig.III.13.(a)**). The first minimum was not noticed by the earlier workers Ghosh *et al.* and Ganguly, may be because it occurs at very low concentration of SDS[165,319-321].

The first minimum in the FI (**Fig.III.13**) can be attributed to increase in the micropolarity of the dye in the DSIP. The small increase in the FI starting from the CMC_{IP} up to the maximum at $2.0x10^{-4}$ mol dm^{-3} of SDS may be due to prominence of somewhat irregular shaped DSIP micelles, where, the dye remains in contact with more than one surfactant hydrophobic chains and experiences low micropolarity.

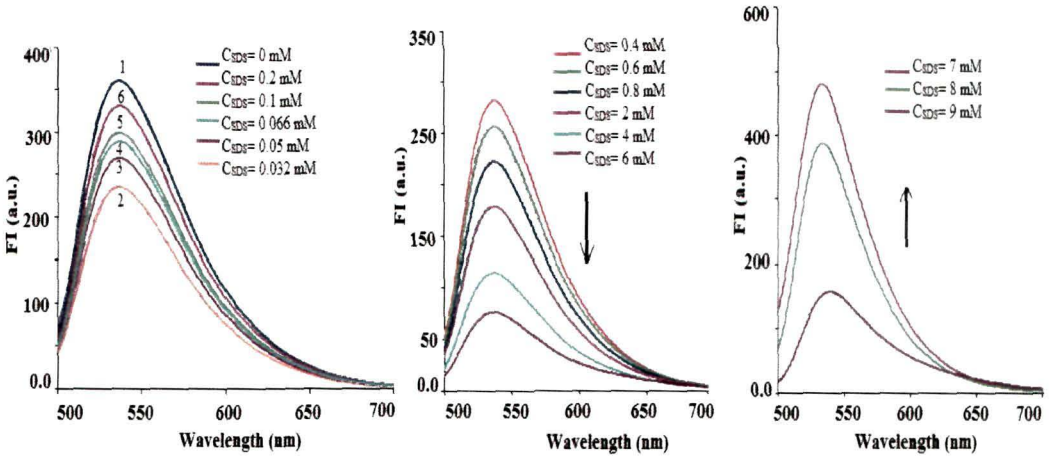

Fig.III.14. Fluorescence spectra of AO in varying concentration of SDS.

This effect is opposed by the formation of PDSIP which dominates just above the SDS concentration corresponding to the maximum of the FI. The PDSIP formation, which probably peaks at around 4.0×10^{-4} mol dm^{-3} of SDS gives a polar environment to the dye, lowering the FI. Above 4.0×10^{-4} mol dm^{-3} of SDS, although the PDSIP gradually breaks down, as indicated by decreasing absorbance at 523 nm, the dye probably experiences the highest micropolarity in the surface region of the SDS dominated DSIP-SDS mixed micelles at the second minimum of FI. The final marked increase in the FI above 6.3×10^{-3} mol dm^{-3} of SDS is attributed to the commencement of formation of normal SDS micelles[320]. The changes in the FI of AO showed similar trends in presence of SDBS (**Fig.III.13(c)**). However, the positions of the two minima and the maximum in between were at lower concentrations of the surfactant which can be attributed to the lower surface activity of SDBS than SDS. The second minimum in the FI curve is lower than the CMC* of the surfactant as indicated by surface tension.

III.2.4. The interactions at fixed pH

The plots of absorbances at 523 nm, FI at 535 nm and surface tension of 1.0×10^{-5} mol dm^{-3} aqueous AO at *p*H 7.00 as functions of log [SDS] are shown in **Fig.III.13(b)** along with surface tension without the dye. The absorbance and surface tension curves are almost similar to those in the absence of the buffer except for a relatively small increase in the absorbances at 523 nm and the lowering of CMC*, which has been found to be 7.0×10^{-3} mol dm^{-3} of SDS. Such decrease in the absorbances at 523 nm may be attributed to increase in the ionic strength due to the buffer components[218]. The lowering in the CMC*

is due to the presence of the buffer components and 1.0×10^{-5} mol dm^{-3} AO. Higher concentration of the dye (2.5×10^{-5} mol dm^{-3}) does not bring out any noticeable changes in the values of CMC* except in the pC_{20} values (**Table III.5.**). Similar variations are seen in case of SDBS. The FI vs. [SDS] plots in presence of the buffer of *p*H 7.00 were similar to that in the absence of the buffer except that the two minima are closer in the presence of the buffer than in its absence. The present model is consistent with the observed trend in the fluorescence curve in the presence of the buffer where the changes in the intensity and the positions of the minima and the maximum can be attributed to variations in the prominence of the different interactions, including the PDSIP formation.

III.2.5. The Thermodynamics of PDSIP Formation

The equilibrium of the submicellar PDSIP formation between AO and SDS can be represented by

$$[H^+] + [AOH^+] + [SDS^-] = [AOH_2^{2+}SDS^-] \qquad \text{III.3.}$$

Or,

$$K_c = [AOH_2^{2+}SDS^-] / ([H^+][AOH^+][SDS^-] \qquad \text{III.4.}$$

Here, $[SDS^-]$ and K_c are the concentrations of the surfactant anion and the equilibrium constant of the interaction, respectively. The pH of the mixed solutions of AO and SDS remained around 6.61 (within the experimental concentration range of SDS). Therefore, assuming that the $[H^+]$ constant, the above equation can be written as:

$$K_c^* = K_c [H^+] = [AOH_2^{2+}SDS^-] /[AOH^+][SDS^-] \qquad \text{III.5.}$$

Using Ketelaar's equation[214]

$$[AOH^+]_o/(d - d_o) = 1/(\varepsilon - \varepsilon_o) + 1/K_c(\varepsilon - \varepsilon_o)[SDS^-]_o \qquad \text{III.6.}$$

Here, $[AOH^+]_o$ and $[SDS^-]_o$ are the initial concentrations of the dye and the surfactant, respectively. d and ε are the absorbance and molar extinction coefficient of the PDSIP, $[AOH_2^{2+}SDS^-]$ at 523 nm in the presence of the surfactant, respectively and d_o and ε_o are the absorbance the molar extinction coefficient of the dye at 523 nm in absence of the

surfactant. Only those absorbance values of the λ_{max} of the PDSIP in the submicellar concentration ranges have been considered in the calculations whose spectra passed through the isosbestic point at 508 nm. The plots of $[AOH^+]_o/(d - d_o)$ *vs.* $(1/[S]_0)$ for various temperatures yielded straight lines in a wide range of the concentration of SDS (**Fig.III.15**). The true equilibrium constants K_c (where $K_c = K_c^*/ [H^+]$) have been determined and consequently the thermodynamic parameters have been calculated (**Table III.5**).

Table III.5. Thermodynamic parameters of the PDSIP formation by AO with SDS and SDBS in absence of any buffer.

Surfactant	T/K	K_c*	$K_c/10^9$	$-\Delta G^\circ$/kJmol^{-1}	ΔH°/kJmol^{-1}	ΔS°/JK^{-1}mol^{-1}
SDS	298	750	3.0	54.0	31.9	74.2
	303	600	2.4	54.4		
	308	500	2.0	54.8		
SDBS	298	333	1.3	52.0	23.9	94.2
	303	285	1.4	52.5		
	308	250	1.0	52.9		

*Average of at least three experiments with maximum error limit of 5%. The squired correlation coefficients are included in the respective plots in the inset of **Fig.III.15**.

The standard Gibbs free energy change for the PDSIP formation has been determined from the following equation:

$$\Delta G^\circ = - RT \ln K_c \qquad \text{III.7.}$$

ΔH^o and ΔS^o have been determined from the slope and intercept of the van't Hoff plot of $\ln K_c$ versus 1/T (**Fig.III.15, inset**) at temperatures 298K, 303K and 308K. The values of the thermodynamic parameters are shown in **Table III.5.** The high values of equilibrium constants are comparable with those reported earlier for similar systems[212,214,217,218]. The equilibrium constant (K_c) and the ΔG^o values of the interaction of AO with the premicellar anionic surfactants, SDS and SDBS show that the PDSIP formation interaction is stronger with SDS than with SDBS. The overall PDSIP formation in both the cases is driven by entropy, indicative of an increase in the entropy by breaking the ordered water structure around the DSIP due to the PDSIP formation which probably dominates over an endothermic transfer of the proton from water to the dye, the reverse of an exothermic acid-base reaction.

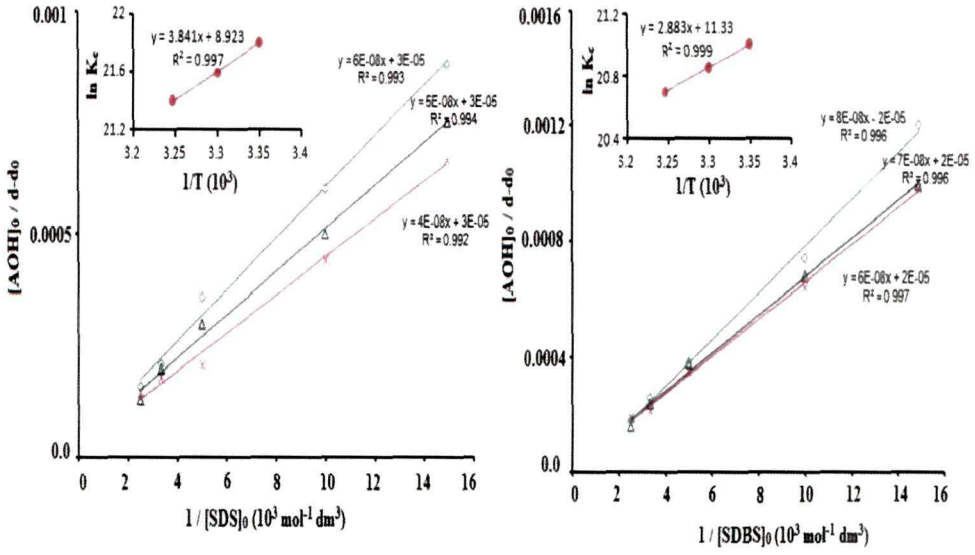

Fig.III.15. Plot of $[AOH^+]_o/(d - d_o)$ *vs.* $(1/[S]_0)$ and the $\ln K_c$ versus 1/T (inset).

III.2.6. DFT Optimized Structures of DSIP and PDSIPs

It is well known that in the ground state AO is protonated on the intracyclic nitrogen where the resulting positive charge is mainly located **(Fig.III.16)**. On the other hand, the second protonation of some phenazinium cationic dye, e.g., neutral red[212] in presence of anionic surfactants are reported to occur at the terminal dimethylamino N-atom which is supposed to be rich in electron density due to the presence of the two electron donating methyl groups present in it.

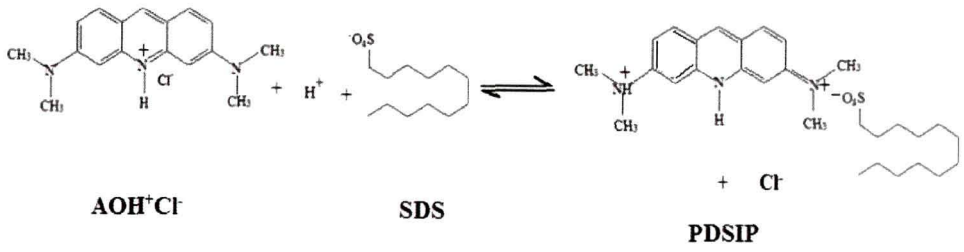

Fig.III.16. Schematic figure of formation of protonated dye-surfactant ionpair (PDSIP).

The structure with protonation at one of the terminal diamino N-atom with surfactant near the other terminal N-atom, was considered for optimization. As these are charged systems, we optimized the doubly protonated AO ($AOH_2^{2+}Cl^-$), DSIP ($AOH^+Cl^-.ES^-$) and PDSIP with higher level of calculation including more polarization, 6-311++ g (d,p). It has been found that the shortest separation (as measured from the two H-atoms of the terminal methyl groups of the dye to the O-atoms of the surfactant) between the dye and surfactant moiety in the DSIP is 2.50 Å in water phase and 2.08 Å in gas phase. It can be noted that in gas phase, the cationic dye and the anionic surfactant come closer to make O-H hydrogen bond and get stabilized, while with inclusion of solvent, the cationic dye and anionic surfactant get more separated and are stabilized by interacting through the dielectric medium (water).

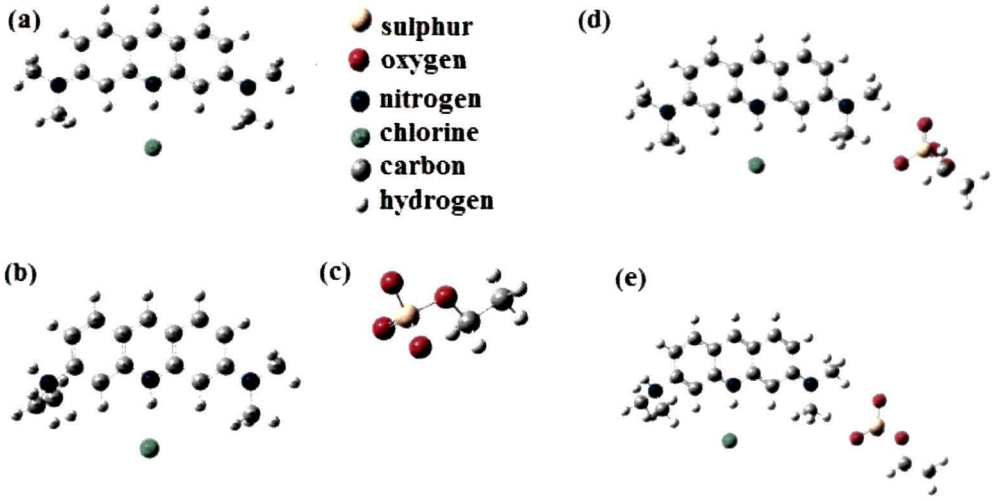

Fig.III.17. The optimized structures of all the individual molecules and complexes: (a) AOH^+Cl^-, (b) $AOH_2^{2+}Cl^-$ (c) ES^- (d) DSIP, and (e) PDSIP.

In the PDSIP, the shortest distance of separation between the H-atom of the methyl groups of the terminal amino group of AO and the O-atom of the sulphonate group of the surfactant head group is 2.43 Å. The DFT optimized structures are given in **Fig.III.17.** The stabilization energy of the PDSIP has been calculated as follows[324]:

Stabilization energy:

PDSIP $I_{S\,E} = E_{PDSIP} - (E_{ES} + E_{dication})$

$= -2063.3117 - (-778.4519 - 1284.8600)$

$= -0.0703$ Hartrees

$= -184.5727$ kJ $mole^{-1}$

III.2.7. Prediction of Spectral Properties of DSIP and PDSIP

The experimental UV-Vis spectra showed the appearance of a new band, at the higher wavelength side of AO in aqueous solution of concentrated H_2SO_4 and also in the presence of submicellar concentration range of SDS, which have been attributed to the formation of a new species with doubly protonated dye. To support and understand these experimental findings, we have also calculated the absorption spectra of the protonated cationic dye in aqueous solution as well as the PDSIP in the presence of aqueous submicellar SDS. These calculations were also done using the same level of calculations. The calculated absorption spectra of AOH^+Cl^- was now found at $\lambda_{max} = 444.30$ nm in water (433.33 nm, in gas phase) which matches fairly well with the previous reported values, λ_{max} = 444.10 nm in water (432.90 nm, in gas phase)[290,291] and are in qualitative agreement with the current experimental findings within a percentage error of 10% (12%) in water (gaseous) phase. However, a small red shift of 1.99 nm (**Fig.III.18**) from 444.30 nm to 446.29 nm of the cationic dye is found in presence of ES in water phase on ionpair formation. The calculated absorption maximum for $AOH_2^{2+}Cl^-$ **(Table III.6)** was found to be 475.22 nm which is red shifted by 3.72 nm form 475.22 nm to 478.94 nm on PDSIP formation (**Fig.III.18**) which qualitatively supports the observed new shoulder or band at 523 nm in submicellar SDS. The different experimental conditions could not be captured to reproduce 530 nm for $AOH_2^{2+}Cl^-$ and 523 nm for PDSIP, as observed experimentally. It can however be mentioned that even 20-30% of errors are reported in the literature as even with this much error one can get some qualitative agreements.

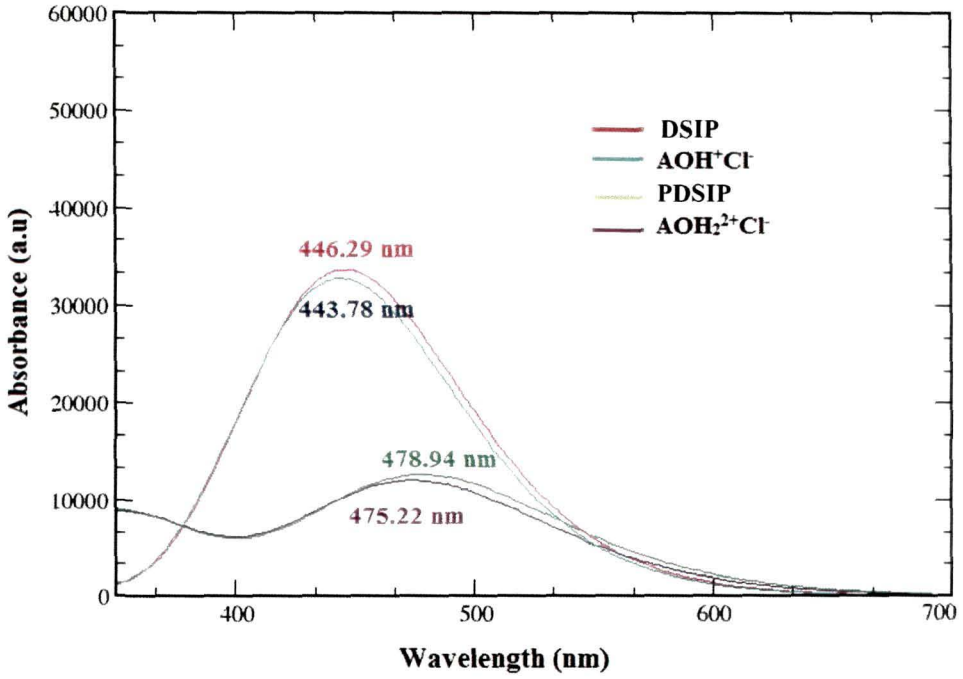

Fig.III.18. Computed absorption spectra of AOH^+Cl^-, $AOH_2^{2+}Cl^-$, DSIP and PDSIP.

Fig.III.18 shows the plots of the absorption spectra and **Table III.6** includes the corresponding absorption wavelengths (λ_{max}), oscillator strengths, transition dipole moments, and the molecular orbitals involved in the main excited states together with the error (%) in λ_{max} with respect to the experimentally observed values in the aqueous solution.

To have a better picture of this transition we plot the important FMOs and calculated the transition dipole moment and the contribution of FMOs to the transitions as shown in **Table III.6.** To rationalize the experimental observations, we focus on the occupation of relevant frontier molecular orbitals (FMOs) responsible for these lower energy electronic transitions. As can be seen from **Table III.6**, the HOMO-1, HOMO, LUMO, and LUMO+1 are mainly governing the observed transitions. In **Fig.III.19**, we present the energy levels and orbital plots of the important FMOs along with the corresponding absorption wavelength. As can be seen from **Fig.III.19,** the FMOs are mostly localized on the dye moiety in the DSIP, AOH^+SDS^-. Ionpair formation leads to a change in the symmetry of the relevant FMOs which may lead to the absorption in the higher wavelength.

Table III.6. Oscillator strengths (f), transition dipole moment (μ_x, μ_y and, μ_z), molecular orbital contributions (H = HOMO and L = LUMO), and corresponding absorption wavelength (λ_{max}) together with percentage error in λ_{max} for each system. The values in bracket correspond to gaseous phase.

System	F	Transition	λ_{max}(nm)	Error in λ_{max} (%)[a]
AOH^-Cl^-	0.81	H→L = 0.69 H-1→L+1=0.13	443.78 (433.33)	10 (12)
DSIP	0.82	H→L = 0.69 H-1→L+1 =0.13	446.29 (458.76)	10 (8)
$AOH_2^{2-}Cl^-$	0.29	H→L = 0.60	475.22 (473.13)	10 (11)
PDSIP	0.31	H→L = 0.60	478.94 (476.22)	8 (9)

[a]Error (%) corresponds to the difference between the calculated λ_{max} (nm) and the experimental values in aqueous solution.

Thus, from the UV-Visible absorption spectral observation supported with fluorescence and surface tension data of the systems, for the first time, we show that AO undergoes protonation in some of the DSIPs. The experimental observations have been supported by theoretical calculations using time dependent density functional theory (TD-DFT). The electronic structures and spectral characteristics of these complexes have been studied extensively and our computed results validate the experimental prediction that the dye gets partially protonated in presence of surfactant in submicellar concentrations.

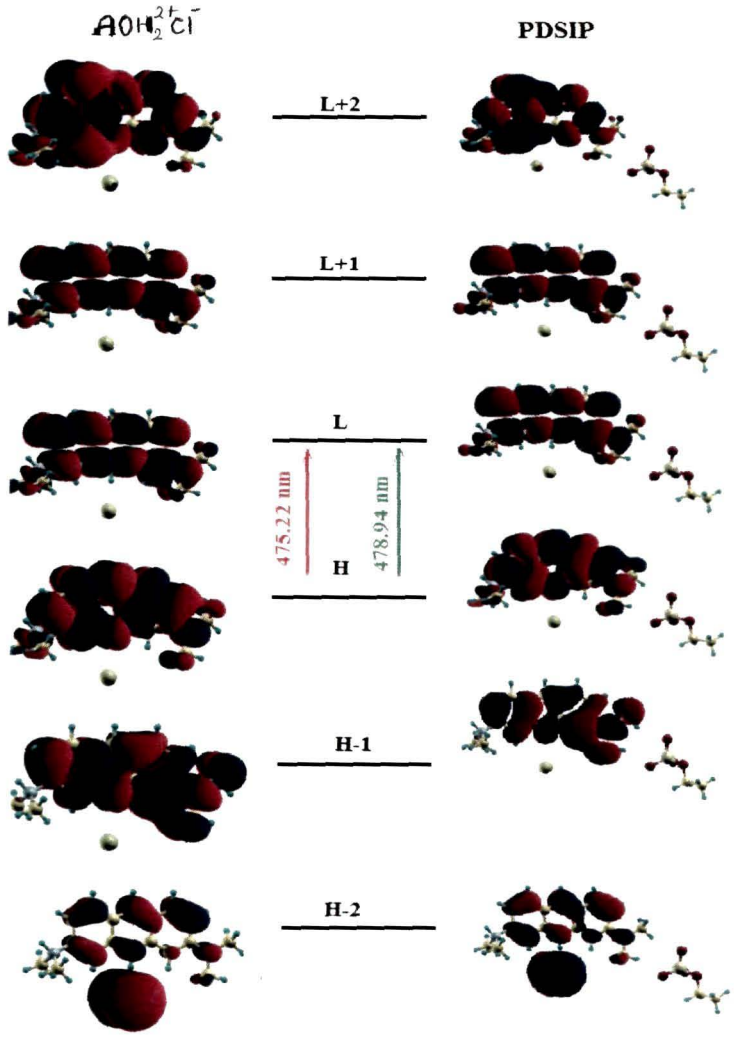

Fig.III.19. Orbital energies and of FMOs of $AOH_2^{2+}Cl^-$ and $AOH_2^{2+}Cl^-$.ES (PDSIP) and their wave function plots together with corresponding transitions.

III.3. Stabilization of the β-diketo tautomer of curcumin in premicellar ionic surfactants

Curcumin, (1E,6E)-1,7-bis(4-hydroxy-3-methoxy phenyl)-1,6-heptadiene-3,5-dione, also known as C.I. Natural Yellow (**Fig.III.20.**), is a hydrophobic polyphenol obtained from the dried rhizomes of *Curcuma longa* Linn[325]. It was first isolated from turmeric nearly two centuries ago and its chemical structure as diferuloylmethane was identified in 1913[326] and confirmed in 2005[327]. It is approved as a food additive by World Health Organization and Food and Agriculture Organization[328]. It is used as a spice and as a coloring agent in cosmetics, pharmaceuticals, and hair dyes[329]. It has attracted great interest in recent years because of its outstanding divergent medicinal activities, *viz.*, anticancer[330], antioxidant[331], antimicrobial[332], antiamyloid[333], anti-ischaemic[334], anti-inflammatory[335] etc., adding new dimensions in the branch of medicinal chemistry. The upsurge in research activities over the past decade on Curcumin is largely due to the discovery that Curcumin possess the ability to prevent protein aggregation in debilitating diseases such as Alzheimer's and Parkinson's[336-338]. It also has potential in the treatment of cystic fibrosis[336] and can be considered as a model substance for the treatment of HIV infection[340-342].

Curcumin has two tautomeric forms - the *cis* enol curcumin and the β-diketo curcumin, and these keto and enolic forms can also exist in different *cis* and *trans* forms[343,344]. The relative contribution of the different keto and the enol forms depends on the factors such as temperature, polarity of the solvent and the substitution on the aromatic rings. Under physiological conditions, it exhibits keto-enol tautomerism having a predominant β-diketo form in acidic and neutral solutions and a stable keto-enol form in alkaline media[346]. Some important medicinal activities of curcumin were attributed to its β-diketo tautomeric form[345]. Aqueous curcumin exists in its neutral (AH_3) form up to *p*H 8 and in protonated (AH_4^+) form at *p*H < 1[344,346] (**Fig.III.20**). It is reported to have three pK_a values at 8.38, 9.30 and 10.69 [347,348] which correspond to its deprotonation of the AH_3, AH_2^- and AH_2^- forms, respectively. Aqueous curcumin is characterized by a broad peak at 425 nm with a small shoulder at 355 nm corresponding to the absorbances of the diferuloyl structure and the feruloyl unit, respectively[347].

Most of the previous reports on curcumin-surfactant systems were with concentrations of the surfactant above CMC, where the nature of the interactions is somewhat simple and better-known[220-224]. Leung *et al.* and Tonnensen *et al.* used

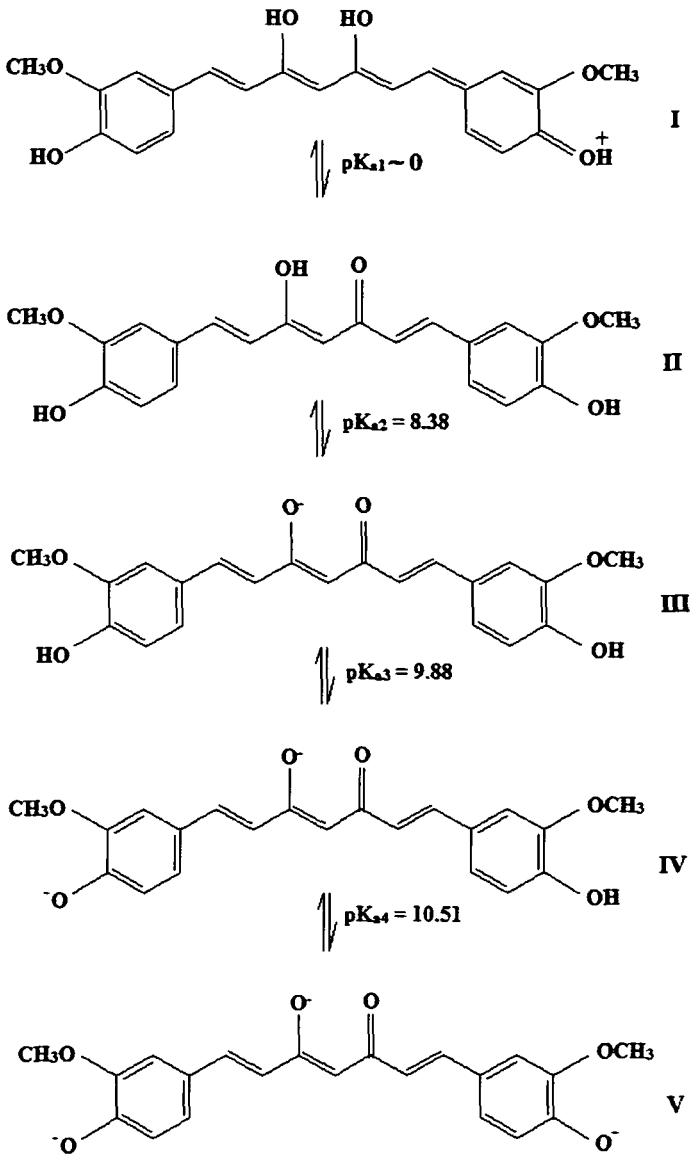

Fig.III.20. Prototropic equilibria of aqueous (25.0 μmol dm^{-3}) curcumin along with the pK_a's [344].

cationic micelles to entrap the curcumin molecule within its hydrophobic micellar core[220,222]. Within the nonpolar core only the keto-enol forms of curcumin is predominant irrespective of the medium *p*H.

As already mentioned in the introduction section, Ke *et al.* have reported a striking interaction of curcumin with a cationic surfactant, viz., dodecyltyimethylammonium bromide (DTAB) in submicellar concentrations at *p*H 5.00[276]. Based on the fluorescence spectral evidences, they attributed an observed UV-Visible band at λ_{max} of 355 nm of

curcumin under the experimental conditions to a complex formation between curcumin and the cationic surfactant. After this, a spectral study on the stabilization of the β-diketo tautomer in presence of submicellar cationic and anionic surfactants as well as in polymers was also carried out[277]. In considering the potential mechanisms for its range of biological activities, it is important to acknowledge the inherent chemical features of the curcumin molecule, specially, because the antioxidant activity of curcumin is attributed to its diketo tautomer. Therefore, we extended the study to surface tension and a detail steady state fluorescence measurements and TD-DFT calculations. To have a complete picture of the interaction, UV-visible study was also done in the entire *p*H range of 2.00 to 7.50. We also have examined the salt effect on the keto-enol tautomerism of curcumin observed in the submicellar solutions. The study on the stabilization of β-diketo tautomer curcumin in aqueous premicellar ionic surfactants has been presented in two different subsections below.

III.3.1. Curcumin in Submicellar Cationic Surfactant Solutions*

III.3.1.1. UV-Visible spectral study

Although the changes in absorption behavior of aqueous curcumin caused by cationic surfactants have been studied[276,277], the absorption spectra of curcumin in the presence of cationic surfactants varying in chain length as well as head group and counter ion, have been studied in the entire *p*H range of 2.00 to 7.50 for clarity and completeness. The variations in spectral properties of aqueous curcumin (25.0 μmol dm^{-3}) in the presence of five cationic surfactants, in buffered solutions have been studied. **FigIII.21** shows that as the concentration of the CTAB increases from $1.8x10^{-5}$ mmol dm^{-3}, the main absorption band of curcumin at 425 nm loses its intensity gradually into a broad shoulder at 355 nm while this shoulder at 355 nm increases gradually into a clear peak. .

It is also observed that the new absorption peak at 355 nm above CTAB $8x10^{-5}$ mol dm^{-3} has some red shifts when [CTAB] increases from $8.0x10^{-5}$ to $2.0x10^{-4}$ mol dm^{-3} (**Fig.III.21**). This indicates that there is an allowance of a low-energy π-π^* excitation of the conjugated curcumin structure because of the coupling between the electric transition dipole moments of the two feruloyl chromophore units[349].

This work has been published in **J. Mol. Liq. 187 (2013) 350-358.*

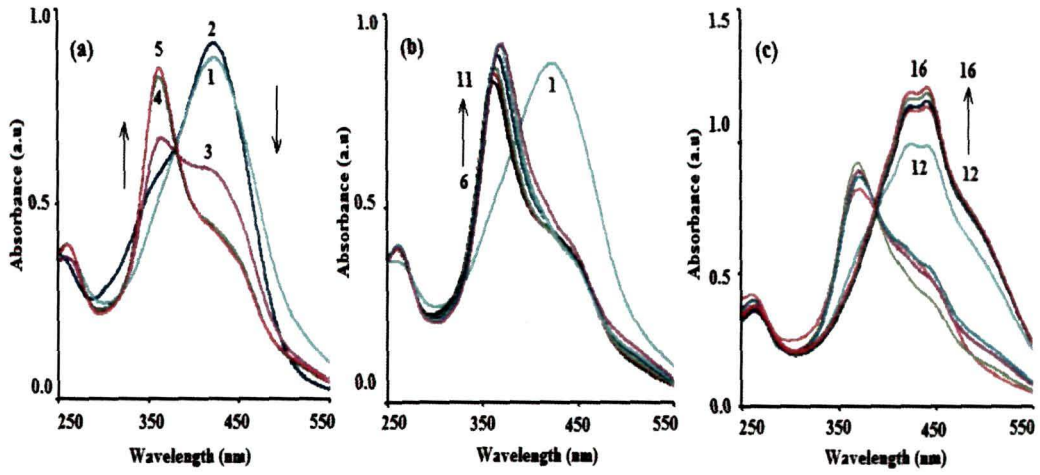

Fig.III.21. UV-visible spectra of curcumin ($2.5x10^{-5}$ mol dm^{-3}) in presence of various concentrations of CTAB at *p*H 7.00 and 298 (±1) K: [CTAB] / (10^{-5} mol dm^{-3}) = (a): (1) 0.00, (2) 1.0, (3) 2.0, (4) 4.0 and (5) 6.0; **(b):** (6) 8.0, (7) 10.0, (8) 12.0, (9) 14.0, and (10) 18.0; (11) 20.0; **(c)** (12) 40.0, (13) 60.0, (14) 80.0, (15) 100.0, and (16) 120.0.

Therefore, the absorption peak of aqueous curcumin at 425 nm and a shoulder at 355 nm, correspond to the absorptions of the conjugated diferuloyl structure and the feruloyl unit respectively. The opposite changes of the absorption bands at 425 nm and at 355 nm at [CTAB] less than $0.20x10^{-3}$ suggests that binding of CTAB with curcumin can destroy or recover the conjugated structure of curcumin. Moreover, had the binding between the CTAB and curcumin occurred at the active groups in the aromatic rings of curcumin, the added surfactant would have lowered the absorption intensities of curcumin at both 425 nm and 355 nm. However, this is not observed.

The β-diketone group has maximum electron density[350] in the structure of curcumin and it has been reported to form chelated complexes with metal ions such as Na^{+}, Cu^{2+}, Mg^{2+} and Al^{3+} (ref. 351), etc. The positively charged head group of CTAB interacts electrostatically with the β-diketone group of curcumin to form CTAB/curcumin complex. The binding of the CTAB molecule to the central methylene bridge of the two feruloyl units breaks the extended aromatic conjugation in the planar geometry of curcumin. Thus, at [CTAB] from $0.18x10^{-5}$ mol dm^{-3}, the 355 nm bands appears persists up to [CTAB] of $0.20x10^{-3}$ mol dm^{-3}, and then at [CTAB] > 20 mmol dm^{-3}, the 425 nm band reappears at 420 nm. The inversion of the absorption pattern of curcumin above [CTAB] = 20 mmol dm^{-3} indicates the departure of the head of CTAB from the β-diketone group of curcumin and the recovery of the planar conjugated enol form.

It is reported that ionic micelles can shift the pK_a of dyes up to 2 units due to difference in electric potential between the bulk and the micelle surface[180]. On the other hand the ionic submicellar surfactants are reported to shift the pK_a of dyes up to 5-6 units in dye-surfactant ion pairs through combined hydrophobic-electrostatic interactions, including H-bonding, resulting in a strong electron withdrawing or releasing effects[296]. We could find a new peak at 454 nm at surfactant concentrations above the CMC at *p*H 7.00 unlike that obtained earlier[277]. This new peak is due to deprotonation of enolic proton whose pK_a corresponds to 8.38. Thus cationic micelles at *p*H 7.00 which is close to the second pK_a (**Fig.III.20**) of curcumin can deprotonate the proton stabilized by hydrogen bonding. This new peak was observed in case of all the cationic surfactants except DTAB[277] at *p*H 7.00 which can be seen in **Fig.III.22** and **Fig.III.23** for CPB and CPC, respectively.

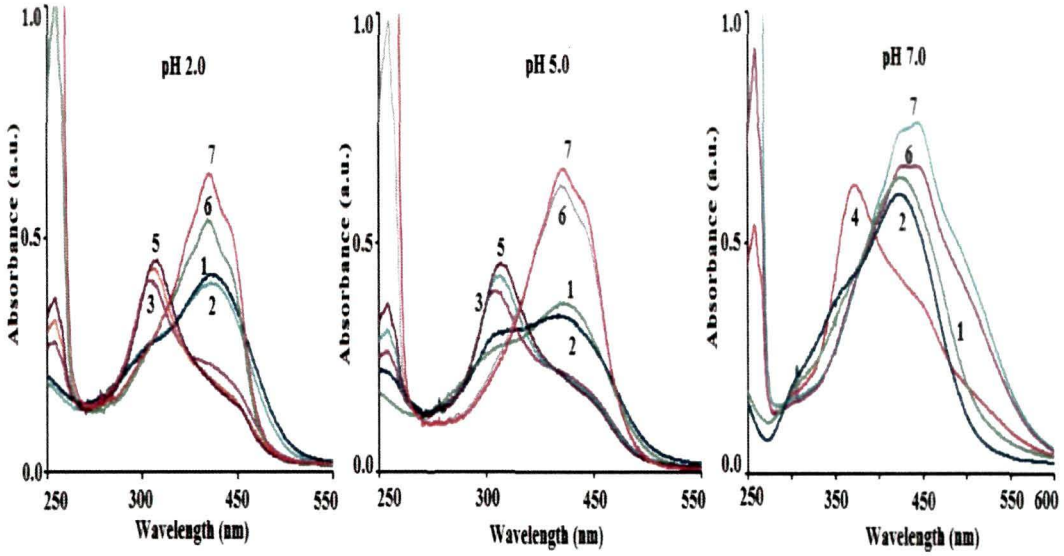

Fig.III.22. UV-visible spectra of curcumin (2.5×10^{-5} mol dm^{-3}) in presence of various concentrations of CPB at 298 (±1) K: [CPB] / (10^{-5} mol dm^{-3}) = (a): (1) 0.00, (2) 1.0, (3) 5.0, (4) 10.0 (5) 20.0, (6) 40.0, (7) 60.0

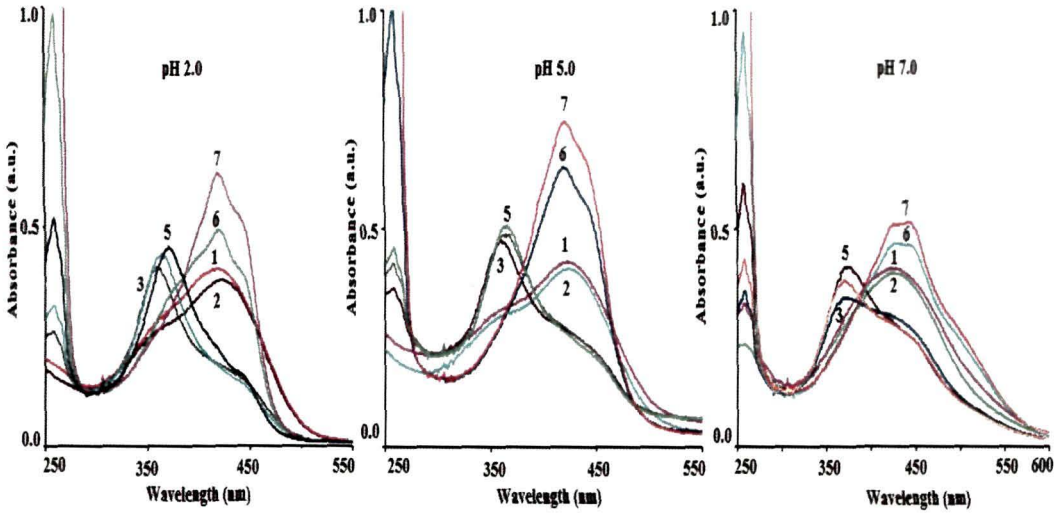

Fig.III.23. UV-visible spectra of curcumin (2.5×10^{-5} mol dm^{-3}) in presence of various concentrations of CPC at 298 (±1) K: [CPC] / (10^{-5} mol dm^{-3}) = (a): (1) 0.00, (2) 1.0, (3) 5.0, (4) 10.0, (5) 20.0, (6) 40.0, and (7) 60.0.

The spectra of aqueous curcumin observed at a higher ionic strength of 0.06 (in presence of 0.05M KBr) at *p*H 5.00 in presence of varying concentrations of CTAB, TTAB and DTAB have been studied and are also presented in **Fig.III.24, Fig.III.25** and **Fig.III.26,** respectively.

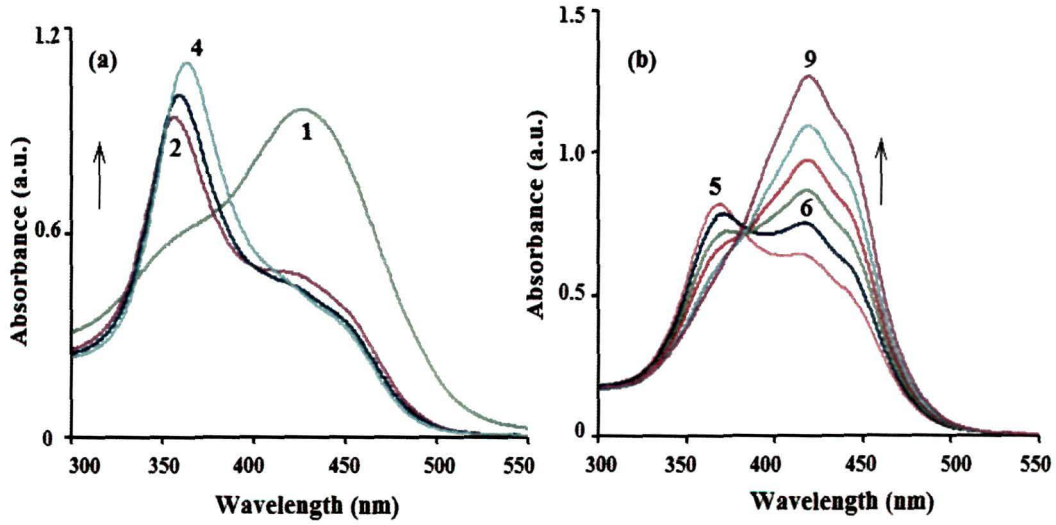

Fig.III.24. UV-visible spectra of curcumin (2.5×10^{-5} mol dm^{-3}) in presence of various concentrations of CTAB at *p*H 5.00 (*I = 0.06*) and 298 (±1) K: [CTAB] / (10^{-5} mol dm^{-3}) = (a): (1) 0.00, (2) 0.9, (3) 1.0, (4) 3.0; **(b):** (5) 6.0, (6) 8.0, (7) 10.0, (8) 12.0, and (9) 14.0

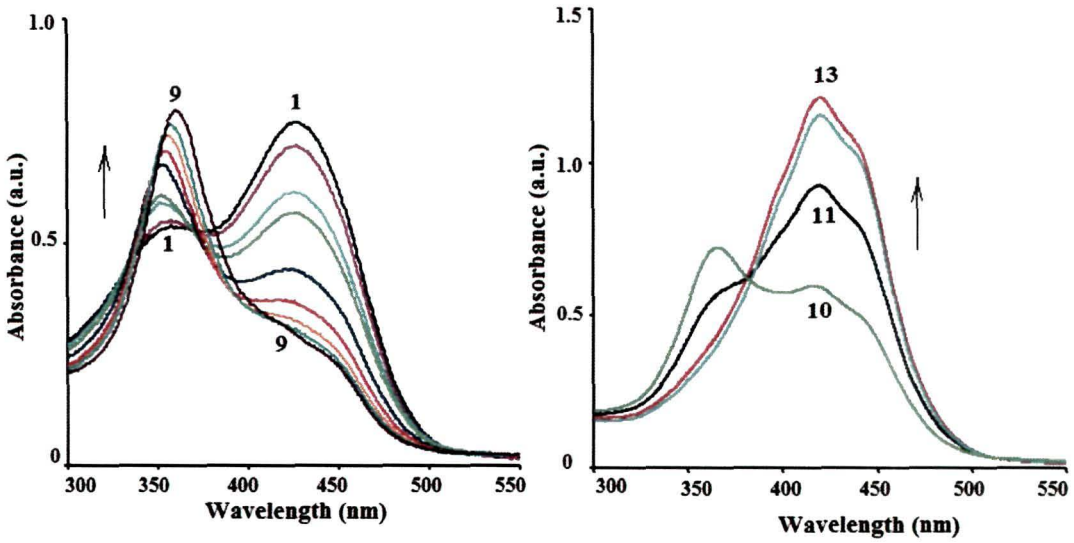

Fig.III.25. UV-visible spectra of curcumin (2.5×10^{-5} mol dm^{-3}) in presence of various concentrations of TTAB at *p*H 5.00 (*I = 0.06*) and 298 (±1) K: [TTAB] / (10^{-5} mol dm^{-3}) = (a): (1) 0.00, (2) 1.0, (3) 2.0, (4) 4.0 (5) 6.0 (6) 8.0, (7) 10.0, (8) 20.0, (9) 30.0; **(b):** (10) 40.0, (11) 60.0, (c) (12) 80.0, and (13) 10.0.

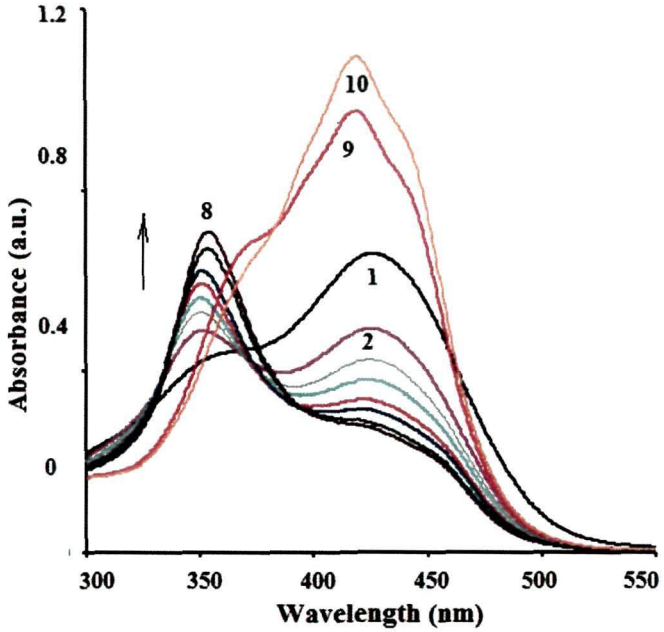

Fig.III.26. UV-visible spectra of curcumin (2.5×10^{-5} mol dm^{-3}) in presence of various concentrations of DTAB at *p*H 5.00 (*I = 0.06*) and 298 (±1) K: [DTAB] / (10^{-3} mol dm^{-3}). (1) 0.00, (2) 0.90, (3) 1.20, (4) 2.0, (5) 3.0, (6) 4.0, (7) 5.0, (8) 6.0, (9) 8.0, (10) 10.0.

It is observed that at higher ionic strength, aqueous curcumin exhibited similar trends of appearance/disapperance of the band at 355 nm, however, the band appeared with higher absorption intensities at a lower concentration (e.g., 0.9×10^{-5} mol dm^{-3} CTAB) also reverted to the 425 nm band at a lower concentration (e.g., 1.0×10^{-4} mol dm^{-3} of CTAB) compared to that at the ionic strength of 0.01.

III.3.1.2. Equilibrium analysis

The presence of isosbestic points in the spectra of curcumin in presence of the cationic surfactants indicates equilibrium between the free dye and surfactant with their complex. Assuming the interaction to be of 1:1 stoichiometry, the interaction can be represented as follows:

$$S^+ + C \underset{}{\overset{K_c}{\rightleftharpoons}} S^+C \qquad \text{III.8}$$

and

$$K_c = [S^+.C] / [S^+] [C] \qquad \text{III.9}$$

where, S^+, C and $S^+.C$ represent the surfactant, the dye and their complex, respectively. The equilibrium binding constant, K_c has been determined by using the equation[277,352]:

$$\frac{d_o}{d-d_o} = \frac{\varepsilon_d}{\varepsilon_c} + \frac{\varepsilon_d}{\varepsilon_c K_c}\left(\frac{1}{C_S}\right) \qquad \text{III.10.}$$

where, d and d_o are the observed absorbances of the curcumin solutions at the λ_{max} of the complex in the presence and absence of surfactant, respectively. ε_d and ε_c are molar extinction coefficients of the dye and its complex, respectively and $C_s = [S^+]$.

The plots of $1/(d-d_o)$ *vs.* $1/C_s$ were found to be linear with squired correlation coefficient between 1 and 0.981. The observed large values of K_c (**Table III.7**) are comparable to those reported in similar oppositely charged dye-surfactant systems[212,217,218]. The K_c increased by over an order on increasing the ionic strength from 0.01 to 0.06. We report the K_c values at ionic strength of 0.06 of all the surfactants at *p*H 5.00 only (**Table III.8**). Since, curcumin is as such electrically neutral in the experimental *p*H range, the increase in the interaction with ionic strength may be indicative of a secondary salt effect suggesting involvement of an acid-base interaction in the complex formation. The presence of aromatic pyridinium ring in the head group did not show any prominent effect

on the spectra of aqueous curcumin. The K_c was found to increase on changing the surfactant in the order: DTAB < TTAB < CPB < CPC < CTAB[151].

The K_c showed a considerable increase with increase in the chain length of the surfactant indicating an important role of hydrophobic interaction in the complex

Table III.7: The binding constants (K_c) of curcumin with cationic surfactants at 298 (±1) K.

Surfactant	λ_{max} of the complex (nm)	pH	$K_c/(10^3 M^{-1})$* at ionic strength 0.01	$K_c/(10^3 M^{-1})$* at ionic strength 0.06
CTAB	353.5	7.00	3.26[a]	42.4
		6.00	3.42	
		5.00	3.47[a]	
		4.00	3.28	
		3.00	3.21	
		2.00	3.12[a]	
TTAB	351.5	7.00	2.83[a]	36.9
		5.00	2.99[a]	
		2.00	2.68[a]	
DTAB	349.5	7.00	2.47[a]	35.2
		5.00	2.59[a]	
		2.00	2.29[a]	
CPC	357.5	7.00	3.14	31.1
		5.00	3.34	
		2.00	3.07	
CPB	356.5	7.00	3.12	26.5
		5.00	3.20	
		2.00	2.88	

*Experimental error limit = ±5%, [a]data from ref. 277.

formation. Moreover, the appearance of the 355 nm UV-band of curcumin is not seen in presence of Tetra-n-butylammonium bromide (TBAB) salt which lacks a hydrophobic tail in its structure which indicates that the interaction is hydrophobicity induced. As the head group of the surfactant changes from cetyltrimethyl ammonium to pyridinium ring in CPC and CPB, delocalization of positive charge of the head group occurs and the electrostatic attraction between the head group and electronegative oxygen atoms of curcumin becomes weaker, so the complex formation decreases and the K_c gives smaller values (**Table III.7**) compared to that of CTAB inspite of having similar tail lengths. Replacement of the counterion of the surfactant from Br^- in CPB to Cl^- in CPC causes an increase of the complex formation as observed from the pC_{20} values (**Table III.8**). This phenomenon is

originated from the size difference between the ions. A larger size of Br^- makes its hydration difficult, so these ions are preferred rather than Cl^- ions to bind to the surfactant molecules. As a result, freedom of the surfactant molecules to interact with curcumin molecules is lowered. Cl^- counterion is reported to have larger contribution towards micellization[1] and submicellar dye-surfactant interactions[238] than the Br^- counterion. These observations indicate that the interaction between the dye and the surfactants is highly influenced by conditions of the medium and the structural properties of both the dye and the surfactant

The value of K_c is largest at *p*H 5.00 and decreases gradually as we go away from it to either side (**Table III.7**). Although the Ketelaar does not give highly accurate K_c, this trend vs. *p*H is very clear from the table. This analogy with enzyme reactions can be explained on the basis of dominance of the nonionic form of curcumin at *p*H 5.00. The interaction gradually disappears as the nonionic form changes to the mono-anionic form of curcumin on approaching the 2^{nd} pK_a (7.7-8.5) and also as the nonionic form changes to the mono-cationic form on approaching the 1^{st} pK_a (<0) (**Fig.III.20**). The ionic forms of curcumin are obviously less hydrophobic than the nonionic form predominating around *p*H 5.00. A strong hydrophobic interaction between the surfactant tail and the curcumin molecule seems to be crucial for the stabilization of the β-diketo form as only the nonionic form of curcumin shows the interaction.

The observed secondary salt effect in the present case indicates an involvement of acid-base interaction in the dye-surfactant complex formation. However, the absence of such complex formation by the ionic curcumin forms (I, III, IV & V) makes it difficult to understand the mechanism of the salt effect. An increase in the hydrogen ion concentration probably facilitates protonation of the central methylenic carbon atom of curcumin which in turn facilitates the removal of the enolic proton from oxygen atom favoring the formation of the diketo tautomer. Since only the diketo form complexes with a cationic surfactant head group, the complex formation is favored by the increase in the ionic strength.

III.3.1.3. Surface Tension study

The surface tension behavior of the buffered solutions on increasing the concentration of the surfactants in the absence and presence of curcumin at *p*H 7.00 are shown in **Fig.III.27**. The CMC of the surfactants in the buffer solution in the absence of curcumin

(**Table III.8**), as estimated from the curves, are lower than the CMCs in water because of the presence of the buffer components[217,218].

But, interestingly, the decrease in the surface tension of the solutions was more rapid in the presence of curcumin (25.0 μmol dm^{-3}) than that in its absence indicating a considerably higher efficiency[212,217,218,253,254] of the surfactant in the presence of curcumin. The values of pC_{20}, also markedly decreased in the presence of curcumin (**Table III.8**). For, example, the pC_{20} has been found to be 3.69 and 4.69 for CTAB in the absence and the presence of curcumin, respectively, which were attributed to a nonionic surfactant-like nature having a large head group of the dye- surfactant ion pairs formed at submicellar concentrations. Curcumin, being nonionic in the experimental *p*H range, is incapable of forming ion pairs. But the observed higher efficiency of the complex suggests that the complex still behaves like a cationic surfactant with a larger head group than the original cationic surfactant. A larger head group of the complex occupies larger surface area of the solution reducing the surface tension more rapidly[311]. The complex may form a monolayer at the air/water interface and any change in the structure of the monolayer at the air/water interface affects the surface tension, γ of a solution. In this case, the dye-surfactant complexes have larger head groups than that of the corresponding cationic surfactants and therefore occupy a larger surface area per surfactant in the monolayer at the air/water interface compared to that of the individual cationic surfactant. A larger surface area per surfactant leads to a lower CMC of the complex (CMC_c). **Fig.III.27** shows change in trend in the surface tension behavior in the surface tension *vs.* surfactant concentration curves

Table III.8: CMC* of the surfactants, pC_{20} values in presence of buffer and in presence of buffer and aqueous (25.0 μmol dm^{-3}) curcumin at *p*H 7.00.

Surfactant	CMC/(mol dm^{-3})		pC_{20}, in	
	Buffer	Buffer and curcumin	Buffer	Buffer and curcumin
CTAB	4.08×10^{-4}	4.00×10^{-4}	3.69	4.69
TTAB	2.82×10^{-3}	3.01×10^{-3}	2.92	4.22
DTAB	1.02×10^{-2}	8.13×10^{-3}	2.52	3.22
CPB	8.12×10^{-4}	9.01×10^{-4}	3.698	4.39
CPC	6.03×10^{-4}	4.07×10^{-4}	3.698	4.32

Experimental error limit = ±5%

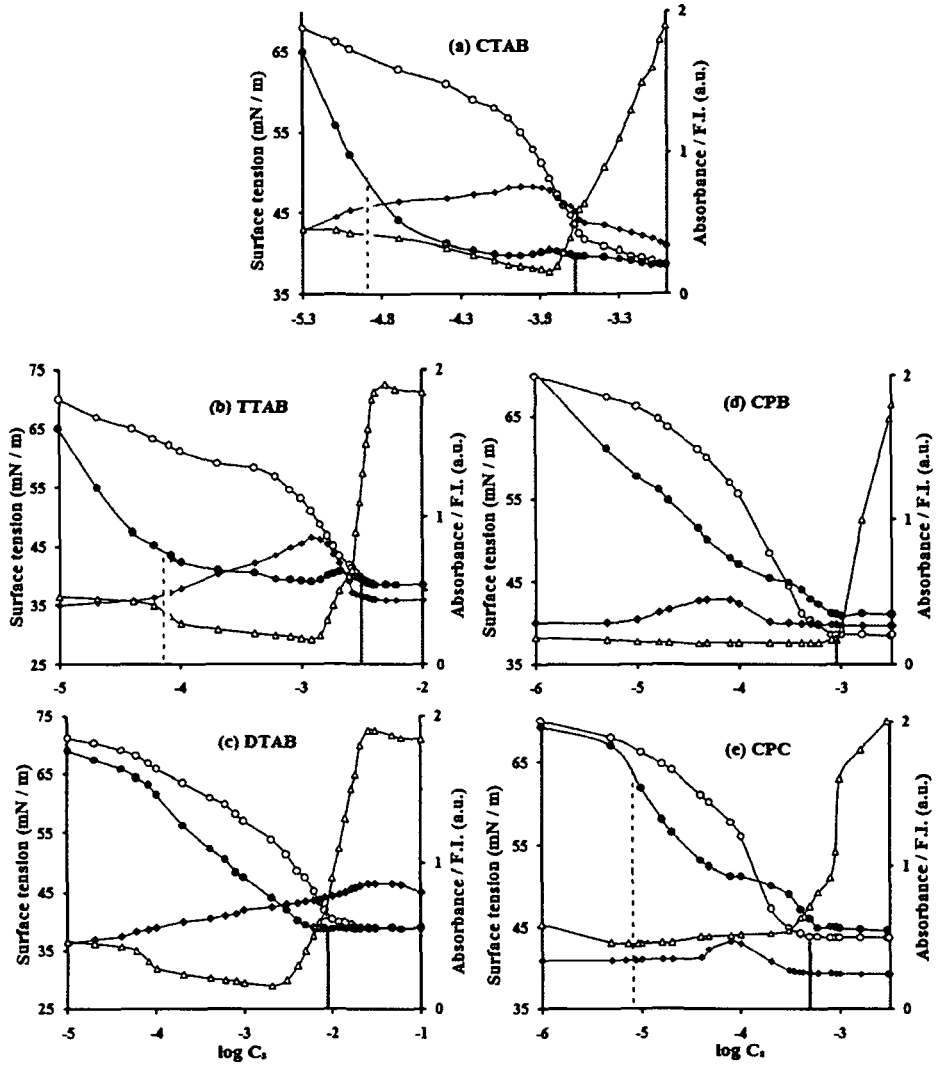

Fig.III.27. Plot of surface tension and absorbance of curcumin (25.0 μmol dm^{-3}) as a function of concentration of (a) CTAB (b) TTAB and (c) DTAB (d) CPB, and (e) CPC at *p*H 7.00 at 298 (±1) K. Symbols: Surface tension of aqueous surfactant in absence (○) and in the presence (●) curcumin, absorbance (♦) at 355 nm and FI / 10^2 (Δ) at 535 nm. The vertical orange bars indicate the CMC values.

with CTAB, TTAB and CPC as was reported with oppositely charged dye-surfactant ion pairs[217]. These points (concentration of the surfactant) after which the rapid decrease in surface tension of the surfactant in presence of curcumin decreases, correspond to micellization of the respective complexes. The surface tension *vs.* logarithm of surfactant concentration plots, in the presence of curcumin; also indicate changes in the slopes around the concentrations of surfactants where the β-diketo band starts to appear as shown

in **Fig.III.27**. The slopes of the curve before the breaks showed a significant decrease with decrease in the surfactant chain length. The changes in the slopes and the increase in the efficiency of the cationic surfactants in the presence of curcumin can be attributed as the possibility of formation of surface active curcumin-surfactant complexes. The complex is formed due to cooperative attractive forces between the partial negative charges of the electron rich electronegative O-atoms of curcumin and the positively charged cationic surfactant head groups and the hydrophobic forces.

III.3.1.4. Fluorescence spectral behavior:

The λ_{max} of the fluorescence band of curcumin shifts from 517 nm to 439 nm on lowering the polarity of the solvent[353-357]. Similarly, with decrease in the hydrogen bonding ability of the solvent, i.e., on going from protic to aprotic solvent, the λ_{max} showed blue shift[355,357]. Thus, the greater the interaction with water, the lesser is the extent of blue-shift. It was reported that the fluorescence intensity (FI) of the fluorescence band of curcumin with emission λ_{max} at 570 nm decreases with increase in the concentration of DTAB up to the CMC and above that along with a shift of the λ_{max} to about 500 nm[277]. We have examined the fluorescence behavior of curcumin in more detail as a function of the surfactant concentration in presence of all the five surfactants. The spectra with CTAB have been shown in **Fig.III.28**. The fluorescence intensities (FI) at 535 nm for all five surfactants have been included in **Fig.III.27**. Though we observed the λ_{max} of emission at 570 nm in pure water, we have observed the λ_{max} of emission at 535 nm (after being excited at 425 nm) in our solutions as the solutions in our case contained a small amount of methanol used for dissolving curcumin may be one of the possible reason for the shift. This small shift in emission λ_{max} may be attributed to a variation in the solvent polarity[353-357]. This red-shift in the fluorescence maximum as observed here after going water : methanol mixture to pure water ($\Delta\lambda \approx 20$ nm), indicates that the exited singlet state must be very polar.

It can be noted that the FI actually started to decrease only on addition of surfactant above the CMC_c, i.e., on micellization of the curcumin-surfactant complex. The FI decreased to a minimum indicating an increase in the polarity of its environment as the micelles of the complex consolidate with increase in the surfactant concentration (**Fig.III.27**). However, over the range of *p*H 2.00-7.50, the FI is not much affected with the change in *p*H. In presence of submicellar CTAB, curcumin may experience a more polar environment through increased exposure to more hydrophilic region and hence the

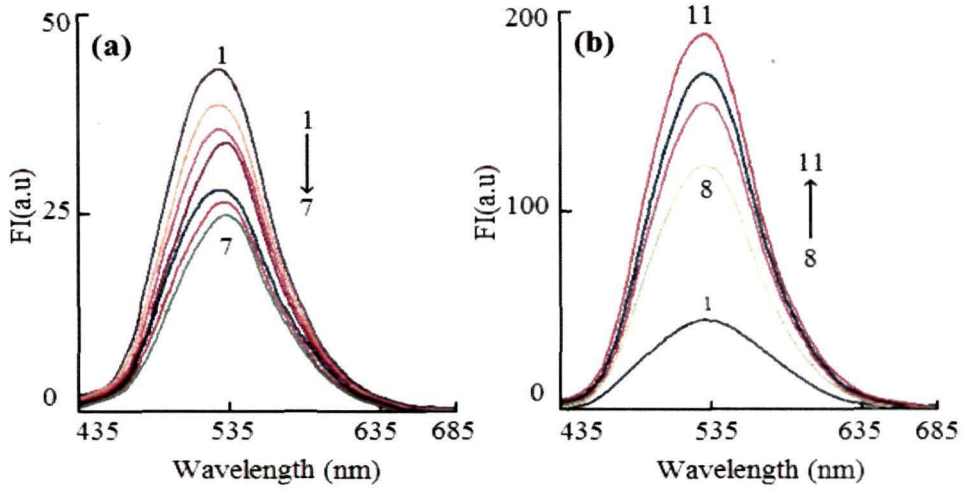

Fig.III.28. Fluorescence spectra of curcumin (25.0 μmol dm^{-3}) in presence of CTAB at *p*H 7.00 and temperature 298 (±1) K: [CTAB] / (mmol) **(a):** (1) 0.00 (2) 0.05 (3) 0.08 (4) 1.00 (5) 1.40 (6) 1.80 **(b):** (7) 2.00 (8) 3.00 (9) 4.00 (10) 6.00 (11) 8.00.

fluorescence quenching. The presence of bromide ion may partly affect the fluorescence intensity (FI) as reported for DTAB surfactant[276]. Our observations for curcumin in submicellar cationic surfactants indicate that, there is a probability of formation of a weak fluorescent complex between the fluorescent curcumin and the cationic surfactants. We can attribute it as the formation of a weak dye-surfactant complex between the β-diketo form of the curcumin and the $CTA^+/TTA^+/DTA^+/CP^+$ head groups.

Even though all curcumin molecules may exist in several tautomeric forms as well as geometric (*cis-trans*) isomeric forms of enol configuration, the fluorescence spectra exhibit no wavelength dependency on these forms[346]. The spectra recorded at different absorption maxima gave fluorescence maximum at 535 nm only. The fluorescence intensity (FI) of the band with λ_{max} of 535 nm of 25.0 μmol dm^{-3} buffered curcumin decreased slightly as [CTAB] increased above 0.025 mmol, reached a minimum 1.80 mmol dm^{-3} of CTAB and then showed a marked increase (**Fig.III.28**). As the changes in the trends in the surface tension behavior coincide with the appearance of the UV band of the β-diketo tautomer and the lowering of the FI, the tautomerization perhaps takes place upon micellization of the complex (premicelles). This suggests that the β-diketo tautomer is stabilized in the curcumin-cationic surfactant premicelles. While the marked increase in the intensity at higher concentrations of the surfactant can be attributed to curcumin solubilized in nonpolar environment of micelle core, the initial decrease in the intensity is indicative of a more polar environment of the dye which is possible only through ion-

dipole interaction of the cationic head group of the surfactant with the two electronegative oxygen atoms of the curcumin molecule.

At concentrations above 10 mmol dm^{-3}, there was a shift of the fluorescence maximum to ≈500 nm. The increase in the fluorescence intensity above 2.00 mmol dm^{-3} of CTAB coincided with the disappearance of the UV- absorption band of the diketo form. At [CTAB] > 2.00 mmol dm^{-3}, curcumin is solubilized in the planar keto-enol form in the nonpolar micellar core of CTAB, which is reflected by the appearance of the 420 nm band. Therefore, the ion-dipole binding must be through the β-diketo group breaking the conjugation of the dye to be consistent with the observed changes of the UV-Vis spectra. Since the UV-band does not appear in the high concentration above the CMC of the surfactants, we have not studied further in this concentration range.

The FIs at 535 *vs.* the surfactant concentrations showed almost similar trends for all five surfactants except observation of change in the trends at different concentrations for different surfactants. This indicates similar interactions of curcumin with all five cationic surfactants with variation in the strengths of the interaction and the concentration ranges where the dye is under a particular type of microenvironment.

III.3.1.5. Computational study of curcumin – cationic surfactant interactions

The DFT optimized structures of curcumin, the model surfactant (EA) and the proposed interaction products have been shown in **Fig.III.29**. We have also performed the vibrational energy calculations to confirm the local energy minimum structures for all the molecules. From the fully optimized geometries, we find that the keto-enol curcumin stabilizes in planar geometry with a cis-configuration of two oxygens forming hydrogen bonds while the diketo curcumin stabilizes in a V-shaped geometry as reported earlier[348,357]. Geometry optimization starting with the syn-diketo structure did not produce a minimum, and it rearranged to the anti-diketo form. The calculated gas phase and methanol phase energy of the keto-enol form of curcumin has been found to be lower than that of the diketo form by ≈ 7.39 kcal mol^{-1} and 7.81 kcal mol^{-1} respectively which agrees with the reported values[348,357]. A possibility of preferred complexation of the surfactants with diketo curcumin compared with its keto-enol tautomeric form exists which could rationalize the observed experimental UV band at submicellar solutions.

To obtain insight on the charge density profile and bonding aspects, we have performed calculations of the natural bond orbital (NBO) and natural electronic configuration. As can be seen from the relaxed structures of the individual molecules and

the complex as shown in **Fig.III.29,** the diketo curcumin could not retain its anti-configuration in presence of EA. In presence of EA, the anti-diketo curcumin stabilizes with the orientation of the electronegative oxygen atoms towards the positive EA moiety. This indicates interaction between the EA moiety with the two electron rich O-atoms of the β-diketo tautomer of curcumin which would otherwise take an anti orientation. We find that the shortest distance of separation (as measured from the closest H-atom of the methyl group attached to the N-atom of EA to the closest O atom of curcumin) between curcumin and EA is within 2.395 Å. From natural population analysis (NPA), we also find that there is a small amount of fractional charge transfer from diketo curcumin to EA. We also observe that the re-distribution of electronic charges in diketo curcumin moiety occurs in presence of EA and the excess transferred charge is mainly localized on $2P_z$ orbital of N. The very small value of charge transfer in the complex indicates that the interaction does not mainly govern through the electrostatic Coulombic interaction, ion (EA)-dipole (curcumin) and van der Waals interactions may significantly contribute to the overall stability of the complex between the β-diketo curcumin and EA. Inclusion of solvent effect causes a very huge change in the of EA complex stabilization viz. -21.27 kcal $mole^{-1}$ in gas phase to -6.71 kcal $mole^{-1}$ in methanol phase. We find that the HOMO-LUMO energy of diketo curcumin reduces ≈ 0.44 e.V on complexation (**Table III.9**) with EA.

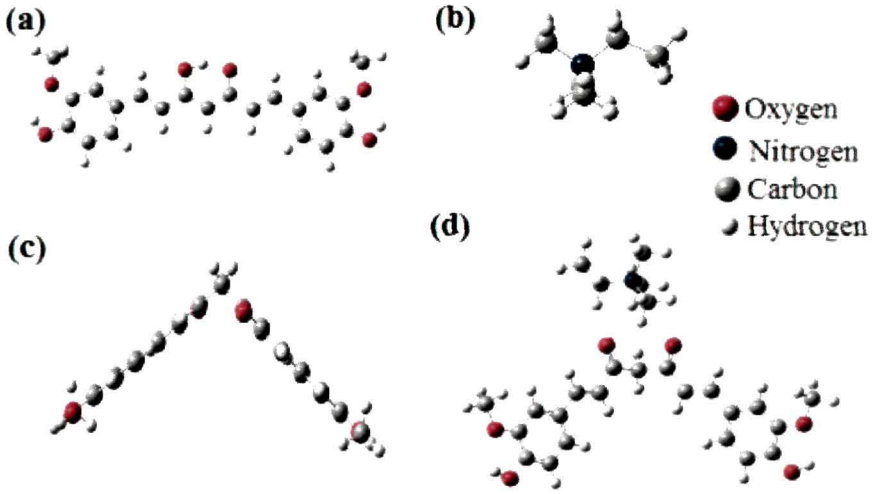

Fig.III.29. The optimized structures of all the individual molecules and complexes: (a) ketoenol curcumin, (b) EA, (c) β-diketo curcumin and (d) β-diketo curcumin.EA complex.

To understand the observed shifts in peak position in UV-Visible absorption spectra upon complexation with the surfactant, we have carried out TD-DFT computations on the ground state optimized geometries of free keto-enol and diketo

Table III.9. Relevant terms for the individual tautomers and the complex with EA. ΔE_{stab}, ΔE_{H-L} and CT representing stabilization energy, HOMO-LUMO energy gap, and charge transfer, respectively. The values within parentheses correspond to methanol as solvent. H and L stand for HOMO and LUMO respectively.

System	ΔE_{stab} (kcal mol^{-1})	ΔE_{H-L} (eV)	CT (e)	Transition energy (nm)	Oscillator Strength	MOs contribution
Keto-enol Curcumin	-	3.15	-	429.90 (461.95)	1.53 (1.66)	H→L (0.64)
Diketo Curcumin	-	3.59	-	391.59 (408.57)	0.26 (0.52)	H→L (0.45) H-2→L (0.48)
				378.37 (350.36)	0.15 (0.37)	H-2→L (0.43)
Diketo Curcumin. EA	-21.27 (-6.71)	3.15	0.03	443.80 (425.38)	0.23 (0.43)	H→L (0.66)
				417.44 (407.43)	0.22 (0.13)	H-1→L (0.60)
				375.19 (369.22)	0.30 (0.15)	H-1→L+1 (0.54)
				365.61 (368.72)	0.28 (0.16)	H→L+1 (0.40)

curcumin and of the diketo curcumin complex with EA. In solution, curcumin predominantly exists as the keto-enol tautomeric form with a strong intramolecular hydrogen bond in the ground state as shown in **Fig.III.29.** As shown in **Table III.9**, the TD-DFT computed gas phase excitation energies for keto-enol curcumin and its diketo

curcumin tautomer are 429.90 nm and 391.59 nm, respectively, with strong absorption resulting mainly from the HOMO to LUMO electronic excitations (**Fig.III.30**). The calculated results for free curcumin tautomers match quantitatively with the previously reported values[348,357] of 419 nm of the keto-enol form and 389 nm for the diketo form, respectively, in gas phase. The calculated values in methanol solvent obtained also match qualitatively with the experimental findings. Experimentally, we find that the presence of low concentration of surfactants in curcumin solution results in a new absorption peak at higher energy, at ≈ 355 nm, along with the original peak at 425 nm. Interestingly, we do find new absorption peaks at 350.36 nm for diketo curcumin and 369.22 nm, 368.72 nm for diketo curcumin complexed with EA. Here the situation is completely different from the case of metal ion chelation of curcumin which report the absorption peak at lower energy, *i.e.*, red shift[358] due to the significant amount of charge transfer effect between the metal ion and curcumin in the metal chelated complexes.

To rationalize this observation, we focus on the occupation of relevant FMOs responsible for these higher energy electronic transitions. As can be seen from **Table III.9**, the HOMO–2, HOMO–1, HOMO, LUMO, LUMO+1, LUMO+2 FMOs are mainly governing the observed shift to the higher energy side. It is also clear from the **Fig.III.30** that the LUMO+2 is mainly localized on the one half and the HOMO–2 is mainly localized at the central region of the diketo curcumin. On the other hand, the LUMO is de-localized almost over the entire molecule but the HOMO–1, HOMO and LUMO+1 are predominantly localized over the two arms with a kink at the central tetrahedral methylenic carbon (**Fig.III.30**). Whereas, complexation of diketo curcumin with EA render changes in the delocalization of FMOs as seen in **Fig.III.30**. The significant changes in relevant FMOs occupation for curcumin complexed with EA render the transition energy towards higher energy values. Thus, the theoretical results help in understanding the origin of the UV absorption peak of curcumin in presence of the submicellar cationic surfactants.

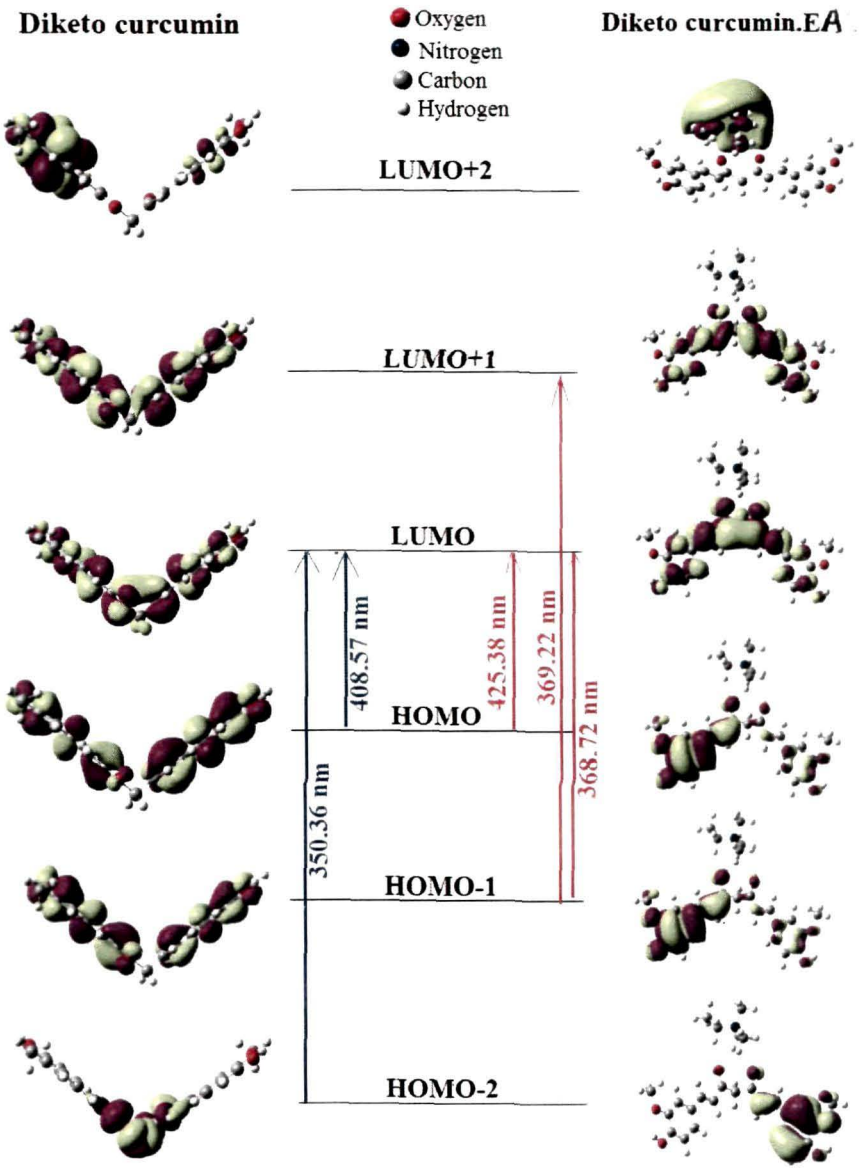

Fig.III.30. The transitions of the complex, chosen on the basis of higher oscillator strength in methanol.

III.3.2. Curcumin in Submicellar Anionic Surfactant Solutions*

III.3.2.1. UV-Visible spectral study

The variations in spectral properties of 25.0 μmol dm^{-3} aqueous curcumin in presence of different concentrations of SDS at *p*H 7.00 and 298 K have been shown in **Fig.III.31**. As our subsequent discussions are focused on the UV-Vis spectral observations, we briefly describe the spectral variations of curcumin on additions of SDS though the same has been reported earlier[276,277]. The absorption of the 425 nm band of curcumin solution starts decreasing with appearance of the new band with λ_{max} at 355 nm as the concentration of SDS is increased to 0.50 mmol dm^{-3}. Further addition of SDS increases the intensity of the new band with corresponding decrease of the 425 nm band with a slight bathochromic shift from 355 nm to 362 nm. The intensity of the new band increases up to a concentration of SDS of 1.80 mmol dm^{-3} and then again starts decreasing on further addition of SDS. In the concentration range of 2.0-4.0 mmol dm^{-3}, there was the reversal of the 425 nm band. The UV band disappeared completely at 6.00 mmol dm^{-3} SDS with simultaneous appearance of the original band at 420 nm above the CMC of SDS.

The spectra recorded between 0.50 mmol dm^{-3} and 1.80 mmol dm^{3} of the surfactant concentrations passed through a clear isosbestic point at 374 nm. It is interesting to note that the new band at 355 nm corresponding to the β-diketo curcumin, appears as the same manner as observed in presence of cationic surfactants at the *p*H range 2.00-7.50. The β-diketone moiety of curcumin can chelate cationic metal ions[347] such and cetyltrimethyl ammonium ion. Here, the interaction of curcumin is with a negatively charged head group. Here, at the [SDS] = 0.50 mmol dm^{-3} to 1.80 mmol dm^{-3}, the twisted diketo form of curcumin is stabilized by a complex formation with SDS. At [SDS] = 2.00 mmol dm^{-3}, the complex begins to break down due to formation of premicelles[276]. The disappearance of the UV band above [SDS] > 6.00 mmol dm^{-3} and the simultaneous appearance of the 420 nm band can be attributed to micellar solubilization of curcumin in the keto-enol form. The CMC of SDS is 8.21 mmol dm^{-3} (ref.218), which is reduced to 6.00 mM due to the presence of buffer components[218]. The 420 nm band can be attributed to the keto-enol form of curcumin in the nonpolar SDS micellar core[133] The 5 nm hypsochromic shift of the band from 425 nm to 420 nm may be attributed to change in the microenvironment of the dye on incorporation to the micelle[276].

This work has been published in **Spectrochim. Acta A 104 (2013) 150-157.*

However, this high energy band was not observed in presence of Triton X-100, a nonionic surfactant.

As observed that cationic micelles at *p*H 7.00 (**Fig.III.21**) can deprotonate the most acidic H-atom, the anionic micelles cannot as indicated the non appearance of the band at 454 nm. The present experiments have been carried out in acidic and neutral medium. It is possible that the diketo curcumin interacts with surrounding water through H-bond formation with the oxygen atoms of the carbonyl groups and then the H atom bound to one of the oxygen atoms binds with the dodecylsulfate group of the surfactant. The H-bond with either of the oxygen atoms, more likely to that of the sulfate group, may be close to a protonation. The whole process may be assisted by ion-dipole and hydrophobic interactions involving the dye-surfactant combination. Thus, the monomeric surfactant stabilizes the twisted diketo curcumin by means of a dye-surfactant complex involving H-bond formation.

Addition of SDSN to aqueous curcumin in the experimental pH range also induced spectral variations analogous to that observed with SDS. The λ_{max} of the submicellar band of the dye was the same as that with SDS and the absorption spectra passed through an isosbestic point. A slight red shift from 355 nm to 365 nm is observed on increasing [SDSN] from 0.30 mmol dm^{-3} to 1.20 mmol dm^{-3}.

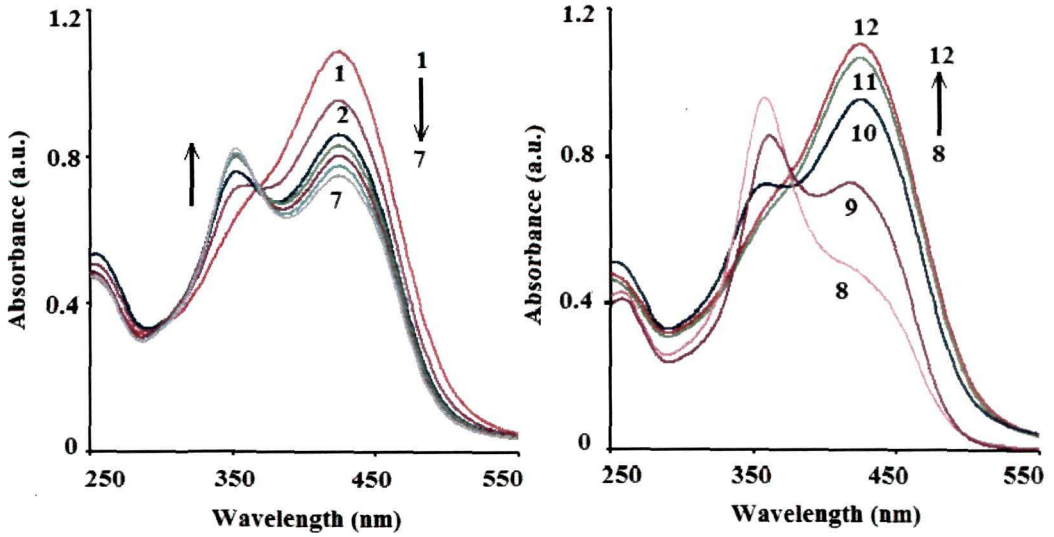

Fig.III.31. UV-visible absorption spectra of curcumin (25.0 μmol dm^{-3}) in various concentrations of SDS at *p*H 7.00 and temperature 298 (±1) K: [SDS] / (mmol dm^{-3}) **(a):** (1) 0.00 (2) 0.50 (3) 0.80 (4) 1.00 (5) 1.40 (6) 1.80 **(b):** (7) 2.00 (8) 3.00 (9) 4.00 (10) 6.00 (11) 8.00. (12) 9.00

With SDBS under similar experimental conditions, the spectral variations were somewhat different from that observed with SDS and SDSN[277] (**Fig.III.32**). The new submicellar absorption band appears at 360 nm in presence of 0.30 mmol dm^{-3} SDBS. A gradual red shift of 360 nm to 387 nm is observed on going from 0.30 mmol dm^{-3} to 1.00 mmol dm^{-3} of SDBS. The original curcumin band appears at 416 nm above 1.20 mmol dm^{-3} concentration of the surfactant with gradual disappearance of the UV band. The only significant difference in SDBS from the other two anionic surfactants that may bring about the observed difference in the spectra is the presence of the benzene ring in SDBS. The interaction of the aromatic π-electrons of SDBS with curcumin may affect the H-bond formation and as a consequence may weaken the diketo curcumin-surfactant complex.

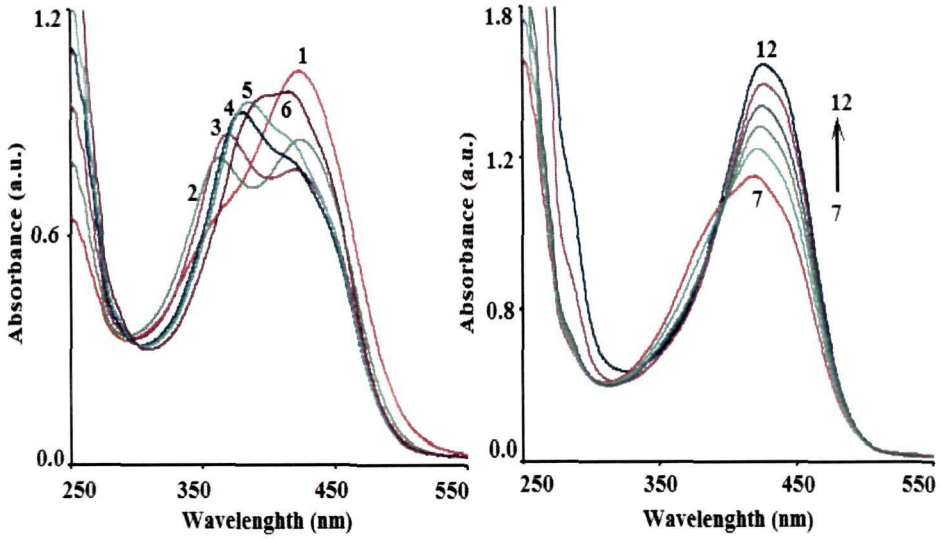

Fig.III.32. Absorbance spectra of curcumin (25.0 μmol dm^{-3}) in presence of various concentrations of [SDBS] / (mmol dm^{-3}) at pH 7.00 and 298 (±1) K **(a):** (1) 0.00 (2) 0.30 (3) 0.40 (4) 0.60 (5) 0.80 (6) 1.00 (6) 1.20 **(b):** (7) 1.50 (8) 1.80 (9) 2.10 (10) 4.00 (11) 6.00 (12) 8.00.

III.3.2.2. Equilibrium analysis

The presence of isosbestic points in the spectra of curcumin in presence of SDS and SDSN indicate equilibrium between the free dye and surfactant with their complex. Assuming the interaction to be of 1:1 stoichiometry, the interaction can be represented as follows:

$$S^- + C \underset{}{\overset{K_c}{\rightleftharpoons}} S^-C \qquad \text{III.11.}$$

and

$$K_c = [S^-.C] / [S^-] [C] \quad \text{III.12.}$$

where, S^-, C and $S^-.C$ represent the surfactant, the dye and their complex, respectively. The equilibrium binding constant, K_c has been determined by using the **equation III.10**. The plots of $1/(d-d_o)$ *vs.* $1/C_s$ were found to be linear with squired correlation coefficient between 1 and 0.979. The determination of K_c with SDBS, however, may not be as reliable as with SDS and SDSN since no isosbestic point was observed in this system. Addition of an electrolyte (*viz.*, 0.05M Na_2SO_4) to the solutions increasing the ionic strength from 0.01 to 0.06 increased K_c by over an order for all three surfactants **(Table III.10)**. Since, curcumin is as such electrically neutral in the experimental *p*H range, the observed increase in the interaction with ionic strength may be indicative of a secondary salt effect suggesting involvement of an acid-base interaction in the form of protonation or deprotonation. In the present case there may be a protonation of either the diketo group of curcumin or the anionic surfactant headgroup. The observed secondary salt effect supports our assumption made in ***Sec III.3.2.1*** about binding between the diketo oxygen and the anionic surfactant head group oxygen through a proton.

Table III.10. The binding constants (K_c), of the interaction of buffered aqueous curcumin with the submicellar anionic surfactants at 298 (±1) K and ionic strength of 0.01 and 0.06.

Surfactant	*p*H	K_c/ ($10^3 M^{-1} dm^3$)* at ionic strength 0.01	K_c/ ($10^3 M^{-1} dm^3$)* at ionic strength 0.06
SDS	5.00	1.48[a]	29.4
SDBS	5.00	1.28[a]	18.1
SDSN	5.00	1.34[a]	20.4

*Experimental error limit = ±5%. [a]Data from ref.277

III.3.2.4. Surface Tension Study

Fig.III.33 shows the variation of surface tension with variation in the surfactant concentrations of the buffered aqueous anionic surfactant solutions in absence and in the presence of 25.0 μmol dm^{-3} curcumin at *p*H 7.00. The surface tension gradually decreased with increase in the concentration of the surfactant, reached a minimum (*e.g*, at 2.50 mmol dm^{-3} in the case of SDS) and then almost levelled off. The concentration 2.50 mmol dm^{-3} is therefore the CMC of SDS in the experimental buffered medium. The CMCs obtained from the surface tension *vs.* concentration plots are indicated by vertical bars in **Fig.III.33**

at *p*H 7.00. It can be mentioned here that the CMCs of the surfactant in the buffered media were within the experimental error in the absence and the presence of curcumin. The insignificant difference in the CMC due to curcumin may be due to already drastic decrease in the CMC caused by the buffer components. The surface tension in the presence of the dye was less than that in the absence at very low concentration of SDS probably due to adsorption of curcumin initially at the air/water interface. Between [SDS] of 0.10 mmol dm^{-3} and 2.50 mmol dm^{-3}, the surface tension in the presence of curcumin is slightly higher than that in its absence, which indicates the formation of a less surface active curcumin-SDS complex. The crossover (**Fig.III.33(b)**) of surface tension curves also coincided by the appearance of the diketo curcumin UV-Visible band at 355 nm. The values of pC_{20} have been found to be 3.25 and 3.19 in the presence and absence of curcumin, respectively. The surface tension of SDBS and SDSN showed similar variations in the absence and presence of curcumin (**Fig.III.33**).

The absence of significant lowering of surface tension of the surfactants and absence of two CMCs in the presence of curcumin as reported earlier with other ionic dyes[296] indicate that the curcumin-anionic surfactant complex does not behave like a nonionic surfactant but retains the anionic charge with comparable surface activity. At [SDS] = 18 mmol dm^{-3}, the intensity of the 355 nm band is maximum and at this concentration the surface tension of SDS in presence of curcumin is lower than that in absence. This indicates that some of the surfactant molecules occupy the surface monolayer.

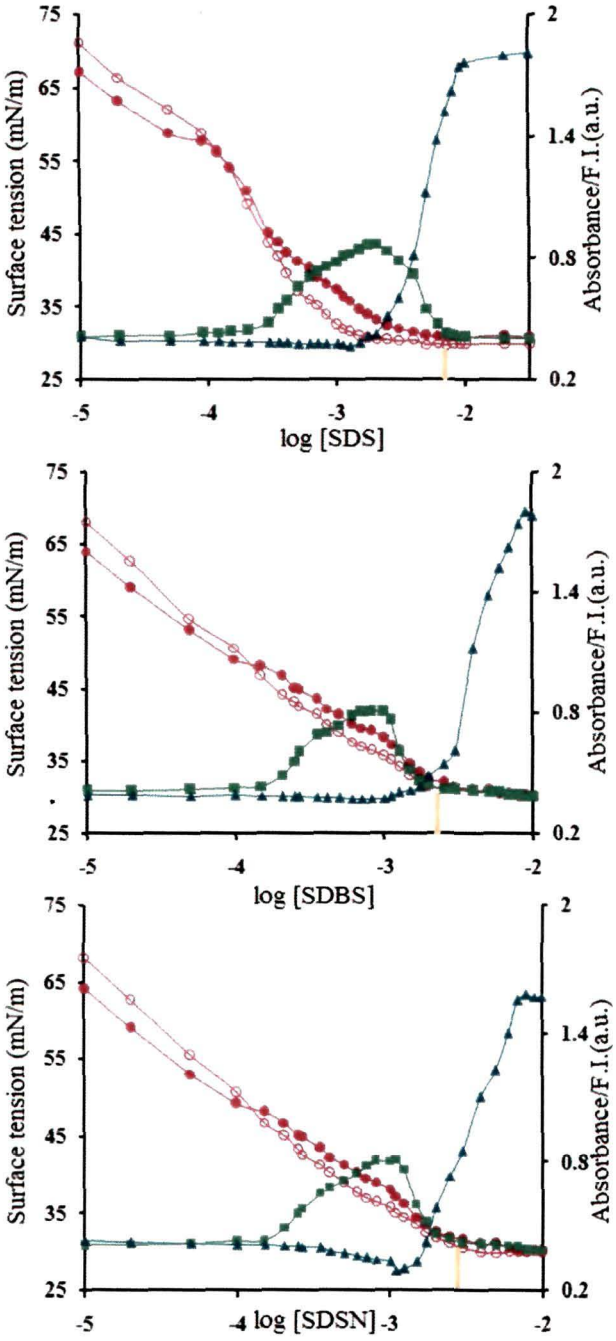

Fig.III.33. Plot of UV absorbance at 355 nm, fluorescence intensity at 550 nm and surface tension of aqueous solution of curcumin (25.0 μmol dm^{-3}) as a function of concentration of (a) SDS (b) SDBS and (c) SDSN at *p*H 7.00 at 298 (±1) K. Symbols: Absorbance (■), FI / 10^2 (▲) and surface tension of aqueous surfactant in the absence ( ) and the presence (●) of curcumin.

III.3.2.5. Fluorescence spectral behavior

The changes in fluorescence behavior of curcumin have been attributed to the solute-solvent interactions, intramolecular charge transfer character, intermolecular hydrogen bonding with polar solvents, and π-π interaction with molecules possessing aromatic entity[269]. The plots of fluorescence intensity (FI) *vs.* concentration of the surfactants are shown in **Fig.III.34**. After being excited at 425 nm curcumin exhibits an intense fluorescence maximum at ≈ 550 nm in aqueous solution. The FI of the band at λ_{max} of 550 nm, of 25.0 μmol dm^{-3} buffered curcumin decreased very slightly as [SDS] increased above 0.50 mmol dm^{-3}, reached a minimum 1.80 mmol dm^{-3} of SDS and then showed a marked increase. While the marked increase in the FI at higher concentrations of the surfactant can be attributed to curcumin solubilized in nonpolar environment due to premicelles, the initial slight decrease is indicative of a slightly more polar environment of the dye which is possible only through ion-dipole or H-bond interaction of curcumin with the anionic head group of the surfactant. The increase in the FI above 2.00 mmol dm^{-3} of SDS coincided with the disappearance of the visible absorption band of the proposed diketo form. Therefore, the ion-dipole interaction or the H-bond interaction is perhaps through the β-diketo group breaking the conjugation of the dye to be consistent with the observed changes of the UV-Visible spectra.

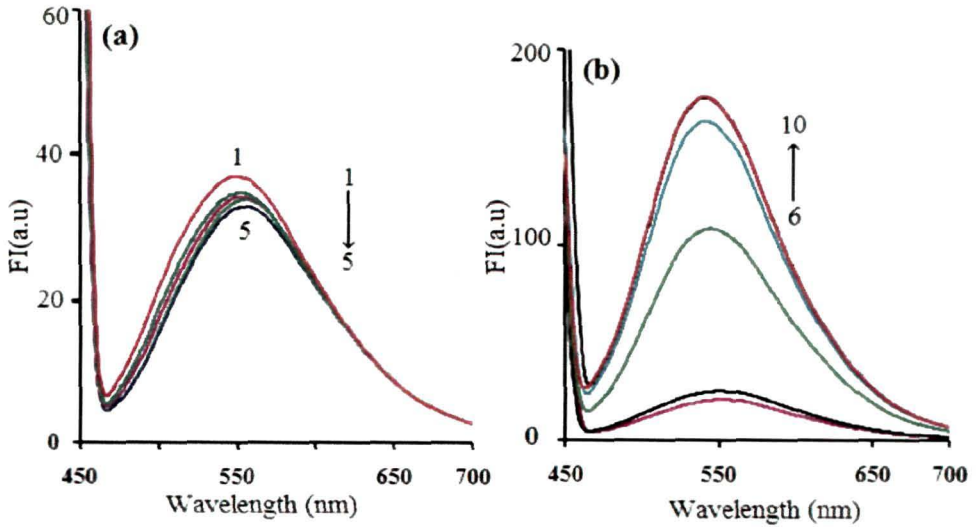

Fig.III.34. Fluorescence spectra of curcumin (25.0 μmol dm^{-3}) in presence of various concentrations of SDS at *p*H 7.00 and 298 (±1K). [SDS] / (mmol dm^{-3}) **(a):** (1) 0.00, (2) 0.50, (3) 1.00, (4) 1.40, (5) 1.80; **(b):** (6) 2.00 (7) 3.00 (8) 4.00 (9) 6.00 (10) 8.00.

III.3.2.6. Computational study of curcumin – anionic surfactant interactions

The calculated gas phase energy of the keto-enol form of curcumin has been found to be lower than that of the diketo form by ≈ 7.39 kcal mol^{-1} which agrees with the reported values[348,357]. A possibility of preferred complexation of the surfactants with diketo curcumin compared with its keto-enol tautomeric form exists which could rationalize the observed experimental UV band at submicellar solutions. To ensure that the diketo curcumin forms the complex with the surfactant, we considered both the tautomeric forms of curcumin to interact with ES and compared the calculated stabilization energies. All the DFT optimized structures are shown in **Fig.III.35**. From the fully optimized geometries, we find that the keto-enol curcumin stabilizes in planar geometry with a cis-configuration of two oxygens forming hydrogen bonds while the diketo curcumin stabilizes in a V-shaped geometry with anti-configuration of two keto groups. The methanol phase stabilization energy of the diketo curcumin.ES and keto-enol.ES have been calculated as -19.51 kcal $mole^{-1}$ and -15.8132 kcal mol^{-1}, respectively. Thus, the diketo complex is more stabilized than the keto-enol complex by ≈ 4-5 kcal mol^{-1}.

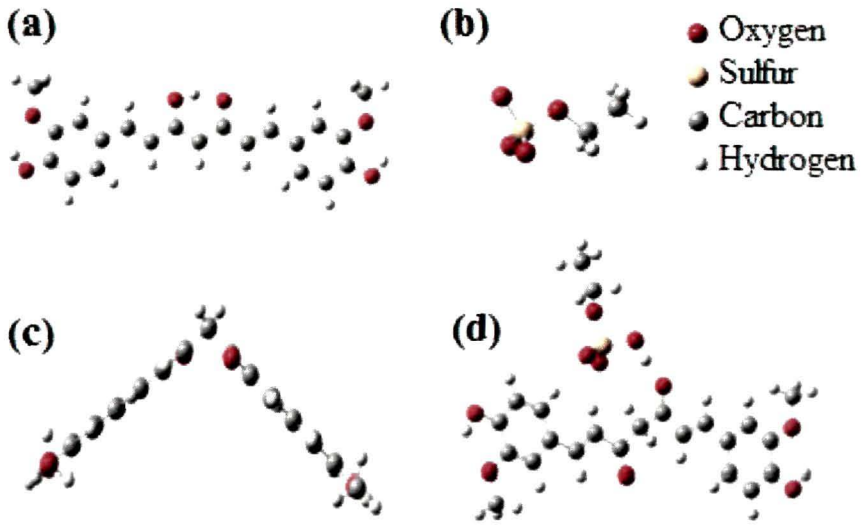

Fig.III.35. The optimized structures of all the individual molecules and complexes: (a) ketoenol curcumin, (b) ES, (c) diketo curcumin and (d) diketo curcumin.ES complex.

To obtain insight on the charge density profile and bonding aspects, we have performed calculations of the natural bond orbital (NBO) and natural electronic configuration. As can be seen from the relaxed structures of the individual molecules and

the complex as shown in **Fig.III.35**, the diketo curcumin retains its anti-configuration in presence of ES. We find that the shortest distance of separation (as measured from the closest O atom of ES to the closest O atom of curcumin, hydrogen atom in between) between curcumin and ES is within 2.574 Å. From natural population analysis (NPA), we also find that there is a small amount of fractional charge transfer from diketo curcumin to ES. We also observe that the re-distribution of electronic charges in diketo curcumin moiety occurs in presence of ES and the excess transferred charge is mainly localized on 3d orbitals of S atom of ES. The very small value of charge transfer in the complex indicates that the interaction does not mainly govern through the electrostatic Coulombic interaction. The dipole-dipole, H-bonding and van der Waals interactions may significantly contribute to the overall stability of the complex between the diketo curcumin and ES. Inclusion of solvent effect causes a very small change in the of ES complex stabilization. We find that the formation of the complex by the diketo form decreases the HOMO-LUMO energy by about 0.45 eV (**Table III.11**).

To understand the observed shifts in peak position in UV-Visible absorption spectra upon complexation with the surfactant, we have carried out TD-DFT computations on the ground state optimized geometries of free keto-enol and diketo curcumin and of the diketo curcumin complex with ES. As shown in **Table III.11**, the TD-DFT computed gas phase excitation energies for keto-enol curcumin and its diketo curcumin tautomer are 429.90 nm and 391.59 nm, respectively, with strong absorption resulting mainly from the HOMO to LUMO electronic excitations (**Fig.III.36**). The calculated results for free curcumin tautomers match quantitatively with the previous reported values[348,357] of 419 nm of the keto-enol form and 389 nm for the diketo form respectively, in gas phase. The calculated values in methanol solvent obtained also match qualitatively with the experimental findings. Experimentally, we find that the presence of low concentration of surfactants in curcumin solution results in a new absorption peak at higher energy, at ≈ 355 nm, along with the original peak at 425 nm. The transitions of the complex, chosen on the basis of higher oscillator strength in methanol, are shown in **Fig.III.36.**

Interestingly, we do find new absorption peak at 350.36 nm for diketo curcumin and 366.93 nm, 362.03 nm for diketo curcumin complexed with ES. Here the situation is completely different from the case of metal ion chelation of curcumin where generally one finds the new absorption peak at lower energy, *i.e.*, red shift[358] due to the significant amount of charge transfer effect

Table III.11. Relevant terms for the individual tautomers and the complex with ES. ΔE_{stab}, $\Delta E_{H\text{-}L}$ and CT representing stabilization energy, HOMO-LUMO energy gap, and charge transfer, respectively. The values within parentheses correspond to methanol as solvent. H and L stand for the HOMO and LUMO, respectively.

System	ΔE_{stab} (kcal mol^{-1})	$\Delta E_{H\text{-}L}$ (eV)	CT (e)	Transition energy (nm)	Oscillator Strength	MOs contribution
Keto-enol Curcumin	-	3.15	-	429.90 (461.95)	1.53 (1.66)	H→L (0.64)
Diketo Curcumin	-	3.59	-	391.59 (408.57)	0.26 (0.52)	H→L (0.45) H-2→L (0.48)
				378.37 (350.36)	0.15 (0.37)	H-2→L (0.43)
Diketo Curcumin.ES	-17.36 (-19.51)	3.14	0.07	452.65 (434.55)	0.07 (0.34)	H→L (0.69)
				386.87 (412.82)	0.44 (0.30)	H-1→L+1 (0.39)
				366.71 (366.93)	0.25 (0.41)	H-1→L (0.39) H-2→L+1 (0.44)
				350.05 (362.03)	0.28 (0.10)	H→L+1 (0.54)

To rationalize this observation, we focus on the occupation of relevant FMOs responsible for these higher energy electronic transitions. As can be seen from **Table III.11**, the HOMO–2, HOMO–1, HOMO, LUMO, LUMO+1 FMOs are mainly governing the observed shift to the higher energy side. It is also clear from the **Fig.III.37** that the LUMO+2 is mainly localized on the one half and the HOMO–2 is mainly localized at the central region of the diketo curcumin. On the other hand, the LUMO and LUMO+1 are de-localized almost over the entire molecule but the HOMO–1 and HOMO are predominantly localized over the two arms with a kink at the central tetrahedral methylenic carbon. Whereas, complexation of diketo curcumin with ES render changes in the delocalization of FMOs as seen in **Fig.III.37.** The significant changes in relevant

FMOs occupation for curcumin complexed with ES render the transition energy towards higher energy values. Thus, the theoretical results help in understanding the origin of the UV absorption peak of curcumin in presence of the submicellar anionic surfactants.

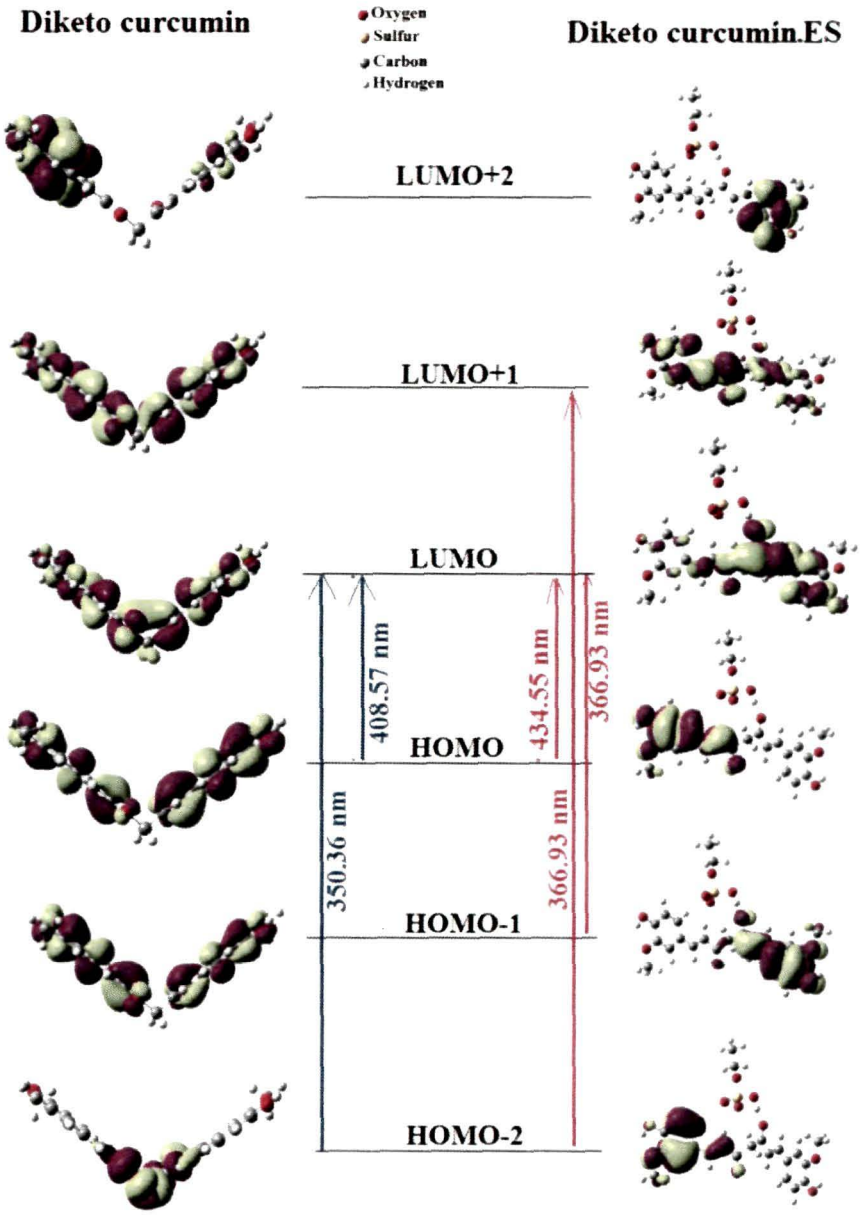

Fig.III.36. The relevant frontier molecular orbitals (FMOs) involved in the absorption processes. The blue and red lines indicate the transitions of the free and complexed β-diketo curcumin, respectively.

The above experimental and theoretical evidences including the salt-effect clearly demonstrate that the observed UV band of aqueous curcumin in the presence of the premicellar anionic surfactants is due to the diketo tautomeric form of curcumin stabilized by binding of the diketo group with the anionic surfactant headgroup through a proton.

CONCLUSIONS AND FUTURE SCOPE

IV. Conclusions:

The present experimental and computational study of the three chosen dyes in the environment of aqueous surfactant solutions with more focus in the submicellar concentration ranges has revealed some interesting novel information regarding the dye-surfactant interactions, which have been summarized below:

IV.1. *Cis-trans* Isomerism of Methyl Orange in Cationic Premicelles

- The *cis*-MO stabilized by submicellar cationic surfactants has been reported to be highly fluorescence active compared to the *trans* form.
- The *cis* form of MO is stabilized in the premicelles formed by the MO-surfactant ionpairs in presence of cationic surfactants below the normal CMC. The dye isomerizes to the *cis* form to reduce its molecular volume to minimize the steric restrictions in the ionpair premicelles.
- The intensity of the 575 nm fluorescence band due to formation of *cis* MO increases when there is DSIP micelle formation and starts to decrease when the *cis* form reverts back to the *trans* form near the normal CMC of the cationic surfactants.
- The observed unusual fluorescence behavior of MO in the presence of the submicellar and micellar surfactants may be attributed to a greater fluorescence of the *cis* form compared to that of the *trans* form, a factor that dominates over the solvent-polarity factor.
- The symmetry forbidden $S_1 \rightarrow S_0$ ($n\text{-}\pi^*$) fluorescence becomes allowed in a twisted *cis*-MO stabilized in cationic premicelles, unlike the usual azobenzenes.
- A broad moderate intensity emission band appears in the range of 420 – 530 nm which has been attributed to a stabilization of MO in intermediate conformations between the *trans* and the *cis* isomers.
- TD-DFT calculations show that MO_{cis}.EA is stable over the MO_{trans}.EA complex by $\approx$2.94 kJ mol^{-1}. On complexation of the *cis* form with EA, there is no significant change in the FMOs, however, complexation brings about changes in the symmetry of the lobes of the relevant FMOs which renders the wavelength of absorption to the higher energy side.
- The ground state geometries of the free and complexed MO confirm that UV band of MO observed in the presence of the submicellar cationic surfactants is due to the *cis* form of the dye which arises from HOMO→LUMO and HOMO-1 →LUMO transitions.

- The enhancement of F.I. at 575 nm of MO in the *cis* form is originated through initial absorption around 375 nm when excited with 270 nm radiation.

IV.2. Protonation of Acridine Orange in Dye-Surfactant Ion Pair Micelles

- The present study of the interactions of aqueous AO with submicellar anionic surfactants unequivocally establishes the formation of PDSIP in the DSIP micelles in addition to the well known induced dimerization of the dye.
- The anionic surfactants clearly exhibit two CMCs in presence of AO as is exhibited also by some other cationic dyes, which do not show induced dimerization, as reported earlier.
- The PDSIP formation by AO is entropy driven and stronger with SDS than with SDBS.
- The plots of FI of AO in the presence of an anionic surfactant *vs.* concentration of the anionic surfactant show two minima along with a short maximum in between contrary to the previous reports. The first minimum (shallow) and the short maximum of the FI curve have been attributed to formation of DSIP and DSIP micelle, respectively. The second minimum (deep) has been attributed to formation of PDSIP and location of AO at highly polar surface region of the surfactant rich DSIP-surfactant mixed micelles.
- The anionic surfactant approaches AO through one of the terminal N-atom and protonation occurs at the other basic terminal diamino N-atom, as shown by TD-DFT calculations.

IV.3. Stabilization of the β-diketo tautomer of aqueous curcumin in premicellar ionic surfactants

IV.3.1. *Curcumin in Submicellar Cationic Surfactant Solutions*

- The present work consolidates the newly observed phenomenon of keto-enol tautomerism of curcumin in premicellar ionic surfactants in addition to the other well known interactions. Stabilization of the β-diketo tautomer increases on increasing the tail length or the charge density of the head group of the cationic surfactant.
- Though the curcumin-cationic surfactant complex is formed at a very low concentration of the surfactants, the β-diketo tautomer is stabilized only on micellization of the curcumin-surfactant complex.

- The V-shaped β-diketo form of curcumin is probably a more favored form than the planar keto-enol form in the compact aggregates (premicelles) of the complex due to steric reasons. The V-shape allows more hydrophobic interaction between the surfactant tail and the two hydrophobic feruloyl moieties of curcumin.
- An observed secondary salt-effect indicates the involvement of a proton in the mechanism of the interaction. It is suggested that as the surfactant head group approaches curcumin, a protonation of the central methylenic carbon breaks down the π-conjugation in curcumin and facilitates deprotonation of the enolic proton stabilizing the β-diketo tautomer and hence the curcumin–cationic surfactant complex.
- The formation of the complex by the β-diketo tautomer further lowers the HOMO-LUMO energy by about 0.44 eV. The complex formation is mainly governed by ion-dipole, van der Waals interactions and a small charge transfer component as was reported with anionic surfactant.
- Natural population analysis reveals that there is a small amount of fractional charge transfer from diketo curcumin to cationic surfactant and the excess charge is localized on the $2P_z$ orbital of N-atom of CTAB.
- The significant changes in relevant FMOs occupation for curcumin complexed with anionic surfactants also render the transition energy towards higher energy values.

IV.3.2. Curcumin in Submicellar Anionic Surfactant Solutions

- The medicinally active diketo tautomer of curcumin observed in submicellar anionic surfactants is stabilized in a complex formed between curcumin and monomeric anionic surfactant involving a proton.
- The curcumin moiety experiences a higher polarity in the complex than in its free form indicating a role of ion–dipole or H-bonding interaction as suggested by fluorescence behavior.
- Enhancement of the interaction by secondary salt-effect indicates involvement of the protonation in the interaction.
- The formation of the complex by the diketo form further decreases the HOMO-LUMO energy by about 0.45 eV. The complex formation is mainly governed by ion-dipole, dipole-dipole, H-bonding, van der Waals interactions and a small charge transfer component.
- Natural population analysis reveals that there is a small amount of fractional charge transfer from diketo curcumin to anionic surfactant also and the excess

charge is transferred to the 3d orbitals of S-atom of the anionic surfactant, viz., SDS.

- The significant changes in relevant FMOs occupation for curcumin complexed with anionic surfactants also render the transition energy towards higher energy values.

Finally we can say that the complex formation between the electron-rich diketo group and the anionic surfactant head group is quite unusual unlike that between curcumin and cationic surfactant head group. Such unusual ability of curcumin to bind with species of both charge types may have pertinence to the reported versatile medicinal activities of curcumin.

Future scopes

The fluorescence behaviour of methyl orange can be further studied to know in detail, particularly, the broad fluorescence band and the variation in its intensity on changing the concentration of cationic surfactant. The connection between the β-diketo form of curcumin and the versatile medicinal activities of curcumin can be studied in detail. The possibility of utilizing the various changes in dyes induced by submicellar surfactants, e.g., *cis-trans* isomerism, dye aggregation, dye protonation and deprotonation and keto-enol tautomerism can be explored.

1. Rosen, M.J. Surfactants and Interfacial Phenomena, 2nd ed., John Wiley and Sons, New York, 1989.
2. Schramm, L.L., & Marangoni, D.G. (ed.) Surfactants: Fundamentals and Application in Petroleum Industry, Cambridge University Press, Cambridge, UK, 2000.
3. Ismaeel, A.R., & Edbey, K.M. Thermodynamics, and kinetic study of physical removal of high concentration of sodium dodecyl sulphate during recycling of industrial and household waste water by adsorption at activated charcoal using pH measurements, *J. Chem. Pharm. Res.* **2** (3), 459--466, 2010.
4. Rosen, M.J. Geminis: A new generation of surfactants, *Chemtech* 23, 30--33 1993.
5. Menger, F.M., & Littau, C.A.J. *J. Am. Chem. Soc* Vol. 113, p.1451, 1991; Vol. 115, p.10083, 1993.
6. Patist, A., et al. Effect of Tetraalkylammonium Chlorides on Foaming Properties of Sodium Dodecyl Sulfate Solutions, *Langmuir* **14** (16), 4471--4474, 1998.
7. Gibbs, J.W. The Collected Works of J.W. Gibbs, Longmans, Green, London, 119, 1928.
8. Anacker, E.W. Modeling Dye-Surfactant Interactions, *J. Colloid Interface Sci.* **164** (1) 54--62, 1994.
9. Manual of Symbol and Terminology, Appendix II, Part I, IUPAC, *Pure and Appl. Chem.* **31**, 612, 1972.
10. McBain, J.W. *Trans. Faraday Soc.* **9**, 99--101, 1913.
11. Hartley, G.S. Aqueous Solutions of Paraffin Chain Salts: A Study in Micelle Formation, Hermann & cie, Paris, 1936.
12. Hinze, W.L., & Armstrong, D.W. (eds.) Ordered Media in Chemical Separations, *J. Am. Chem. Soc.* Washington D.C., 1987.
13. Janini, G.M., & Attari, S.A. Determination of Partition Coefficient of Polar Organic Solutes in Octanol/Micellar Solutions, *Anal. Chem.* **55** (4), 659--661, 1983.
14. Adamson, A.W. *Physical Chemistry of Surfaces*, 3rd ed., John Wiley and Sons, New York, 1976.
15. Fendler, J.H., & Fendler, E.J. *Catalysis in Micellar and Macromolecular Systems*, Academic Press, New York, 1975.
16. Fendler, J.H. *Membrane Mimetic Chemistry*, John Wiley and Sons, New York, 1982.
17. Fendler, J.H., & Tundo, P. Polymerized surfactant aggregates: Characteristics and utilization, *Acc. Chem. Res.* **17** (1), 3--8, 1984.

18. Gunnarsson, G., et al. Surfactant Association into Micelles. An Electrostatic Approach, *J. Phys. Chem.* **84** (23), 3114--3121, 1980.

19. Moulik, S.P. Micelles : Self Organized Surfactant Assemblies, *Curr. Sci.* **71** (5), 368--576, 1996.

20. Hoffman, H., & Ebert, D.C.G. Surfactant, Micelles and Fascinating Phenomena, *Angew. Chem. Int. Ed. Engl.* **27** (7), 902--912, 1988.

21. Tanford, C. The Hydrophobic Effect: Formation of Micelles and Biological Membranes, Wiley; New York, 1980.

22. Jiang, X. Hydrophobic-lipophilic interactions. Aggregation and self-coiling of organic molecules, *Acc. Chem. Res.* **21** (10), 362--367, 1988.

23. Menger, F.M. The structure of micelles, *Acc. Chem. Res.* **12** (4), 111--117, 1979.

24. Elworthy, P.H., et al. Solubilization by Surface Active Agents and Its Application in Chemistry and in Biological Sciences, Chapman and Hall, London, 1968.

25. Menger, F.M., et al. Self-assembling systems: Mining a rich vein, *J. Colloid Interface Sci.* **344** (2), 241--246, 2010.

26. Shimizu, K., & Iwatsuru, M. Measurement of Critical Micelle Concentration of Nonionic-Nonionic Mixed Surfactant Systems by the First Derivative Absorption Spectrum and the Region of Cooperative Micelles, *Chem. Pharm. Bull.* **38** (5), 1353--1358, 1990.

27. Lyklema, J. *Fundamentals of interface and colloid science: soft colloids,* Elsevier, UK, 2005.

28. van Os, N.M., et al. *Physico-chemical properties of selected anionic, cationic and nonionic surfactants,* Elsevier, Netherlands, 1993.

29. Cates, M.E., & Candau, S.J. Statics and dynamics of worm-like surfactant micelles, *J. Phys.: Condens. Matter* **2** (33), 6869--6892, 1990.

30. Zana, R. Dimeric and oligomeric surfactants. Behavior at interfaces and in aqueous solution: a review, *Adv. Colloid Interface Sci.* **97** (1-3), 205--253, 2002.

31. Shiloach, A., & Blankschtein, D. Predicting Micellar Solution Properties of Binary Surfactant Mixtures, *Langmuir* **14** (7), 1618--1636, 1998.

32. Moulik, S.P., et al. Micellar Properties of Cationic Surfactants in Pure and Mixed States, *J. Phys. Chem.* **100** (2), 701--708, 1996.

33. Saenger, W., & Muller-Fahrnow, A. Cyclodextrins Increase Surface Tension and Critical Micelle Concentration of Detergent Solutions, *Angew. Chem. Int. Ed. Engl.* **27** (3), 393--394, 1988.

34. Dasgupta, P.K., & Moulick, S.P. Effects of urea and a nonionic surfactant on the micellization and counterion binding properties of cetyltrimethyl ammonium bromide and sodium dodecyl sulfate, *Colloid Polym. Sci.* **267** (3), 246--254, 1989.

35. Patist, A., et al. On the measurement of critical micelle concentrations of pure and technical-grade nonionic surfactants, *J. Surfactants Deterg.* **3** (1), 53--58, 2000.

36. Shi, Y., et al. Determination of the critical premicelle concentration, first critical micelle concentration and second critical micelle concentration of surfactants by resonance Rayleigh scattering method without any probe, *Spectrochim. Acta A* **78** (5), 1403--1407, 2011.

37. Israelachvil, J.N., et al. Theory of Self-Assembly of Hydrocarbon Amphiphiles into Micelles and Bilayers, *J. Chem. Soc. Faraday Trans. II,* **72**, 1525--1568, 1975.

38. Turro, N.J., & Yekta, A. Luminescent Probes for Detergent Solutions. A Simple Procedure for Determination of the Mean Aggregation Number of Micelles, *J. Am. Chem. Soc.* **100** (18), 5951--5952, 1978.

39. Kay, R.L., & Lee, K.S. Micelle molecular parameters from surfactant ionic mobilities, *J. Phys. Chem.* **90** (21), 5266--5271, 1986.

40. Rathman, J.F., & Scamehorn, F.J. Counterion Binding on Mixed Micelles, *J. Phys. Chem.* **88** (24), 5807--5816, 1984.

41. Schott, H. Hydration of micellar nonionic detergents, *J. Colloid Interface Sci.* **24** (2), 193--198, 1967.

42. Fendler, J.H., & Fendler, E.J. *Catalysis in Micellar and Macromoleular Systems*, Academic Press INC, London, 1975.

43. Kato, T. et al. Intermicellar Interactions and Micelle Size Distribution in Aqueous Solutions of Polyoxyethylene Surfactants, *J. Chem. Soc. Faraday Trans. 1* **85** (8), 2499--2506, 1989.

44. Zielinski, R., et al. Effect of temperature on the salt-induced sphere–rod transition of micelles of dodecyltrimethylammonium bromide in aqueous NaBr solutions, *J. Chem. Soc. Faraday Trans. 1* **85** (7), 1619--1629, 1989.

45. Lipfert, J., et al. Size and Shape of Detergent Micelles Determined by Small-Angle X-ray Scattering, *J Phys. Chem. B.* **111** (43), 12427--12438, 2007.

46. Watanabe, K., & Klein, M.L. Shape fluctuations in ionic micelles, *J. Phys. Chem.* **93** (19), 6897--6901, 1989.

47. Rojas, O.J., et al. Fluorosurfactant Self-Assembly at Solid/Liquid Interfaces, *Langmuir* **18** (21), 8085--8095, 2002.

48. Sakaiguchi, Y., & Hirata, H. Some Aspects through Sedimentation Study on the Extremely Elongated Micelle Formed in Cationic Surfactant-Aromatic Additive Systems, *Bull. Chem. Soc. Jpn.* **61** (8), 2743--2746, 1988.

49. Moroi, Y. *Micelles: Theoretical and Applied Aspects*, Plenum Press, New York, 1992.

50. Sein, A., & Engberts, J.B.F.N. Micelle to Lamellar Aggregate Transition of an Anionic Surfactant in Dilute Aqueous Solution Induced by Alkali Metal Chloride and Tetraalkylammonium Chloride Salts, *Langmuir* **11** (2), 455--465, 1995.

51. Fuhrlop, J.H., & Koning, J. in *Membranes and Molecular Assemblies*: *The Synthetic Approach*, The Royal Society of Chemistry, Cambridge, 1994.

52. Dobos, Z., et al. Micellar proportion: A parameter to compare the hydrophobicity of the pseudostationary phases or that of the analytes in micellar electrokinetic chromatography, *Electrophoresis* **26** (4-5), 849--857, 2005.

53. Schulman, J.H., et al. Mechanism of Formation and Structure of Micro Emulsions by Electron Microscopy, *J. Phys. Chem.* **63** (10), 1677--1680, 1959.

54. Shinoda, K., & Kunieda, H. Conditions to produce so-called microemulsions: Factors to increase the mutual solubility of oil and water by solubilizer, *J. Colloid Interface Sci.* **42** (2), 381--387, 1973.

55. Fletcher, P.D.I., & Robinson, B.H. Dynamic Processes in Water-in-Oil Microemulsions, *Berichte der Bunsengesellschaft fur physikalische Chemie* **85** (10), 863--867, 1981.

56. Eastoe, J., et al. Variation of surfactant counterion and its effect on the structure and properties of Aerosol-OT-based water-in-oil microemulsions, *J. Chem. Soc. Faraday Trans.* **88** (3), 461--471, 1992.

57. Attwood, D., et al. A study on factors influencing the droplet size in nonionic oil-in-water microemulsions, *Int. J. Pharm.* **88** (1-3), 417--422, 1992.

58. Lawrence, M.J. & Rees, G.D. Microemulsion-based media as novel drug delivery systems, *Adv. Drug Delivery Rev.* **45** (1), 89--121, 2000.

59. Gradzielski, M. Effect of the Cosurfactant Structure on the Bending Elasticity in Nonionic Oil-in-Water Microemulsions, *Langmuir* **14** (21), 6037--6044, 1998.

60. Kumar, P., & Mittal, K.L. *Handbook of Microemulsion Science and Technology*, CRC Press, USA, 1999.

61. Paul, B.K., & Moulik, S.P. Uses and applications of microemulsions, *Curr. Sci.* **80** (8), 990--1001, 2001.

62. Kohlwein, S.D. Biological Membranes: Function and Assembly, *J. Chem. Edu.* **69** (1), 3, 1992.

63. Pullman, A. Contribution of theoretical chemistry to the study of ion transport through membranes, *Chem. Rev.* **91** (5), 793--812, 1991.

64. Helenius, A., & Simons, K. Solubilization of membranes by detergents, *Biochimica et Biophysica Acta (BBA) - Reviews on Biomembranes* **415** (1), 29--79, 1975.

65. Vick, S.C. Soap/Cosmetics/Chemical Specialties **60**, 36, 1984.

66. Rieger, M.M., & Rhein, L.D. (ed.). *Surfactants in Cosmetics*, Marcel Dekker, New York, 1997.

67. Guyot, A., & Tauer, K. Reactive surfactants in emulsion polymerization, *Adv. in Polym. Sci.* **111**, 43--65, 1994.

68. Broxton, T.J. Micellar catalysis of organic reactions. 23. Effect of micellar orientation of the substrate on the magnitude of micellar catalysis, *J. Org. Chem.* **53** (13), 3081--3084, 1988.

69. Banat, I.M. Biosurfactants production and possible uses in microbial enhanced oil recovery and oil pollution remediation: A review, *Bioresource Technol.* **51** (1), 1--12, 1995.

70. Kvammen, O., et al. Surfactants in Enhanced Oil Recovery, *Surfactants in Solution*, **11**, 653--660, 1991.

71. Pope, G.A., & Wade, W.H. Lessons from Enhanced Oil Recovery Research for Surfactant-Enhanced Aquifer Remediation, *ACS Symposium Series*, **594**, 142--160, 1995.

72. Drummond, C.J., & Fong, C. Surfactant self-assembly objects as novel drug delivery vehicles, *Curr. Opin. Colloid Interface Sci.* **4** (6), 449--456, 1999.

73. Maibaum, L., et al. Micelle Formation and the Hydrophobic Effect, *J. Phys. Chem. B* **108** (21), 6778--6781, 2004.

74. Shaw, D.J. *Introduction to Colloid and Surface Chemistry*, 4th ed., Butterworths-Heinmann, London, 1992.

75. Mukherjee, K., et al. Thermodynamics of micellization of aerosol OT in binary mixtures of water, formamide, ethylene glycol, and dioxane, *J. Phys. Chem.* **98** (17), 4713--4718, 1994.

76. Turro, N.J., et al. Photoluminescence probes for the investigation of interactions between sodium dodecylsulfate and water-soluble polymers, *Macromolecules* **17** (7), 1321--1324, 1984.

77. Nazário, L.M.M. Nonionic Cosurfactants in AOT Reversed Micelles: Effect on Percolation, Size, and Solubilization Site, *Langmuir* **12** (26), 6326--6335, 1996.

78. Riegelman, S., et al. The ultraviolet absorption spectrum as a criterion of the type of solubilization, *J. Colloid Sci.* **13** (3), 208--217, 1958.

79. Eriksson, J.C. NMR-Experiments on Solubilization in Soap Micelles, *Acta Chem. Scand.* **17**, 1478--1481, 1963.

80. Nagarajan, R., et al. Locus of solubilization of benzene in surfactant micelles, *J. Phys. Chem.* **88** (13), 2916--2922, 1984.

81. Abu-Hamdiyyah, M., & Kumari, K. Partitioning of Amphiphilic Additives between the micelles of n-Alkyltrimethylammonium Bromides and the Surrounding Aqueous Solutions as a Function of Surfactant Chain Length, *J. Phys. Chem.* **94** (6), 2518--2523, 1990.

82. Christian, S.D., et al. Precise vapor pressure measurements of the solubilization of cyclohexane by sodium octyl sulfate and sodium octyl sulfate micelles, *J. Colloid Interface Sci.* **84** (2), 423-432, 1981.

83. Kitahara, A. The study on solubilization of water from its vapor pressure over nonionic and ionic surfactant solutions in various nonpolar solvents, *J. Colloid Interface Sci.* **23** (2), 243--247, 1967.

84. Friberg, S.E. Vapour pressure of some fragrance ingredients in emulsion and microemulsion formulations, *Int. J. Cosmetic Sci.* **19** (2), 75--86, 1997.

85. Alauddin, M. Apparent molar volume, apparent molar adiabatic compressibility, and solubilization studies of aqueous solutions of sodium p-(n-dodecyl)benzenesulfonate as a function of surfactant and solubilizate concentrations and temperature, *J. Phys. Chem.* **92** (5),1301--1307, 1988.

86. Heerklotz, H., & Seelig, J. Titration calorimetry of surfactant–membrane partitioning and membrane solubilization, *Biochimica et Biophysica Acta (BBA) - Biomembranes* **1508** (1–2), 69--85, 2000.

87. Smith, G.A., et al. Use of the semi-equilibrium dialysis method in studying the thermodynamics of solubilization of organic compounds in surfactant micelles. System*n*-hexadecylpyridinium chloride-phenol-water, *J. Solution Chem.* **15** (6), 519--529, 1986.

88. Christian, S.D., et al. On the interpretation of solubilization results obtained from semi-equilibrium dialysis experiments, *Colloid Polym. Sci.* **272** (6), 745--754, 1994.

89. Rouse, J.D., et al. Micellar Solubilization of Unsaturated Hydrocarbon Concentrations As Evaluated by Semi-equilibrium Dialysis, *Environ. Sci. Technol.* **29** (10), 2484--2489, 1995.

90. Mukherjee, P. Solubilization in Aqueous Micellar Systems, *Solution Chem. of Surfactants*, 153-174, 1979.

91. Klevens, H.B. Effect of Electrolytes Upon the Solubilization of Hydrocarbons and Polar Compounds, *J. Am. Chem. Soc.* **72** (8), 3780--3785, 1950.

92. Naeem, B. Solubilization of Different Organic Compounds in Micellar System, Department of Chemistry/Quaid-i-Azam University Islamabad, 2003.

93. Bolkhus, A.M., et al. The effect of inorganic salt on the solubilization of alcohols in aqueous surfactant solutions, *J. Colloid Interface Sci.* **124** (1), 125--129, 1988.

94. Sata, N., & Saito, S. Solubilizing von Polyvinylacetat in emulgamator losengen, *Kolloid-Z.* **128** (3), 154--158, 1952.

95. Myers, D. in *Surfactant Science and Technology*, John Wiley and Sons, 2005.

96. Mittal, K.L., et al. *Solution behavior of surfactants: theoretical and applied aspects*, Plenum Press, 1982.

97. Watanabe, Y., et al. Novel ELISA for the detection of raw and processed egg using extraction buffer containing a surfactant and a reducing agent, *J. Immunological Methods* **300** (1–2), 115--123, 2005.

98. Fellows, P.J. Food Processing Technology: Principles and Practice, Wood Publishing, 2009.

99. Mezzenga, R., et al. Understanding foods as soft materials, *Nature Materials* **4**, 729--740, 2005.

100. Chmielewski, R.A.N., & Frank, J.F. Biofilm Formation and Control in Food Processing Facilities, **2** (1), 22--32, 2003.

101. Tadros, T.F. *Surfactants in Agrochemicals*, CRC Press, New York, 1994.

102. Stock, D., & Holloway, P.J. Possible mechanisms for surfactant-induced foliar uptake of agrochemicals, *Pesticide Sci.* **38** (2-3), 165--177, 1993.

103. Basu, S., et al. The Effects of surfactants on adhesion spreading and retention of herbicide droplet on the surface of the leaves and seeds, *J. Environ. Sci. Health* **37** (4), 331--334, 2002.

104. Hari, A.C. Effects of pH and Cationic and Nonionic Surfactants on the Adsorption of Pharmaceuticals to a Natural Aquifer Material, *Environ. Sci. Technol.* **39** (8), 2592--2598, 2005.

105. Costi, E.M., et al. Determination of cationic surfactants in pharmaceuticals based on competitive aggregation in ternary amphiphile mixtures, *Analytica Chimica Acta* **577** (2), 257--263, 2006.

106. Zhang, Z.L., & Zhou, J.L. Simultaneous determination of various pharmaceutical compounds in water by solid-phase extraction–liquid chromatography-tandem mass spectrometry, *J. Chromatography A* **1154** (1–2), 205--213, 2007.

107. Sabagh, A.M., et al. Surface activity and thermodynamic properties of water soluble polyester surfactants based on 1,3-dicarboxymethoxybenzene used for enhanced oil recovery, *Polym. Adv. Technol.* **11** (1), 48--56, 2000.

108. Sharma, M.K. & Sharma, G.D. Surfactants in enhanced petroleum recovery processes: an overview, in *Particle Technology and Surface Phenomena in Minerals and Petroleum Production*, Plenum Press, New York, 1991.

109. de Caro, P.S., et al. Interest of combining an additive with diesel–ethanol blends for use in diesel engines, *Fuel* **80** (4), 565--574, 2001.

110. Hudson, L.K., et al. Nanotechnology in action: Overbased nanodetergents as lubricant oil additives, *Adv. Colloid Interface Sci.* **123-126** (special issue), 425--431, 2006.

111. Shiao, S.Y., et al. Chain length compatibility effects in mixed surfactant systems for technological applications, *Adv. Colloid Interface Sci.* **74** (1-3), 1--29, 1998.

112. Banat, I.M., et al. Potential commercial applications of microbial surfactants, *Appl. Microbiology Biotechnol.* **53** (5), 495--508, 2000.

113. Maestro, A., Interaction of surfactants with thickeners used in waterborne paints: A rheological study, *J. Colloid Interface Sci.* **288** (2), 597--605, 2005.

114. Chen, X.M., & Ellis, B. in *Chemistry and Technology of Epoxy Resins*, Chapman and Hall, 1993.

115. Schmidt, D.L., et al. Water-based non-stick hydrophobic coatings, *Nature* **368**, 39--41, 1994.

116. De Graaf, L.A., & Kolster, P. Industrial proteins as a green alternative for 'petro' polymers: Potentials and limitations, *Macromolecular Symposia* **127** (1), 51--58, 1998.

117. Adams, J.W. Silicones in the coating industry: flow, levelling and defoaming, in *Surface Phenomena and Additives in Water-Based Coatings and Printing Technology*, M.K. Sharma, eds., Plenum Press, New York, 1991.

118. Lin, S.H., & Juang, R.S. Heavy metal removal from water by sorption using surfactant-modified montmorillonite, *J. Hazard. Mater.* **92** (3), 315--326, 2002.

119. Gupta, V.K., et al. Process development for the removal of lead and chromium from aqueous solutions using red mud-an aluminium industry waste, *Water Res.* **35** (5), 1125--1134, 2001.

120. Rubio, J., et al. Overview of flotation as a wastewater treatment technique, *Minerals Engineering* **15** (3), 139--155, 2002.

121. Tyagi, P., & Tyagi, R. Synthesis, Structural Properties and Applications of Gemini Surfactants: A Review, *Tenside Surfactants Detergents* **46** (6), 373--382, 2009.

122. Hartley, G.S. The Effect Of Long-chain Salts on Indicators : The Valence-Type of Indicators And The Protein Error, *Trans. Faraday Soc.* **30**, 444-450, 1934.

123. Diaz Garcia, M.E., & Sanz-Medel, A. Dye-Surfactant Interactions: A REVIEW, *Talanta* **33** (3), 255--264, 1986.

124. Barni, E., et al. Dye-Surfactant Interactions and Their Applications, *Acc. Chem. Res.* **24** (4), 98--103, 1991.

125. Love, L.J.C., et al. The Micelle, *Anal. Chem.* **56** (11), 1132A--1148A, 1984.

126. Duxbury, D.F. The photochemistry and photophysics of triphenylmethane dyes in solid and liquid media, *Chem. Rev.* **93** (1), 381--433, 1993.

127. Mishra, A., et al. Cyanines during the 1990s: a review, *Chem. Rev.* **100** (6), 1973--2011, 2000.

128. Guan, Y., et al. Ionic Self-Assembly of Dye−Surfactant Complexes: Influence of Tail Lengths and Dye Architecture on the Phase Morphology, *Langmuir* 18 (15), 5939--5945, 2002.

129. Faul, C.F.J., & Antonietti, M. Facile Synthesis of Optically Functional, Highly Organized Nanostructures: Dye-Surfactant Complexes, *Chemistry* **8** (12), 2764--2768, 2002.

130. Chakraborty, A., et al. Surfactant chain-length-dependent modulation of the prototropic transformation of a biological photosensitizer: norharmane in anionic micelles, *Langmuir* **23** (9), 4842--4848, 2007.

131. Chena, K.M., et al. Interactions between new multi-anionic surfactants and direct dyes and their effects on the dyeing of cotton fabric, *Colloids and Surf. A* **356** (1-3), 46--50, 2010.

132. Shimomura, M., et al. Orientation and Spectral Characteristics of the Azobenzene Chromophore in the Ammonium Bilayer Assembly, *Berichte der Bunsengesellschaft fur physikalische Chemie* **87** (12), 1134--1143, 1983.

133. Yamazaki, I., et al. Electronic excitation transfer in organized molecular assemblies, *J. Phys. Chem.* **94** (2), 516--525, 1990.

134. Hayashi, M., Interaction of surface active agents with Congo Red, *Bull. Chem. Soc. Jpn* **34** (1), 110--123, 1961.

135. Quadrifoglio, F., & Crezenzi, V. The interaction of methyl orange and other azo-dyes with polyelectrolytes and with colloidal electrolytes in dilute aqueous solution, *J. Colloid Interface Sci.* **35** (3), 447--459, 1971.

136. Kim, B.K. Resonanace Raman Spectra of Methyl orange Bound to Proteins and Cationic Surfactants, *Bull. Chem. Soc. Jpn.* **48** (5), 1394--1396, 1975.

137. Reeves, R.L., et al. Analysis of the Visual Spectrum of Methyl Orange in Solvents and in Hydrophobic Binding Sites, *Can. J. Chem.* **51** (4), 628--635, 1973.

138. Reeves, R.L. The Effect of Reacting and Competing Counterions on the Hydrolysis Kinetics of an Anionic Dye Ester in Mixed Micelles with CTAB, *J. Am. Chem. Soc.* **97** (21), 6025--6029, 1975.

139. Reeves, R.L. The Nature of Mixed Micelles from Anionic Dyes and Cationic Surfactants. A Kinetic Study, *J. Am. Chem. Soc.* **97** (21), 6019--6024, 1975.

140. Reeves, R.L. & Harkaway, S.A. Mixed micelles of methyl orange dye and cationic surfactants, in *Micellization, Solubilization and Microemulsion*, K.L. Mittal, eds., Plenum Press, New York, 819, 1977.

141. Vijlder, M.De. Ion-pair formation as a determining factor in the effectiveness of the interaction of electrolytes with amphiphilic azo dyes in water, *J. Chem. Soc., Faraday Trans. 1* **81** (12) 1369, 1985.

142. Dawber, J.G., et al. The metachromism of methyl orange with electrolytes and possible salting-out, *J. Chem. Soc. Faraday Trans.* 1 **82**, 119--123, 1986.

143. Alehyen, S., et al. Study of the interaction between methyl orange and mono and bis-quaternary ammonium surfactants, *Infante J Surfact Deterg.* **13**, 225--231, 2010.

144. Rafati, A.A., et al. Conductometric studies of interaction between anionic dyes and cetylpyridinium bromide in water–alcohol mixed solvents, *J. Mol. Liq.* **137** (1-3) 80--87, 2008.

145. Simon, M.M.B., et al. Spectrophotometric determination of cationic surfactants in frozen and fresh squid by ion-pair formation with methyl orange, *Analyst* **115** (3) 337--339, 1990.

146. Lewis, G.N., et al. Isomers of Crystal Violet Ion. Their Absorption and Re-emission of Light, *J. Am. Chem. Soc.* **64** (8) 1774--1782, 1942.

147. Zhang, A., et al. Studies of quenching and enhancement of fluorescence of methyl orange adsorbed on silver colloid, *J. Colloid Interface Sci.* **298** (2), 769--772, 2006.

148. Zhang, A., & Y. Fang, Influence of adsorption orientation of methyl orange on silver colloids by Raman and fluorescence spectroscopy: *p*H effect, *Chem. Phys. 331* (1), 55--60, 2006.

149. Buwalda, R.T., et al. Aggregation of Azo Dyes with Cationic Amphiphiles at Low Concentrations in Aqueous Soultions, *Langmuir* **15** (4), 1083--1089, 1999.

150. Buwalda, R.T., & Engberts, J.B.F.N. Aggregation of Dicationic Surfactants with Methyl Orange in Aqueous Solutions, *Langmuir* **17** (4), 1054--1059, 2001.

151. Dutta, R.K., & Bhat, S.N. Interaction of Methyl Orange with Submicellar Cationic Surfactants, *Bull. Chem. Soc. Jpn.* **66** (9), 2457--2460, 1993.

152. Abe, M., et al. Interaction between anionic surfactants and oil dyes in the aqueous solutions: V. The effects of the oxyethylene chain length and/or the alkyl chain length in surfactant molecule on the tautomerism of an azo dye, *J. Colloid Interface Sci.***104** (1), 228--233, 1985.

153. Shah, S.W.H., et al. Spectroscopic analysis of naphtholazobenzimidazole in organised solution, *Phys. Chem. Liq.* **48** (3), 316--328, 2010.

154. Dakiky, M., et al. Acid alizarin violet interactions with surfactants: ionization and thermodynamic parameters in buffered cationic, anionic and nonionic surfactant solutions, *Dyes Pigments* **63** (1), 101--113, 2004.

155. Biedermann, W., & Datyner, A. The interaction of nonionic dyestuffs with sodium dodecyl sulfate and its correlation with lipophilic parameters, *J. Colloid Interface Sci.* **82** (2), 276--285, 1981.

156. Ghosh, S. Sodium dodecyl benzene sulphonate mediated tautomerism of Eriochrome Black-T: Effect of charge transfer interaction, *Chem. Phys. Lett.* **500** (4-6), 295--301, 2010.

157. Karukstis, K.K., et al. A Spectral approach to determine location and and orientation of azo dyes in surfactant aggregates, *Spectrochim. Acta A* **75** (4), 1354--1361, 2010.

158. Ghoreishi, S.M., & Nooshabadi, M.S. Electromotive force studies about some dyes–cationic surfactants interactions in aqueous solutions, *Dyes Pigments* **65** (2), 117--123, 2005.

159. Nazar, M.F., et al. Interaction of azo dye with cationic surfactant under different pH conditions, *J. Surfactants Deterg.* **13** (4), 529--537, 2010.

160. Fletcher, P.D.I., & Robinson, B.H. Effect of Organized Surfactant Systems on the Kinetics of Metal-Ligand Complex Formation and Dissociation, *J. Chem. Soc. Faraday Trans.1* **80** (9), 2417--2437, 1984.

161. Tatikolov, A.S., & Costa, S.M.B. Complexation of polymethine dyes with human serum albumin: a spectroscopic study, *Biophys. Chem.* **107** (1), 33--49, 2004.

162. Sarangi, M.K., & Basu, S. Photophysical behavior of acridine with amines within the micellar environment of SDS, *Phys. Chem. Chem. Phys.* **13** (37), 16821--16830, 2011.

163. Ngen, E.J., et al. Evaluation of delocalized lipophilic cationic dyes as delivery vehicles for photosensitizers to mitochondria, *Bioorganic & Medicinal Chem.* **17** (18), 6631--6640, 2009.

164. Kononov, A.I., et al. Photophysical processes in the complexes of DNA with ethidium bromide and acridine orange: A femtosecond study, *J. Phys. Chem. B* **105** (2), 535--541, 2001.

165. Ghosh, A.K., et al. Cu^{2+}-Induced Micellar Charge Selective Fluorescence Response of Acridine Orange: Effect of Micellar Charge, pH, and Mechanism, *J. Phys. Chem. B* **115** (41), 11823--11830, 2011.

166. Kawai, K., et al. Charge Separation in Acridine- and Phenothiazine-Modified DNA, *J. Phys. Chem. B* **112** (7) 2144--2149, 2008.

167. Gherghi, I.C., et al. Study of interactions between DNA-ethidium bromide (EB) and DNA-acridine orange (AO), in solution, using hanging mercury drop electrode (HMDE), *Talanta* 61 (2), 103--112, 2003.

168. Zhang, Y. Voltammetric Behavior of Dobutamine at Poly (Acridine Orange) Film Modified Electrode and Its Determination by Adsorptive Stripping Voltammetry, *Anal. Lett.* **37** (10), 2031--2042, 2004.

169. Wang, Z., et al. The fabrication of poly (acridine orange)/graphene modified electrode with electrolysis micelle disruption method for selective determination of uric acid, *Sensors and Actuators B* **161** (1), 131--136, 2012.

170. Ferguson, J., & Mau, A.W.H. Absorption studies of acid-base equilibria of dye solutions , *Chem. Phys. Lett.***17** (4) 543--546, 1972.

171. Falcone, R.D., et al. Acid-base and aggregation Process of Acridine Orange Base in n-Heptane/AOT/Water Reverse Micelles, *Langmuir* **18** (6) 2039--2047, 2002.

172. Panda, K., & Choudhury, A.K. Studies on the interaction of bacterial lipopolysaccharide with cationic dyes by absorbance and fluorescence spectroscopy, *J. Photoche. Photobiol. A: Chem.* **111** (1-3) 157--162, 1997.

173. Xun. C., et al. Advances in the study of luminescence probes for proteins, *J. Chromatography B* **803** (2), 173--190, 2004.

174. Wang, F., et al. Study on the formation and depolymerization of acridine orange dimer in acridine orange–sodium dodecyl benzene sulfonate-protein system, *J. Colloid Interface Sci.* **298** (2), 757--764, 2006.

175. Antonov, L., et al. UV-Vis spectroscopic and chemometric study on the aggregation of ionic dyes in water, *Talanta* **49** (1), 99--106, 1999.

176. Lamm, M.E., & Neville, D.M. Jr. The Dimer Spectrum of Acridine Orange Hydrochloride, *J. Phys. Chem.* **69** (11) 3872--3877, 1965.

177. Brignole, H. DeVoe, Least-squares computer analysis of dye absorption spectra. Acridine orange dimerization equilibrium, *J. Phys. Chem.* 82 (24) 2570--2575, 1978.

178. Costantino, L., et al. Acridine Orange Association Equilibrium in Aqueous Solutions, *J. Chem. Eng. data* **29** (1), 62--69, 1984.

179. Pereira, R.V., & Gehlen, M.H. Fluorescence of acridinic dyes in anionic surfactant solutions, *Spectrochim. Acta A* **61** (13-14), 2926--2932, 2005.

180. Drummond, C.J., et al. Acid-base equilibria in aqueous micellar solutions. Part 3-Azine derivatives, *J. Chem. Soc. Faraday Trans. 1* **85** (3), 551--560, 1989.

181. Bujdák, J., & Iyi, N. Visible Spectroscopy of Cationic Dyes in Dispersions with Reduced-Charge Montmorillonites, **50** (4), 446--454, 2002.

182. Reichardt, C. Solvatochromic Dyes as Solvent Polarity Indicators, *Chem. Rev.* **94** (8), 2319--2358, 1994.

183. Bhowmik, B.B., & Ganguly, P. Photophysical studies of some dyes in aqueous solution of triton X-100, *Spectrochim. Acta A* **62** (4-5), 808--813, 2005.

184. Chakraborty, M., & Panda, A.K. Spectral behaviour of eosin Y in different solvents and aqueous surfactant media, *Spectrochim. Acta A* **81** (1), 458--465, 2011.

185. Bhowmik, B.B., & Mukhopadhyay, M. Spectral and photophysical studies of thiazine dyes in Triton X-100, *Colloid Polym. Sci.* **266** (7), 672--676, 1988.

186. Guha, S.N., & Mittal, J.P. Pulse radiolysis study of redox reactions of safranine T in sodium dodecylsulphate (SDS) micellar medium, *Proc. Indian Acad. Sci. (Chem Sci.)* **104** (4), 497--507, 1992.

187. Dutta, R.K., & Bhat, S.N. Association of neutral red with micelles and its effect on the pK_a, *Can. J. Chem.* **71** (8), 1785--1791, 1993.

188. Baker, R.H. Drastic fluorescence enhancement and photochemical stabilization of cyanine dyes through micellar systems, *J. Am. Chem. Soc.* 102 (2), 847--848, 1980.

189. Harrison, W.J. Liquid-Crystalline J-Aggregates Formed by Aqueous Ionic Cyanine Dyes, *J. Phys. Chem.* **100** (6), 2310--2321, 1996.

190. Sidorowicz, A. Spectral properties of two betaine-type cyanine dyes in surfactant micelles and in the presence of phospholipids, *J. Mol. Struct.* 744-747, 711--716, 2005.

191. Harrison, W.J. J-aggregates and liquid crystal structures of cyanine dyes, *Faraday Discuss.* **104**, 139--154, 1996.

192. Tatikolov, A.S. & Costa, S.M.B. Photophysics and photochemistry of hydrophilic cyanine dyes in normal and reverse micelles, *Photochem. Photobiol. Sci.* **1** (3), 211--218, 2002.

193. Sato, H., et al. Fluorescence and energy transfer of dye-detergent systems in the premicellar region, *Chem. Lett.* **9** (12), 1529--1532, 1980.

194. Behera, G.B., et al. Cyanine Dyes: Self Aggregation and Behaviour in Surfactants A Review, *J. Surf. Sci. Technol.* **23** (1-2), 1--31, 2007.

195. Basu, S., et al. Photophysical studies of Merocyanine 540 dye in aqueous micellar dispersions of different surfactants and in different solvents, *Spectrochim. Acta A* **66** (4-5), 1255--1260, 2007.

196. Choudhury, S.D., et al. Surfactant-Induced Aggregation Patterns of Thiazole Orange: A Photophysical Study, *Langmuir* **27** (20), 12312--12321, 2011.

197. De, S., et al. Enhanced fluorescence of triphenylmethane dyes in aqueous surfactant solutions at supramicellar concentrations-effect of added electrolyte, *Spectrochim. Acta A* **58** (12), 2547--2555, 2002.

198. Jarosz, M. & Marczenko, Z. Spectrophotometric study of reactions of scandium, ytrium and lanthanum ions with some triphenylmethane dyes in the presence of cationic surfactants, *Anal. Chim. Acta* **159**, 309--317, 1984.

199. Okubo, T., & Ise, N. Catalytic action of polyelectrolytes on the alkaline fading reactions of triphenylmethane dyes, *J. Am. Chem. Soc.* **95** (7), 2293--2297, 1973.

200. Colichman, E.L. Surface and Interfacial Tension Titrations of Long Chain Quaternary Salts in Brom Phenol and Brom Thymol Blue Solutions, *J. Am. Chem. Soc.* **73** (4), 1795--1798, 1951.

201. Rosendorfova, J., & Cermakova, L. Spectrophotometric study of the interaction of some triphenylmethane dyes 1-carbethoxypentadecyltrimethylammonium bromide, *Talanta* **27** (9), 705--708, 1980.

202. Svodoba, B., & Chromy, V. Reactions of metallochromic indicators on micelles-I: General observations, *Talanta* **12** (5), 431--436, 1965.

203. Albrizzio, J., et al. Secondary valence force catalysis. XIII. Kinetics of the alkaline fading of crystal violet in the presence of cationic surfactants, *J. Org. Chem.* **37** (6), 871--874, 1972.

204. Yamamoto, K., & Motomizu, S. Liquid-liquid distribution of ion-associates of acidic dyes with quaternary ammonium counter-ions, *Talanta* **38** (5), 477--482, 1991.

205. Callahan, J.H., & Cook, K.D. Mechanism of Surfactant-Induced Visible Spectrometry of Metal-Chrome Azurol S Complexes, *Anal. Chem.* **56** (9), 1632--1640, 1984.

206. Hashemi, N., & Sun, G. Intermolecular Interactions between Surfactants and Cationic Dyes and Effect on Antimicrobial Properties, *Ind. Eng. Chem. Res.* **49** (18), 8347--8352, 2010.

207. Stevenson, D.M., et al. The Behaviour of Dyes in Aqueous Solutions Part II – Anionic Dye–Nonionic Surfactant Interactions, *J. Society Dyers Colourists* **97** (1), 13--17, 1981.

208. Su, T.L., et al. Interactions and Solubilization of Disperse Dye with Modified Gemini Surfactants: Investigation Using the Taguchi Method, *J. Surfactants Deterg.* **14** (3), 363--369, 2011.

209. Dutta, R.K., & Bhat, S.N. Interaction of phenazinium dyes and methyl orange with micelles of various charge types, *Colloids Surf. A* **106** (2-3), 127--134, 1996.

210. Sarkar, D., et al. Binding Interaction of Cationic Phenazinium Dyes with Calf Thymus DNA: A Comparative Study, *J. Phys. Chem. B* **112** (30), 9243--9249, 2008.

211. Rohatgi-Mukherjee, K.K., et al. Molecular interaction of phenosafranin with surfactants and its photogalvanic effect, *J. Colloid Interface Sci.* **106** (1), 45--50, 1985.

212. Gohain, B., et al. Protonated dye-surfactant ion pair formation between neutral red and anionic surfactants in aqueous submicellar solutions, *J. Mol. Liq.* **142** (1-3), 130--135, 2008.

213. Göktürk, S., & Tunçay, M. Spectral studies of safranin-O in different surfactant solutions, *Spectrochim. Acta A* **59** (8), 1857--1866, 2003.

214. Dutta, R.K., & Bhat, S.N. Dye-surfactant interaction in submicellar concentration range, *Bull. Chem. Soc. Jpn.* **65** (4), 1089--1095, 1992.

215. Saikia, P.M. A partition equilibrium study of sulphonapthalein dyes in anionic surfactant systems: determination of CMC in buffered medium, *Colloids Surf. A* **216** (1-3), 21--26, 2003.

216. Saikia, P.M., & Dutta, R.K. Acid-base equilibria of sulphonapthalein dyes in aqueous polymer-surfactant media, *J. Surfactants Deterg.* **9** (1), 39-45, 2006.

217. Gohain, B., & Dutta, R.K. Premicellar and micelle formation behavior of dye surfactant ion pairs in aqueous solutions: Deprotonation of dye in ion pair micelles, *J. Colloid Interface Sci.* **323** (2), 395--402, 2008.

218. Gohain, B., et al. Hydrophobicity-induced deprotonation of dye in dye-submicellar surfactant systems, *Phys. Chem. Chem. Phys.* **4** (1), 2617--2620, 2002.

219. Yamamoto K, & Adachi K., Interaction between sulfonaphthalein dyes and chitosan in aqueous solution and its application to the determination of surfactants, *Anal Sci.* **19** (8), 1133--1138, 2003.

220. Tønnesen, H.H. Solubility, chemical and photochemical stability of curcumin in surfactant solutions. Studies of curcumin and curcuminoids, XXVIII, *Pharmazie* **57** (12), 820--824, 2002.

221. Iwunze, M.O. Binding and distribution characteristics of curcumin solubilized in CTAB micelle, *J. Mol. Liq.* **111** (1-3), 161--165, 2004.

222. Leung, M.H.M., et al. Encapsulation of curcumin in cationic micelles suppresses alkaline hydrolysis, *Langmuir* **24** (11), 5672--5675, 2008.

223. Wang, Z., et al. The role of charge in the surfactant-assisted stabilization of the natural product curcumin, *Langmuir* **26** (8), 5520--5526, 2010.

224. Ghatak, C., et al. An Understanding of the Photophysical Properties of Curcumin inside a Micelle Formed by an Ionic Liquid: A New Possibility of Tunable Drug Delivery System, *J. Phys. Chem. B* **116** (10), 3369--3379, 2012.

225. Hartley, G.S., & Roe, J.W. Ionic concentrations at interfaces, *Trans. Faraday Soc.* **36**, 101--109, 1940.

226. B. Simončič, & J. Špan, A study of dye-surfactant interactions. Part 1. Effect of chemical structure of acid dyes and surfactants on the complex formation, *Dyes Pigments* **36** (1), 1--14, 1998.

227. Ghoreishi, S.M., et al. Interaction of anionic azo dye and TTAB - cationic surfactant, *J. Braz. Chem. Soc.* **20** (3), 460--465, 2009.

228. Zade, A.B., & Munshi, K.N. Spectrophotometric Studies on Some Dye-Surfactant Complexes, *Surfactants in Solution*, 713--724, 1986.

229. Bračko, S., & Špan, J. Conductometric investigation of dye-surfactant ion pair formation in aqueous solution, *Dyes Pigments* **45** (2), 97--102, 2000.

230. Neumann, M.G., & Gehlen, M.H. The interaction of cationic dyes with anionic surfactants in the premicellar region, *J. Colloid Interface Sci.* **135** (1), 209--217, 2008.

231. Bielska, M., et al. Dye-surfactant interaction in aqueous solutions, *Dyes Pigments* **80** (2), 201--205, 2009.

232. Sato, H., et al. Energy transfer between rhodamine 6G and pinacyanol enhanced with sodium dodecyl sulfate in the premicellar region. Formation of dye-rich induced micelles, *J. Phys. Chem.* **87** (19), 3759--3769, 1983.

233. Ban, T. Fluorescence decay of the acridine orange-sodium dodecyl sulfate system: formation of dye-rich induced micelles in the premicellar region, *Photochem. Photobiol.* **37** (2), 131--139, 1983.

234. Mukerjee, P. & Mysels, K.J. A Re-evaluation of the Spectral Change Method of Determining Critical Micelle Concentration, *J. Am. Chem. Soc.* **77** (11), 2937--2943, 1955.

235. H. Sato, et al., Fluorescence and energy transfer of dye-detergent systems in the premicellar region, *J. Photochem.* **17** (2), 243--248, 1981.

236. Barber, D.C. Atropisomer-specific formation of premicellar porphyrin J-aggregates in aqueous surfactant solutions, *J. Phys. Chem.* **95** (10), 4074--4086, 1991.

237. Dutta Choudhury, S. Surfactant-Induced Aggregation Patterns of Thiazole Orange: A Photophysical Study, *Langmuir* **27** (20), 12312--12321, 2011.

238. Casero, I. Study of the formation of dye-induced premicellar aggregates and its application to the determination of quaternary ammonium surfactants, *Talanta* **45** (1), 167--180, 1997.

239. Dakiky, M., & Nemcova, I. Aggregation of *o,o'*- Dihydroxy azo Dyes III. Effect of cationic, anionic and non-ionic surfactants on the electronic spectra of 2-hydroxy-5-

nitrophenylazo-4-[3-methyl-1-(4"-sulfophenyl)-5-pyrazolone], *Dyes Pigments* **44** (3), 181–193, 2000.

240. Oakes, J., et al. Solubilisation of dyes by surfactant micelles. Part 3; A spectroscopic study of azo dyes in surfactant solutions, *Coloration Technology*, 119 (5), 301--306, 2003.

241. Ouyang, C., et al. Aggregation of azo dye Orange I induced by polyethylene glycol in aqueous solution, *Colloids Surf. A* **301** (1-3), 346--351, 2007.

242. Novaki, L.P., & Seoud, O.A.E. Microscopic Polarities of Interfacial Regions of Aqueous Cationic Micelles: Effects of Structures of the Solvatochromic Probe and the Surfactant, *Langmuir* **16** (1), 35--41, 2000.

243. Moulik, S.P., et al. Interaction of acridine orange monohydrochloride dye with sodiumdodecylsulfate, (SDS) cetyltrimethylammoniumbromide (CTAB) and p-tert-octylphenoxypolyoxy ethanol (Triton X 100) surfactants, *Colloid and Polym. Sci.* **275** (6), 645--655, 1979.

244. Corrin, M.L., & Harkins, D.W. Determination of the Critical Concentration for Micelle Formation in Solutions of Colloidal Electrolytes by the Spectral Change of a Dye, *J. Am. Chem. Soc.* **69** (3), 679--682, 1947

245. Hiskey, C.F., & Downey, T.A. The Colloidal Error of Indicators, *J. Phys. Chem.* **58** (10), 835--840, 1954.

246. Mukerjee, P., & Mysels, K.J. A Re-evaluation of the Spectral Change Method of Determining Critical Micelle Concentration, *J. Am. Chem. Soc.* **77** (11), 2937-2943, 1955.

247. Guha, S.N. Spectral and fluorimetric studies on the effect of surfactants on thionine *Proceedings of the Indian Academy of Sciences - Chemical Sciences* **91** (1), 73--85, 1982.

248. Chernova, R.K. Effect of some colloidal surfactants on spectrophotometric characteristic of metal chelates with chromophoric organic reagents, *Zh. Anal. Khim.* **32** (8), 1477--1486, 1977.

249. Chang, K.L. in *Spectrochemical Methods of Analysis*, Winefordner, J.D. Ed, Wiler, NewYork, p 363, 1971.

250. Goturk, S., & Tuncay, M. Dye-Surfactant Interaction in the Premicellar region, *J. Surfactant Deterg.* **6** (4), 325--330, 2003.

251. Rodriguez, R.B., & Estelrich, J. Photophysical Changes of Pyranine Induced by Surfactants: Evidence of Premicellar Aggregates, *J. Phys. Chem. B* **113** (7), 1972--1982, 2009.

252. Rahman, M.M., et al. Electrochemical Behavior of Malachite Green in Aqueous Solutions of Ionic Surfactants, 1--10, 2013.

253. Gohain, B., et al. Premicellar and micelle formation behavior of aqueous anionic surfactants in the presence of triphenylmethane dyes: protonation of dye in ion pair micelles, *J. Phys. Org. Chem.* **23** (3), 211--219, 2010.

254. Shahir, A.A., et al. Comprehensive study of Tartrazine/Cationic Surfactant Interaction, *J. Phys. Chem. B* **115** (49), 14435--14444, 2011.

255. Kirchherr, A.K., et al. Stabilization of Indocyanine Green by Encapsulation within Micellar Systems, *Mol. Pharmaceutics* **6** (2), 480--491, 2009.

256. Maiti, N.C., et al. Fluorescence Dynamics of Dye Probes in Micelles, *J. Phys. Chem. B* **101** (51), 1051--11060, 1997.

257. Choi, T.S., et al. Solubilization of disperse dyes in cationic gemini surfactant micelles, *Dyes Pigments* **45** (2), 145--152, 2000.

258. Shah, S.H. Solubilization of Amphiphilic Hemicyanine Dyes by a Cationic Surfactant, Cetyltrimethylammonium Bromide, *J. Colloid Interface Sci.* **186** (2), 382--386, 1997.

259. Mukerjee, P. Solubilization in Aqueous Micellar Systems, *Solution Chemistry of Surfactants,* 153--174, 1979.

260. Awan, M.A., & Shah, S.S. Hydrophobic interaction of amphiphilic hemicyanine dyes with cationic and anionic surfactant micelles, *Colloids Surf. A* 122 (1-3), 97--101, 1997.

261. Bielska, M., et al. Dye-surfactant interaction in aqueous solutions, *Dyes and Pigments,* 80 (2), 201--205, 2009.

262. Zaghbani, N., et al. Separation of methylene blue from aqueous solution by micellar enhanced ultrafiltration, *Sep. Purif. Technol.* **55** (1), 117--124, 2007.

263. Mandal, A.B., et al. Determination of the critical micelle concentration of surfactants and the partition coefficient of an electrochemical probe by using cyclic voltammetry, *Langmuir* **4** (3), 736--739, 1988.

264. Shah, S.S., et al. Differential absorbance measurements of amphiphilic hemicyanine dyes, solubilization study in anionic surfactant, *Colloids and Surf. A* **168** (1), 77--85, 2000.

265. Guha, S., & Jaffe, P.R. Bioavailability of Hydrophobic Compounds Partitioned into the Micellar Phase of Nonionic Surfactants, *Environ. Sci. Technol.* **30** (4), 1382--1391, 1996.

266. Guha, S. Bioavailability of Mixtures of PAHs Partitioned into the Micellar Phase of a Nonionic Surfactant, *Environ. Sci. Technol.* **32** (15), 2317--2324, 1998.

267. Saikia, P.M., & Dutta, R.K. A Partition Equilibrium Study of Sulfonephthalein Dyes in Nonionic Surfactant Systems at High pH, *J. Surface Sci. Tech.* **23** (3-4), 195--208, 2007.

268. Saikia, P.M., & Dutta, R.K. Effect of Association of Bromophenol Blue with Tween Surfactants on Its Acid-Base Equilibria at High *p*H, *J. Dispersion Sci. Tech.* **30** (1), 33--37, 2009.

269. Boruah, B., et al. Binding and stabilization of curcumin by mixed chitosan-surfactant systems: A spectroscopic study, *J. Photochem. Photobiol. A: Chem.* **245** (1) 18--27, 2012.

270. Yakatan, G.J., & Schulman, S.G. Electronic spectral study of the ionizations of the naphthalene monosulfonic acids, *J. Phys. Chem.* **76** (4), 508--510, 1972.

271. Bunton, C.A., et al. Electrolyte effects on the cationic micelle catalyzed decarboxylation of 6-nitrobenzisoxazole-3-carboxylate anion, *J. Am. Chem. Soc.* **95** (10), 3262--3272, 1973.

272. Bunton, C.A., & Minch, M.J. Micellar effects on the ionization of carboxylic acids and interactions between quaternary ammonium ions and aromatic compounds, *J. Phys. Chem.* **78** (15), 1490--1498, 1974.

273. Mukherjee, P., & Banerjee, K. A Study of the Surface pH of Micelles Using Solubilized Indicator Dyes, *J. Phys. Chem.* **68** (12), 3567--3574, 1964.

274. Romsted, L.S., & Zanette, D. Quantitative treatment of indicator equilibria in micellar solutions of sodium decyl phosphate and sodium lauryl sulfate, *J. Phys. Chem.* **92** (16), 4690--4698, 1988.

275. He, Z.M., et al. Specific counterion effects on indicator equilibria in micellar solutions of decyl phosphate and lauryl sulfate surfactants, *J. Phys. Chem.* **93** (10), 4219--4226, 1989.

276. Ke, D., et al. Spectrometric Study on the Interaction of Dodecyltrimethylammonium Bromide with Curcumin, *Langmuir* **27** (23), 14112--14116, 2011.

277. Boruah, B., *A study on the interactions of some synthetic and natural dyes of different charge types with surfactants and polymers*, Ph.D thesis, Tezpur University, 2012.

278. Stratmann, R.E., et al. An efficient implementation of time-dependent density-functional theory for the calculation of excitation energies of large molecules, *J. Chem. Phys.* **109** (19), 8218--8224, 1998.

279. Caillie, V., & Amos, R.D. Geometric derivatives of density functional theory excitation energies using gradient-corrected functionals, *Chem. Phys. Lett.* **317** (1-2), 159--164, 2000.

280. Kantchev, E.A.B., et al. Time dependent density functional theory (TD-DFT) modelling of Pechmann dyes- from accurate absorption maximum prediction to virtual dye screening, *Org. Biomol. Chem.* **10**, 6682--6692, 2012.

281. Jacquemin, D., et al. A TD-DFT study of the absorption spectra of fast dye salts, *Chem. Phys. Lett.* **410** (4-6), 254--259, 2005.

282. Bourass, M., et al. DFT and TD-DFT investigations of new thienopyrazine-based dyes for solar cells: Effect of electron donor groups, *Der Pharma Chemica* **5** (5), 144--153, 2013.

283. Zarate, X., et al. A DFT-/TD-DFT study of Porphyrazines and Phthalopcyanines Oxo-Titanium Derivatives as Potential Dyes in Solar Cells, *Int. J. Quantum Chem.* **111** (15), 4186--4196, 2011.

284. Sang-aroon, W., et al. DFT and TD-DFT on the electronic structure and photoelectrochemical properties of dyes derived from cochineal and lac insects as photosentizer for dye-sensitized solar cells, *J. Mol. Model.* **19** (3), 1407--11415, 2013.

285. Petit, L., et al. Absorption Spectra of First-Row Transition Metal Complexes of Bacteriochlorins: A Theoretical Analysis, *J. Phys. Chem. B* **109** (24), 12214--12221, 2005.

286. Quartarolo, A.D., et al. Absorption Spectra of the Potential Photodynamic Therapy Photosensitizers Texaphyrins Complexes: A Theoretical Analysis, *J. Chem. Theory Comput.* **3** (3), 860--869, 2007.

287. Jacquemin, D., et al. Substitution effects on the visible spectra of 1,4-diNHPh-9,10-anthraquinones, *Chem. Phys. Lett.* **405** (4-6), 429--433, 2005.

288. Furchy, F., & Rappoport, D. Density functional methods for excited states: equilibrium structure and electronic states, Chapter III of Computational

Photochemistry edited by M. Olivucci, 16 *Theoretical and Computational Chemistry*, 93--128, 2005.

289. Cossi, M., & Barone, V. Time-dependent density functional theory for molecules in liquid solutions, *J. Chem. Phys.* **115** (10), 4708--4717, 2001.
290. Homem-de-Mello, P., et al. Cationic dye dimers: a theoretical study, *Theor. Chem. Acc.* **118** (2), 305--314, 2007.
291. Homem-de-Mello, P., et al. The effects of solvation in the theoretical spectra of cationic dyes, *Theor. Chem. Acc.* **113** (5), 274--280, 2005.
292. Linnanto, J., & Korppi, T. Quantum chemical simulation of excited states of chlorophylls, bacteriochlorophylls and their complexes, *Phys. Chem. Chem. Phys.* **8** (6) 663--687, 2006.
293. Patrick, J.O.M., & Collins, S.J.J. The Effect of Axial Mg Ligation on the Geometry and Spin Density Distribution of Chlorophyll and Bacteriochlorophyll Cation Free Radical Models: A Density Functional Study, *J. Am. Chem. Soc.* **123** (44), 11042--11046, 2001.
294. Dutta, R.K., et al. Effect of association of sulphonapthalein dyes with sodium dodecyl sulfate micelles on their acid-base equilibria, *J. Chem. Soc., Faraday Trans.*, **91** (4), 681--686, 1995.
295. Khamis, M., et al. Azo dyes interactions with surfactants. Determination of the critical micelle concentration from acid-base equilibrium, *Dyes Pigments* **66** (3), 179--183, 2005.
296. Gohain, B. *A Study on the ionpair formation, protonation-deprotonation equilibria of dyes and micelle formation behavior in aqueous dye surfactant solution,* Ph.D. Thesis, Tezpur University, India, 2009.
297. Perrin, D.D. Buffers of Low Ionic Strength for Spectrophotometric pK_a Determinations, *Aust. J. Chem.* **16** (4), 572--578, 1963.
298. Frisch, M.J., et al. Gaussian 03, revision C.02; Gaussian, Inc.: Wallingford, CT, 2003.
299. Parr, R.G., & Wang, W. Density-Functional Theory of Atoms and Molecules; Oxford University Press: New York, 1989.
300. Tomasi, J., & Persico, M. Molecular Interactions in Solution: An Overview of Methods Based on Continuous Distributions of the Solvent, *Chem. Rev.* **94** (7), 2027--2094, 1994.

301. Karukstis, K.K., et al. Spectroscopic Studies of the Interaction of Methyl Orange with Cationic Alkyltrimethylbromide Surfactants, *J. Colloid Interface Sci.* **203** (1), 157--163, 1998.

302. Cosa, G., et al. Photophysical Properties of Fluorescent DNA-dyes Bound to Single and Double-stranded DNA in Aqueous Buffered Solution, *Photochem. Photobiol.* **73** (6), 585--589, 2001.

303. Mäntele, W. The seven sins of fluorescence measurements, *Spectrochim. Acta A* 96, v-vi, 2012.

304. M. van de Weert, Erratum to: Fluorescence Quenching to Study Protein-ligand Binding: Common Errors, *J. Fluoresc.* **20** (2), 625--629, 2010.

305. Chandra, S., et al. Synthesis, functionalization and bioimaging applications of highly fluorescent carbon, *Nanoscale* **3** (12), 1533--1540, 2011.

306. Lakowicz, J.R. Principles of Fluorescence Spectroscopy, Springer, Berlin, Third edition.

307. Sierocki, P., et al. Photoisomerization of Azobenzene Derivatives in Nanostructured Silica, *J. Phys. Chem. B.* **110** (48), 24390--24398, 2006.

308. Sakamoto, R., et al. *trans-cis* Photoisomerization of Azobenzene-Conjugated Dithiolato-Bipyridine Platinum(II) Complexes: Extension of Photoresponse to Longer Wavelengths and Photocontrollable Tristability, *Chem. Eur. J.* **15** (6), 1429--1439, 2009.

309. Fujino, T., et al. Femtosecond time-resolved fluorescence study of photoisomerization of trans-azobenzene, *J. Phys. Chem. A* **105** (35), 8123--8129, 2001.

310. Cembran, A., et al. On the Mechanism of the cis-trans Isomerization in the Lowest Electronic States of Azobenzene: S_0, S_1, and T_1, *J. Am. Chem. Soc.* **126** (10), 3234--3243, 2004.

311. Bell, G.R., et al. Penfold, Structure of a Monolayer of Hexadecyltrimethylammonium *p*-Tosylate at the Air-Water Interface, *J. Am. Chem. Soc.* **119** (42), 10227--10228, 1997.

312. Ahmadi, F., et al. The effect of anionic and cationic surfactants of indicators and measurement of dissociation constants with two different methods, *Spectrochim. Acta A* **67** (2), 412--419, 2007.

313. O'Neill, M., & Kelly, S.M. Photoinduced surface alignment for liquid crystal displays, *J. Phys. D: Appl. Phys.* **33** (1), 67--84, 2000.

314. Helfrich, W., & Lipsett, F.R. Fluorescence and Defect Fluorescence of Anthracene at 4.2°K, *J. Chem. Phys.* **43** (12), 4368--4357, 1965.

315. Wang, F., et al. Study on the formation and depolymerization of acridine orange dimer in acridine orange-sodium dodecyl benzene sulfonate-protein system, *J. Colloid Interface Sci.* **298** (2), 757--764, 2006.

316. Ghosh, A.K., et al. Anionic micelle-induced fluorescent sensor activity enhancement of acridine orange: Mechanism and *p*H effect, *Chem. Phys. Lett.* **507** (1-3) 162--167, 2011.

317. Costantino, L., et al. Acridine Orange Association Equilibrium in Aqueous Solution, *J. Chem. Eng. Data* **29** (1), 62--66, 1984.

318. Petrossyan, N.O.M. *Pure Appl. Chem.* **80**, 1459--1510, 2008.

319. Lu, J.R., et al. Surfactant layers at the air / water interface: structure and composition, *Adv. Colloid Interface Sci.* **84** (13), 143--304, 2000.

320. Luo, Y., & Shen, H. Study on Acridine Orange dimer as a new fluorescent probe for the determination of protein, *Anal. Commun.* **36** (4), 135--137, 1999.

321. Ban, T., et al. Fluorescence decay of the acridine orange sodium dodecyl sulfate system: formation of dye-rich induced micelles in the premicellar region, *Photochem. Photobiol.* **37** (2), 131--139, 1983.

322. Ganguly, P., Photophysics of some cationic dyes in aqueous micellar dispersions of surfactants and in different solvents, *J. Mol. Liq.* **151** (1), 67--73, 2010.

323. Moulik, S.P., et al. Acid-Base Behavior of Neutral Red in Compartmentalized Liquids (Micelles and Microemulsions), *J. Colloid Interface Sci.* **161** (1), 72--82, 1993.

324. Sharma Yamijala, SRKC et al. Computational Studies on Structural and Excited-State Properties of Modified Chlorophyll f with Various Axial Ligands, *J. Phys. Chem. A* **115** (44), 12298--12306, 2011.

325. Govindarajan, S. Turmeric - chemistry, technology, and quality, *Crit. Rev. Food Sci. Nutr.* **12** (3), 199--301, 1980.

326. Lampe, V. & Milobedzaka, J. *Ber. Dtsch. Chem. Ges.* **41**, 1640-1643, 1913.

327. Jayaprakasha, G.K., et al. Sahariah, Chemistry and biological activities of *C. longa*, *Trends Food. Sci. Technol.* **16** (12), 533-548, 2005.

328. JECFA, Safety evaluation of certain food additives and contaminants. Prepared by the 61st meeting of JECFA WHO Food Additive Series: 52. WHO, pp. 55-60, 2004.

329. Goel, A., et al. Aggarwal, Curcumin as "Curecumin": from kitchen to clinic, Biochem. *Pharmacol.* **75** (4), 787-809, 2008.

330. Anand, P., et al. Curcumin and cancer: An "old-age" disease with an "age-old" solution, *Cancer Lett.* **267** (1), 133--164, 2008.

331. Ruby, A.J., et al. Kuttan, Anti-tumour and antioxidant activity of natural curcuminoids, *Cancer Lett.* **94** (1), 79--83, 1995.

332. Kim, M.K., et al. Fungicidal Property of *Curcuma longa* L. Rhizome-Derived Curcumin against Phytopathogenic Fungi in a Greenhouse, *J. Agric. Food Chem.* **51** (6), 1578--1581, 2003.

333. Ono, K., et al. Curcumin Has Potent Anti-Amyloidogenic Effects for Alzheimer's β-Amyloid Fibrils In Vitro, *J. Neurosci. Research* **75** (6), 742--750, 2004.

334. Shukla, P.K., et al. Anti-ischemic Effect of Curcumin in Rat Brain, *Neurochem. Res.* **33** (6) 1036--1043, 2008.

335. Srimal, R.C., & Dhawan, B.N. Pharmacology of diferuloyl methane (curcumin), a non-steroidal anti-inflammatory agent, *J. Pharm. Pharmacol.* **25** (6), 447--452, 1973.

336. Balasubramanian, K. Molecular Orbital basis for Yellow Curry Spice Curcumin's Prevention Of Alzheimer's Disease, *J. Agric. Food Chem.* **54** (10), 3512--3520, 2006.

337. Cole, G.M., et al. Neuroprotective effects of curcumin, *Adv. Exp. Med. Biol.* **595**, 197--212, 2007.

338. Egan, M.E., et al. Curcumin, a major constituent of turmeric, corrects cystic fibrosis defects, *Science* **304** (5760), 600--602, 2004.

339. Aggrawal, B.B., et al. Curcumin: the Indian solid gold, *Adv. Exp. Med. Biol.* **595**, 1--75, 2007.

340. Mazumder, A., et al. Curcumin analogs with altered potencies against HIV-1 integrase as probes for biochemical mechanisms of drug action, *J. Med. Chem.* **40** (19), 3057--3063, 1997.

341. Sui, Z., et al. Inhibition of the HIV-1 and HIV-2 proteases by curcumin boron complexes, *Bioorg. Med. Chem.* **1** (6), 415--422, 1993.

342. Wright, J.S. Predicting the Antioxidant Activity of Curcumin and Curcuminoids, *J. Mol. Struct. Theochem.* **591** (1-3), 207--217, 2002.

343. Cornago, P., et al. A Study of the tautamerism of β-dicarbonyl compounds with special emphasis on Curcuminoids, *Tetrahedron* **64** (35), 8089--8094, 2008

344. Dyrssen, D.W., et al. Studies on the chemistry of the determination of boron with curcumin, *Anal. Chim. Acta* **60** (1), 139--151, 1972.

345. Jovanovic, S.V., et al. H-Atom Transfer Is A Preferred Antioxidant Mechanism of Curcumin, *J. Am. Chem. Soc.* **121** (41), 9677--9681, 1999.

346. Bong, P.H. Spectral and Photophysical Behaviors of Curcumin and Curcuminoids, *Bull. Korean Chem. Soc.* **21** (1), 81--86, 2000.

347. Bernab'e-Pineda, M., et al. Determination of acidity constants of curcumin in aqueous solution and apparent rate constant of its decomposition, *Spectrochim. Acta A* **60** (5), 1091--1097, 2004.

348. Shen, L., & Ji, H.F. Theoretical study on physicochemical properties of curcumin, *Spectrochim. Acta A* **67** (3-4), 619--623, 2007.

349. Zsila, F., et al. Circular dichroism spectroscopic studies reveal pH dependent binding of curcumin in the minor groove of natural and synthetic nucleic acids, *Org. Biochem. Chem.* **2** (20), 2902--2910, 2004.

350. Zsila, F., et al. Simonyi, Molecular basis of the Cotton effects induced by the binding of curcumin to human serum albumin, *Tetrahedron: Asymmetry* **14** (16), 2433--2444, 2003.

351. Began, G., et al. Interaction of curcumin with phosphatidylcholine: a spectrofluorometric study, *J. Agric. Food Chem.* **47** (12), 4992--4997, 1999.

352. Hosseinzadeh, R., et al. Spectrophotometric study of anionic azo-dye light yellow (X6G) interaction with surfactants and its micellar solubilization in cationic surfactant micelles, *Spectrochim. Acta A* **69** (4), 1183-1188, 2008.

353. Mandal, S. et al. Modulation of the Photophysical Properties of Curcumin in Nonionic Surfactant (Tween-20) Forming Micelles and Niosomes: A Comparative Study of Different Microenvironm, *J. Phys. Chem. B* **117** (23), 6957--6968, 2013.

354. Nardo, L., et al. Studies on Curcumin and Curcuminoids. XXXIX. Photophysical Properties of Bisdemethoxycurcumin, *J Fluoresc.* **21** (2), 627--635, 2011.

355. Barik, A., & Priyadarsini, I.K. Solvent dependent photophysical properties of dimethoxy curcumin, *Spectrochim. Acta A* **105** (1), 267--272, 2013.

356. Patra, D., & Barakat, C. Synchronous fluorescence spectroscopic study of solvatochromic curcumin dye, *Spectrochim. Acta A* 79 (5), 1034--1041, 2011.

357. Priyadarsini, K.I. Photophysics, photochemistry and photobiology of curcumin: Studies from organic solutions, bio-mimetics and living cells, *J. Photochem. Photobiol. C* **10** (2), 81--95, 2009.

358. Borsari, M., et al. Curcuminoids as potential new iron-chelating agents: spectroscopic, polarographic and potentiometric study on their Fe (III) complexing ability, *Inorg. Chim. Acta* **328** (1), 61--68, 2002.

APPENDICES

Research Papers in Journals

1. "Fluorescence behavior of *cis*-methyl orange stabilized in cationic premicelles", A. Dutta and R.K Dutta, ***Spectrochim. Acta A*** 126 (2014) 270-279.
2. "Protonation of acridine orange in dye-surfactant ion pair micelles", A. Dutta and R.K. Dutta, ***J. Mol. Liq.*** 178 (2013) 25-30.
3. "Stabilization of diketo tautomer of curcumin by premicellar cationic surfactants: UV-Vis, fluorescence, tensiometric and TD-DFT evidences", A. Dutta, B. Boruah, P.M. Saikia, R.K. Dutta, ***J. Mol. Liq.*** 187 (2013) 350-358.
4. "Stabilization of diketo tautomer of curcumin by premicellar anionic surfactants: UV-Vis, fluorescence, tensiometric and TD-DFT evidences", A. Dutta, B. Boruah, A.K. Manna, B. Gohain, P.M. Saikia, R.K. Dutta, ***Spectrochim. Acta A*** 104 (2013) 150-157.
5. "Time-dependent density functional theory (TDDFT) modeling of protonated dye-surfactant ion pair", A. Dutta and R.K. Dutta (to be communicated).

Presentation in Conferences

1. Presented a paper titled "Spectroscopic Investigation of the pH dependent Degradation Kinetics of Curcumin in Nonionic Micellar Solutions" in the "**International Conference on Recent Frontiers in Applied Spectroscopy (ICORFAS-2010)**",10-12 September, 2010, Annamalai University Chennai, India
2. Presented a paper titled "A visit to the Nature of *cis-trans* isomerism of methyl orange in premicellar Cationic surfactant solutions: a tensiometric, fluorescence and TD-DFT study, in the **Workshop on Spectroscopic Tools and their applications,** 6th April, 2013, organized by Dept. of Chemical Sciences, Tezpur University, Tezpur, Assam, India.
3. Presented a paper titled "Protonation of Acridine orange in the dye-surfactant ionpair micelle" in the **UGC Sponsored National Seminar on "Recent Challenges for Chemical research and Practices: Moulding Chemistry towards a better tomorrow"**, 9-10 November, 2012, organized by the Dept. of Chemistry, Darrang College, Tezpur Assam, India
4. Presented a poster titled "Monomer-dimer equilibrium of Acridine Orange in polymer-surfactant system" in the **National Conference on Chemistry, Chemical Technology and Society**, 11-12 November, 2011, organized by Dept. of Chemical Sciences, Tezpur University, Assam, India.

Conferences and workshop participated

1. **Frontier Lecture Series**, 20-22 November, 2009, Organized by Jawaharlal Nehru Centre for Advanced Scientific Research (JNCASR), Bangalore in collaboration with the Dept. of Chemical Sciences, Tezpur University, Assam, India.
2. 14th National Workshop on Catalysis, December 21-23, 2009, Department of Chemical Sciences, Tezpur University.
3. **Workshop on Integrated Arsenic and Iron Removal from Groundwater: *Arsiron Nilogon***, 25th June, 2011, Sponsered by the Department of Science and Technology (DST), New Delhi, India and organized by the Dept. of Chemical Sciences, Tezpur University, Assam.
4. Workshop on "**Intellectual Property Rights Sensitization: IPRSW-2010**", on 23rd December, 2010 at Tezpur University, Assam.
5. **International Congress on Renewable energy**, 2-4 November, 2011, at Tezpur University, Tezpur, Assam
6. National Workshop on "**Advances in Applied Microbiology to Bioprocess Engineering with special reference to Petroleum Biotechnology,**" 23024 August, 2012, at the dept. of Molecular Biology and Biotechnology, Tezpur University, Assam, Tezpur.